L-vehicles Emissions and Noise mitigation Solutions

D5.3 Results of field surveys on LV tampering

This project has received funding from the European Union's Horizon Europe research and innovation programme under grant agreement No 101056777

Deliverable No.	D5.3	
Deliverable title	Results of field surveys on LV tampering	
Deliverable type	Report	
Dissemination level	PU - Public	
Deliverable leader	IVL	
Contractual due date	31/08/2025	
Actual submission date	28/08/2025	
Version	1.0	
Written by	Åke Sjödin (IVL), Åsa Hallquist (IVL), Yingying Cha (IVL), Hervé Denayer (KU Leuven), Xian Wu (KU Leuven), Alexandre Ricardo Mauricio (KU Leuven), Konstantinos Gryllias (KU Leuven), Martin Kupper (TUG), Hafiz Hashim Imtiaz (TUG)	30/06/2025
Reviewed by	Michael Dittrich (TNO)	07/07/2025
Reviewed by	Michal Vojtíšek (PRAGUE)	15/07/2025
Approved by	All partners	08/08/2025

Revisions table

Version	Date	Change
1.0	28/08/2025	First submission to the EC

This project has received funding from the European Union's Horizon Europe research and innovation programme under grant agreement No 101056777

Table of contents

This project has received funding from the European Union's Horizon Europe research and innovation programme under grant agreement No 101056777

This project has received funding from the European Union's Horizon Europe research and innovation programme under grant agreement No 101056777

Executive summary

This deliverable report presents the work and results from three emission and noise tampering in-field surveys on L-category vehicles (LVs), conducted in Leuven, the Paris region and Barcelona, respectively, in the summer of 2024. Pollutant (CO, HC, NO_X and particulate matter - PM) emissions and noise were measured from the kerbside on passing individual LVs in real-world settings and were combined with inspections by pulling over a subset of the measured vehicles to the roadside by the local police. The roadside inspections included measuring the idle emissions of CO and HC as well as performing the stationary noise test, and visual inspections by qualified and experienced technical staff to assess whether vehicles were deliberately tampered or illegally modified, which could contribute to elevated emission and/or noise levels.

Roadside measurements in real traffic settings on L-vehicles are a significant challenge when it comes to both pollutant emissions and noise. In the case of pollutant emissions particularly the small exhaust plumes associated with LVs present a major measurement problem, resulting in low hit-rates, rarely exceeding 50% for conventional remote sensing (i.e., the Opus RSE RSD 6000 instrument, mainly aimed for measuring gaseous pollutants) and far less for point sampling remote emission sensing, mainly aimed for measuring particulate pollutants (instruments provided by TU Graz and IVL), and only if traffic and road infrastructure conditions (e.g., road grade, proximity of passing vehicles to the measuring instruments) are optimal. In the case of both pollutant emissions and noise, very dense traffic situations present a common measurement problem with the very short distances between vehicles, stop-and-go situations, etc., which may cause overlaps of both exhaust plumes and vehicle generated noise (from all kinds of vehicles, not only LVs). This was especially the case for the Barcelona campaign. The best conditions for measuring both emissions and noise appeared in the Leuven campaign, but here the number of passing L-vehicles was not that high. The Paris region and Barcelona campaigns both showed relatively high numbers of passing LVs, but with lower hit-rates due to dense traffic and/or complex traffic situations.

Nevertheless, the measurements of both emissions and noise on in total more than 2,000 LVs in the three campaigns, have resulted in new insights in various areas related to L-vehicle air and noise pollution, including the occurrence and environment impact of tampering, such as:

- The on-road/real-world emissions of all regulated pollutants (CO, HC, NO_X and PM) from L-category vehicles have been reduced substantially from around Euro 2 (the early 2000's) to Euro 5 compliant LVs, with reductions in the range of ≈ 60-90%, depending on pollutant.
- Despite differences in fleet composition, driving conditions and background noise, comparable noise levels were measured from the roadside for all campaigns. No clear trends could be observed as function of Euro class or engine displacement, mostly due to the fact that the driving conditions were far from the most critical ones for noise.
- The share of tampered LVs in the roadside inspections, carried out in Leuven and Barcelona (no roadside inspections could be carried out in the Paris region campaign), was around 10% in both cities (11% in Leuven and 12% in Barcelona). Since roller bench tests – to check for tampering of the engine speed restrictor on the smallest LVs – were not included in the

This project has received funding from the European Union's Horizon Europe research and innovation programme under grant agreement No 101056777

roadside inspections neither in Leuven nor Barcelona – these tampering shares are likely (somewhat) underestimated.

- The most frequent tampering types observed were :
  - Illegal or modified exhaust system/engine/air intake;
  - Illegal or modified muffler;
  - Higher noise level than the reference noise level measured in the stationary noise test;
  - No dB killer.
- Emission related tampering increased the fuel-specific on-road emissions of CO, HC and PM by a factor of about 5, 7 and 10, respectively.
- Tampering often leads to an increase of the noise levels, both in the stationary test and measured from the roadside for vehicles driving by, but the difference with non-modified vehicles strongly depends on the metrics used to quantify the noise level and the driving condition.
- Tampering also has an impact on the sound character and often leads to changes in psychoacoustic metrics, such as an increase of the roughness. Such indicators could be used to detect vehicles suspected of tampering, but a larger dataset of noise recordings for inspected vehicles is needed to derive tampering detection algorithms which are reliable in real-life traffic conditions.

List of Abbreviations

CO_2	Carbon dioxide
CO	Carbon monoxide
EU	European Union
ECU	Engine control unit
HC	Hydrocarbons
HEU	Horizon Europe
IQR	Inter quartile range
LENS	L-vehicles Emissions and Noise mitigation Solutions
LVs	L-category Vehicles
CO	Carbon monoxide
HC	Hydrocarbons
NO	Nitrogen oxide
NO_2	Nitrogen dioxide
NO_x	Nitrogen oxides
PM	Particulate matter (or sometimes also particle mass)
PN	Particle number
BC	Black Carbon (soot) particles
RES	Remote emission sensing
PS	Point Sampling

This project has received funding from the European Union's Horizon Europe research and innovation programme under grant agreement No 101056777

List of Figures

This project has received funding from the European Union's Horizon Europe research and innovation programme under grant agreement No 101056777

This project has received funding from the European Union's Horizon Europe research and innovation programme under grant agreement No 101056777

List of Tables

This project has received funding from the European Union's Horizon Europe research and innovation programme under grant agreement No 101056777

1 Introduction

1.1 Background

The operation of L-category vehicles (LVs: mopeds, motorcycles, tricycles, and quadri-mobiles) contribute to numerous harmful effects on both air and noise pollution, due to – historically – more relaxed emission standards than other vehicle categories. Besides pollutant emissions, they are a known source of noise annoyance since their peak sound levels and general sound characteristics are distinct compared to those of other types of vehicles. Such negative effects of LVs operation are particularly manifested for tampered vehicles. According to the EU, tampering refers to "inactivation, adjustment or modification of the vehicle emissions control or propulsion system, including any software or other logical control elements of those systems, that has the effect, whether intended or not, of worsening the emissions performance of the vehicle" [1]. Such modifications may be the removal or replacement of the silencer to alter the sound behavior of the vehicle or the manipulation of the engine control unit (ECU) to alter its powertrain performance. However, these changes often take place without considering the possible negative consequences to emission and noise levels. Anti-tampering measures must be taken with a view to preventing such modifications and decreasing these detrimental effects [2].

This report is part of Work Package 5 and constitutes the deliverable from Work Tasks 5.3 (*Execution of in-field surveys*) and 5.4 (*Results of field surveys on LV tampering*) of the L-vehicles Emissions and Noise mitigation Solutions (LENS) project, funded by the European Union (EU)'s Horizon Europe (HE) research and innovation programme under grant agreement No 101056777. LENS is a three-year HE project with the main aim to assist enforcement authorities, cities, and regulators to decrease the contribution of LVs to both noise and air pollution. It develops and promotes interventions and best practices to address light vehicles' noise and pollutant emissions. It also makes suggestions for regulatory initiatives that could lead to the improvement of the emission performance of future vehicles, including the control of emissions under real-life driving conditions and the enforcement of anti-tampering measures.

1.2 Objectives

The objectives of the work carried out to produce this report were (from the final LENS application and the grant agreement):

- Deploy roadside detection techniques in field surveys to screen for tampered LVs;
- Link results from screening surveys directly to roadside inspections of suspected tampered LVs;
- Synthesize the survey results to propose mitigation actions to prevent tampering of LVs;
- Deploy the system in 3 field surveys (to collect data on at least 3,000 individual LVs);
- Pull-over at least 300 LVs by enforcement agencies staff for visual inspection and simplified emission testing to the extent possible;

This project has received funding from the European Union's Horizon Europe research and innovation programme under grant agreement No 101056777

- Collect data on vehicle specifications from national vehicle registration records based on plate readings;
- Firewall, anonymize and process data;
- Statistically process data from in-field surveys and deploy methods to identify tampered vehicles;
- Determine Type I (false positive) and Type II (false negative) of pulled-over LVs;
- Compile and rank the various kinds of tampering of LVs occurring in Europe;
- Estimate the share of tampered LVs and their contribution to the overall noise and pollutant emissions;
- Propose mitigation actions to prevent tampering of LVs.

1.3 Structure

Following this introduction, chapter 2 describes the instrumentation for roadside pollutant emission measurements, including the Opus RSE remote emission sensing instrument for measuring gaseous pollutants and particle mass; in the latter case based on UV opacity; the TU Graz and IVL point sampling remote emission sensing instruments, and finally the KU Leuven instrumentation for roadside noise measurements. In chapter 2 also the measurement sites used are described, along with the typical set-up of instruments at these sites. Finally, the procedure of the roadside inspections of LVs pulled over is described.

Chapter 3 presents the results for all the roadside pollutant emission measurements by instrument type, followed by the results for the roadside noise measurements and the results from the roadside inspections. The presentation of the results from the pollutant emission measurements focusses on average emissions of the different pollutants by Euro class and by engine capacity (engine displacement volume), while the presentation of the results from the noise measurements focusses on sound pressure levels and the perception of LV sound in psychoacoustic metrics. Chapter 3 ends with a tampering analysis, based on the results from the roadside inspections along with the on-road emissions and noise measured from the roadside and sound signal features for detecting tampering.

The final chapter 4 holds the conclusions of this work.

This project has received funding from the European Union's Horizon Europe research and innovation programme under grant agreement No 101056777

2 Methodology

With regard to methodology, the in-field tampering surveys consisted of a complex mixture of instrumentation (for vehicle recognition by means of automatic license plate readers, sensors for measuring vehicle speed & acceleration and pollutant emission and noise measurement instruments both along the roadside and in the roadside inspections for measurements on LVs pulled over), instrumental set-ups at a number of pre-selected sites and finally the logistics, staff involvement and necessary local permits associated with performing all the measurements:

- Instruments for carrying out measurements from the roadside were well-established (commercial) types for gaseous pollutant emissions by means of optical spectroscopy, used in recent EU research & innovation projects such as CARES [3] and NEMO [4] to measure emissions from cars and heavier vehicles, whereas instruments for measuring particulate matter and noise were research grade, developed and/or further refined, tested and validated in LENS [5].
- For any roadside pollutant emission and noise measurement campaign in a real-world setting, site selection is crucial, thus a large amount of efforts and time was spent in LENS to find good or at least acceptable sites, including to find cities which were able to provide support from local police to carry out roadside inspections. The latter failed after several attempts to carry out one of the surveys in an Italian city, which in the end lead to carrying out the final campaign in Barcelona. Other important criteria for selecting sites were 1) a substantial or at least fair share of L-vehicles, 2) neither too dense nor too light traffic, 3) both speed and acceleration of vehicles should be moderate, therefore sites with a moderate road grade are preferred, and 4) there needs to be an area – not too far downstream or upstream from where the roadside measurements are carried out – where LVs safely can be pulled over to the roadside for inspection. Additionally, sites with few nearby buildings were preferred to limit the influence of reflections on the acoustic measurements. To meet all these criteria is a big challenge and often there needs to be some compromise, which was also the case for the LENS surveys, as can be seen in the results chapter.

2.1 Instrumentation for roadside pollutant emission measurements

2.1.1 Opus RSE remote sensing instrument

Optical remote sensing instruments to measure primarily gaseous pollutant emissions from individual passing L-category vehicles (LVs) were provided by the company Opus Remote Sensing Europe (Opus RSE - https://opusrse.com/). In all three measurement campaigns, a dual remote sensing system (RSD 6000) was deployed in order to measure emissions at two different heights – cf. Figure 1. This was because the position – contrary to passenger cars – in terms of the height over the road surface of the tailpipe of LVs may vary substantially. Two instruments operating in parallel to measure emissions at two different heights might help improve capture rates.

This project has received funding from the European Union's Horizon Europe research and innovation programme under grant agreement No 101056777

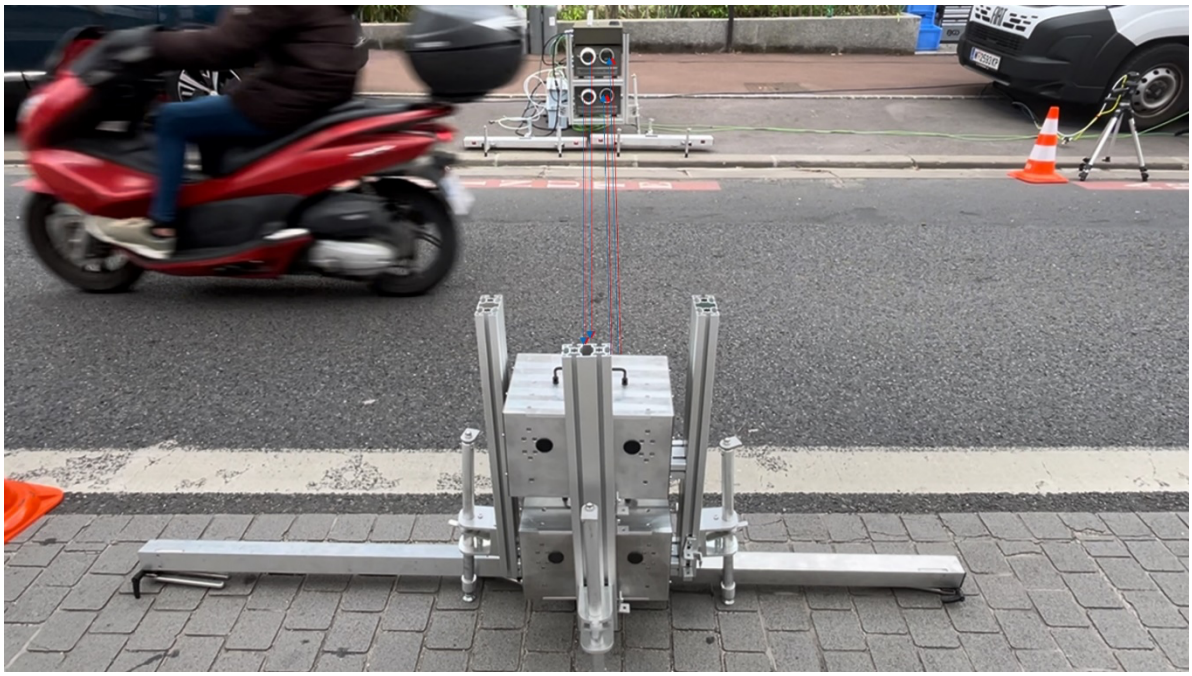

Figure 1. Dual Opus RSE remote sensing instrument system (RSD 6000) deployed for measuring LV emissions at two different heights. The ultraviolet and infrared light beams are indicated by the blue and red arrows.

The Opus RSE remote sensing instrument RSD 6000 measures the molar ratios of a variety of air pollutants – CO, HC[1], NO, NO_2 (i.e., NO_X), NH_3 and total particulate matter PM (as opacity) – over CO_2 in the undiluted exhaust by means of ultraviolet and infrared light traversing the exhaust plume. The pollutant-to-CO_2 ratio in the undiluted exhaust plume is derived from pollutant concentration measurements along the light beams at 100 Hz during half a second, immediately after that the beams have been unblocked by the vehicle after its passage. The measured ratios can be converted to emission factors expressed in gram pollutant per kg fuel burnt and – by applying a fuel consumption factor – emissions in g/km can also be estimated. More information on the measurement and analytical principle can be found on the Opus website (https://opusrse.com/technology/the-remote-sensing-device/) and in the literature [6], [7].

Measured vehicles can be identified from the license plate number sampled by an automatic license plate reader (ALPR). The RSD 6000 unit also measures the speed and acceleration of the vehicles during their passage, i.e., the driving conditions for each vehicle upon passage are known.

Opus RSE remote sensing instruments stem from the original remote sensing instrument developed by researchers at the University of Denver already in the late 1980's [8]. Over the last +35 years the technology has been used to measure on-road emissions from >>100 million vehicles across the globe (https://opusrse.com/about/), mostly passenger cars, but also light commercial vehicles, heavy trucks and buses, however, compared to a very limited number of L-category vehicles [9].

[1] HC is measured using NDIR. It is not equivalent to total HC measurement using a flame ionization detector (FID), which is used in e.g., type approval testing. Rather, it is tuned to general absorption bands, with different sensitivity to different hydrocarbons. NDIR used in PTI have higher sensitivity to alkanes and lower to aromatics. The NDIR/FID ratio depends on fuel and catalyst performance. For NDIR used in miniature PEMS that has been developed by LENS partner this ratio has been determined [10].

This project has received funding from the European Union's Horizon Europe research and innovation programme under grant agreement No 101056777

2.1.2 TU Graz point sampling instruments

The point sampling approach is based on the previous work in the H2020 project CARES and is described in detail in D5.2. The general setup used for the measurement campaigns is shown in Figure 2. From the roadside sampling position, the gas sample is extracted and delivered to the analysers in the point sampling shelter. Furthermore, the setup consists of three light barriers across the road to detect passing vehicles, assign timestamps and speed and acceleration measurement, a radar sensor to differentiate between the vehicle types and for redundant vehicle detection, speed and acceleration measurement and an automated number plate recognition system [11]. The sample is analysed for gaseous and particulate pollutants using a custom-made photoacoustic instrument for black carbon particulate matter measurement, a commercial PN-counter based on diffusion charging, a TSI 3090 Engine Exhaust Particle Sizer (EEPS) – operated by IVL, see section 2.1.3 – and an Airyx iCAD gas analyser for CO_2 and NOx concentration measurement. For the Paris campaign, we added a 3000HM THC ANALYSER to the fixed set of instruments.

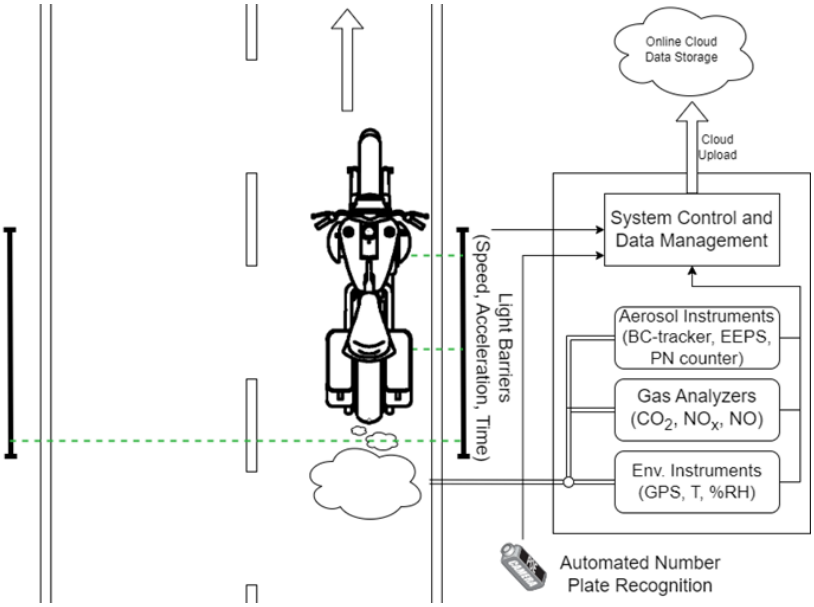

Figure 2. Scheme of the roadside point sampling setup for the in-field campaigns.

Additionally, we used an experimental setup for visualization of the exhaust plumes using Schlieren imaging, details on the setup have been published in [12]. A journal paper describing the data evaluation method was submitted to SAE international (Imtiaz H.H. et al., 2025, *Reconstruction of Density Fields of Category L-Vehicles Exhaust Plumes using Windowed Fourier Transform based Geometrical Phase Analysis and Optical Flow and Comparison with State-of-the-art*, submitted to SAE International Journal of Engines)

2.1.3 IVL EEPS point sampling instrument

In the measurement campaign in Barcelona an additional instrument, an Engine Exhaust Particle Sizer (EEPS, TSI Inc., model 3090), was used for measuring particle number size distributions with high time resolution (10 Hz). The EEPS measures particles in the size range of 5.6 to 560 nm. This instrument has been used previously for determining size-resolved EF from individual vehicles [13, 14,

This project has received funding from the European Union's Horizon Europe research and innovation programme under grant agreement No 101056777

15, 16, 17, 18]. In addition to presenting total particle numbers, also PN >23 nm (PN_{23}) is presented, calculated from the particle number size distribution of the EEPS. Particle mass was calculated assuming sphericity and unit density as in previous studies [13, 14, 15, 19]. When using the EEPS, an additional CO_2 instrument was used (non-dispersive infrared gas analyser, Li-Cor 840A).

2.1.3.1 Data evaluation

The EEPS data was first aligned with the CO_2 data and then aligned with respect to the Opus RSD 6000 passage data and the light barrier data (LB). The delay time between a vehicle passage and detection by the instruments was done by shifting the data to match a known LV passage (Figure 3).

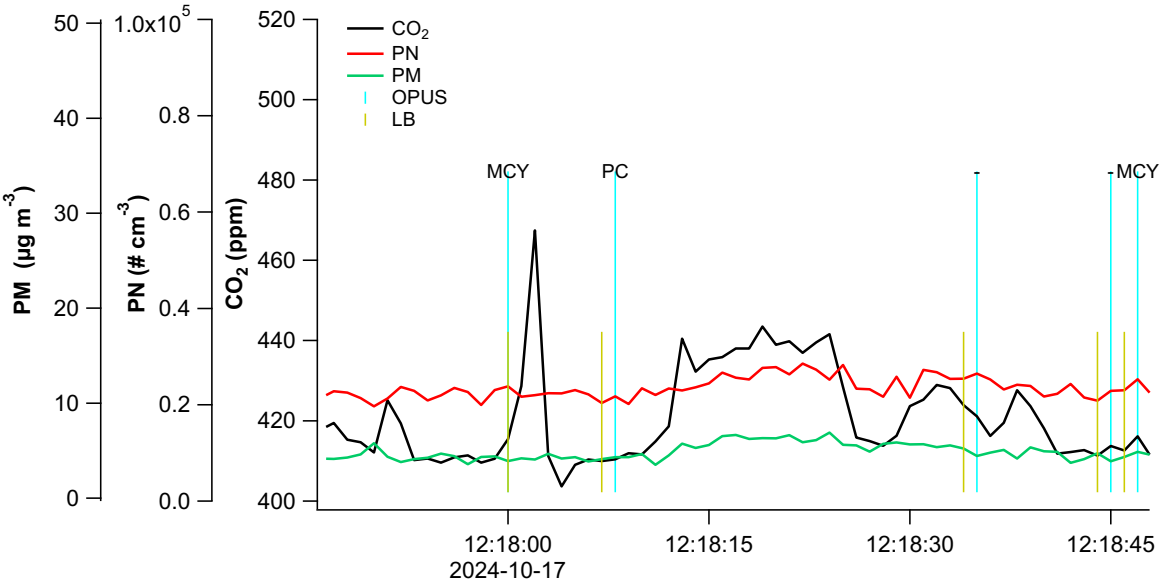

Figure 3. Example of time series observed for CO_2 (black), PN (red) and PM (green) where the emission data has been aligned to the Opus RSD 6000 passage data (light blue vertical lines) and the TUG light barrier data (yellow vertical lines) and to the known L-vehicle (MCY - motorcycle) passage at 12:18:00. PC stands for passenger car.

The data was manually evaluated, where LV passages with a visible peak in CO_2, and or PN, PM were chosen for further analysis. Only passages with a time difference of ≥ 5 s with respect to a prior or subsequent passage, and with a ΔCO_2 > 11 ppm (i.e., the peak maximum CO_2 concentration subtracting the background concentration) were included (Figure 4).

This project has received funding from the European Union's Horizon Europe research and innovation programme under grant agreement No 101056777

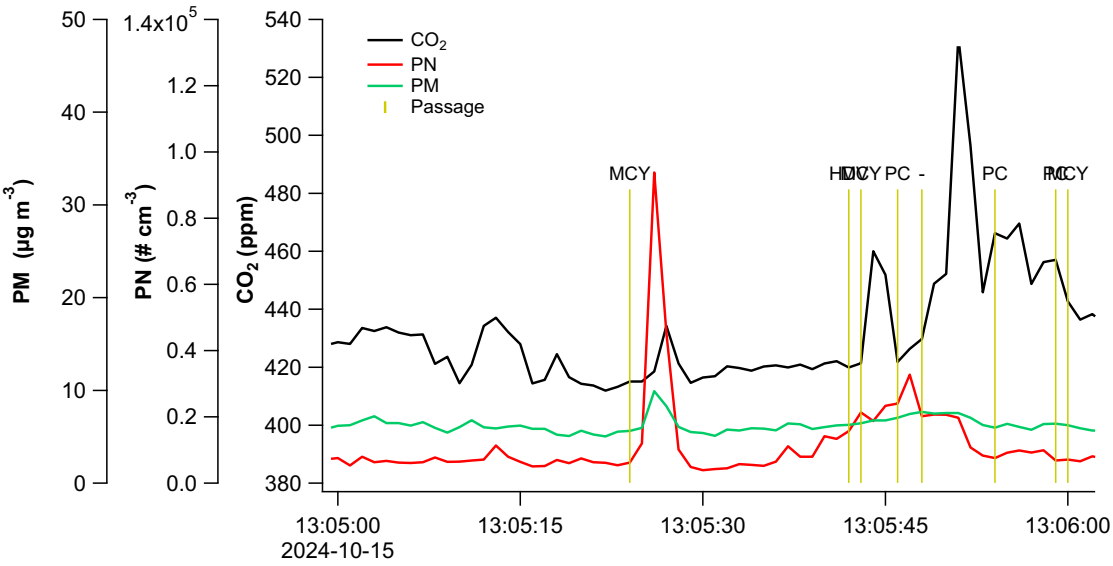

Figure 4. Example of an identified LV passage (MCY) (Euro 3) with significant PN and PM emissions.

However, for five passages, the ΔCO_2 was < 11 ppm, but high emissions of PN and or PM were observed, and they were included in the data analysis. Example of such a passage is shown in Figure 5.

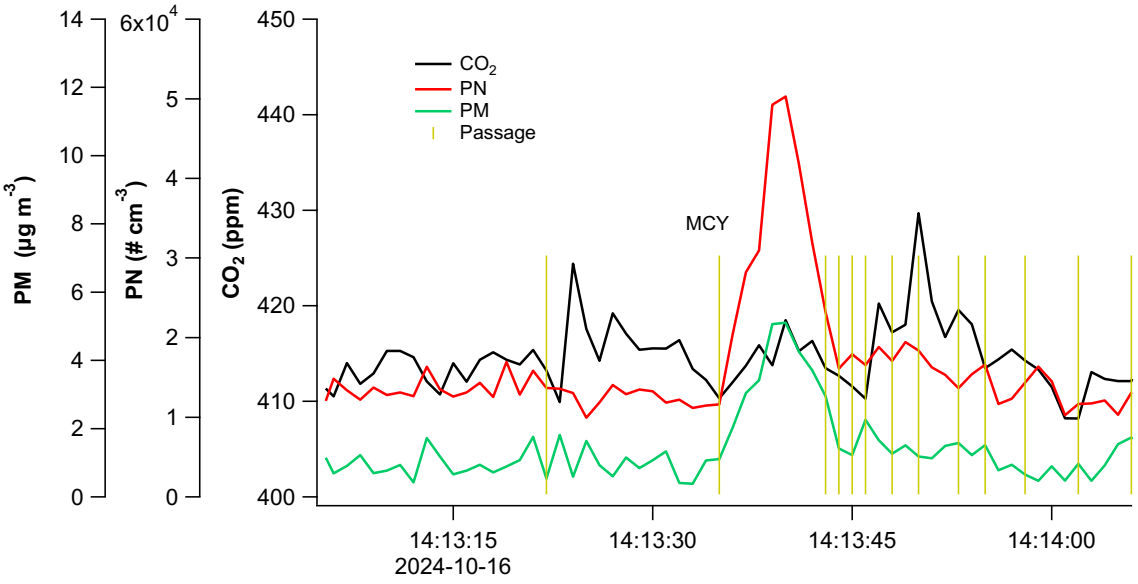

Figure 5. Example of an identified LV passage (MCY) (Euro 2) with significant PN and PM emissions and low CO_2.

The detection limit (DL) of PN was calculated as the standard deviation of the integrated PN during times when there were no vehicle passages. An average of multiple occasions with no traffic was calculated for each day. DL of PM and PN_{23} were calculated in the same way.

This project has received funding from the European Union's Horizon Europe research and innovation programme under grant agreement No 101056777

2.1.3.2 Emission factors

Emission factors (EF) in per kg of fuel burnt were calculated by relating the integrated and background (bkg) corrected particle concentration (*i*) $\int_0^t (i(t) - \overline{i_{bkg}})dt$ to the integrated and bkg corrected CO_2 concentration[2] $\int_0^t (CO_2(t) - \overline{CO_{2_{bkg}}})dt$, and assuming complete combustion and a fuel carbon content of 0.865 (Hallquist et al., 2013) (Equation 1).

$$EF_i = \frac{\int_0^t (i(t) - \overline{i_{bkg}})dt}{\int_0^t (CO_2(t) - \overline{CO_{2_{bkg}}})dt} \times EF_{CO_2} \qquad \text{(Eq. 1)}$$

The background was calculated as 3 s averages if the previous passage was ≥ 10 s. For passages where the distance was <10 s, values at peak start time was used.

If the integrated particle concentration was lower than the calculated DL, the value of half the DL was used in the calculations [20]. The integrated PN was > DL for 100% (Euro 1), 71% (Euro 2), 78% (Euro 3), 76% (Euro 4) and 43% (Euro 5) of the LV plumes. For PM the corresponding values were 100%, 71%, 59%, 35% and 17%. Hence, important to note that for Euro 5, the median PM and PN values are below the detection limit. In Figure 6 a process flow diagram of the data evaluation and EF calculation is shown.

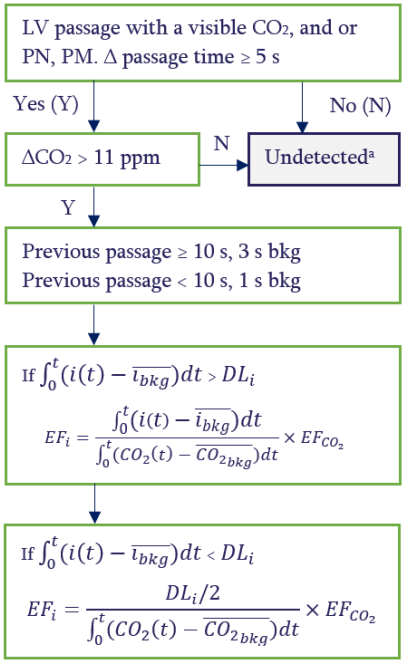

Figure 6. Process flow diagram of the data evaluation. [a]Five passages with ΔCO₂ < 11 ppm with high PN or PM were included.

[2] Using only CO_2 as the denominator for the calculation of emissions in g/kg fuel is an approximation, since it presupposes that measured HC and CO concentrations are negligible compared to measured CO_2 concentrations. However, for L-category vehicles in particular they may not always be negligible, so this approach should be considered as a source of uncertainty.

This project has received funding from the European Union's Horizon Europe research and innovation programme under grant agreement No 101056777

2.2 Instrumentation for roadside noise measurements

In all measurement campaigns, the roadside noise measurements were performed with an optimized linear array with 5 microphones, as shown in Figure 7. In Leuven and Paris, the array was mounted at a height of 1.2 m. In Barcelona, a slightly more compact setup with a height of 0.85 m was used. The data acquisition is performed with a Siemens Simcenter Scadas XS system, controlled via a laptop with Simcenter Testlab software. The system is programmed to continuously monitor the A-weighted sound pressure level (LAF) and automatically start and stop the recording of the microphone signals when thresholds are exceeded. More details on the measurement setup can be found in the LENS deliverable D5.2 (https://www.lens-horizoneurope.eu/).

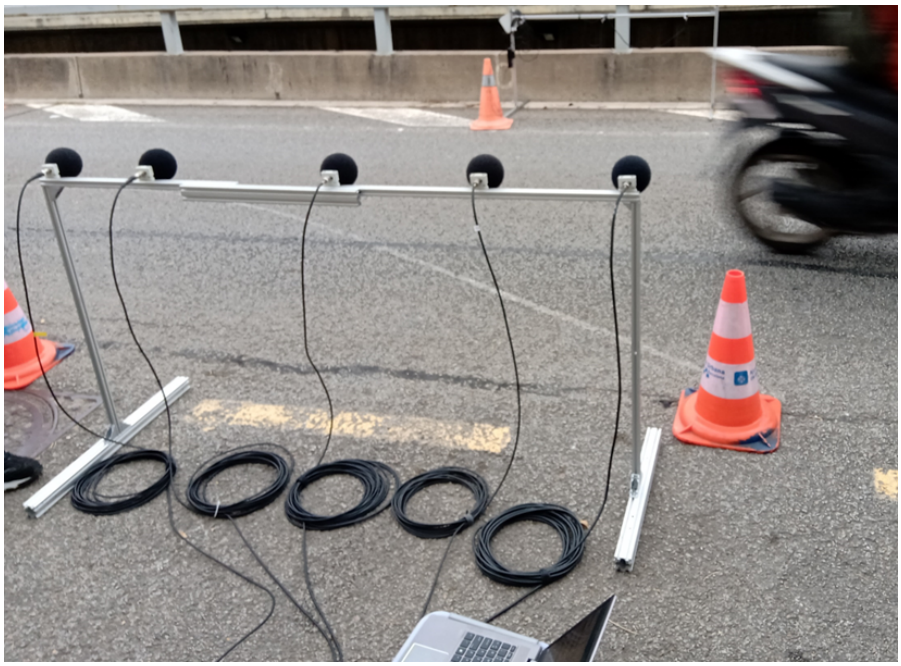

Figure 7. Picture of the microphone array used in the Barcelona campaign. A similar setup, mounted slightly higher, was used in the other campaign.

Because of the triggering based on instantaneous sound pressure level, not all recordings are useable for analysis:

- Also other events, such as other types of vehicles, background noise, people talking near the microphones, etc., could trigger a sound recording. All recordings not containing a clear L-vehicle sound were immediately discarded from the dataset.
- After each recording, the measurement system takes a fraction of a second to save the data and prepare for the next measurement. Trigger events occurring in this short time window lead to a number of missed L-vehicle passes and recordings starting too late. All recordings which were too short to recognize a clear L-vehicle signature, were discarded from the dataset.

The remaining recordings contain the sound signature of one or more L-category vehicles passing the measurement site.

This project has received funding from the European Union's Horizon Europe research and innovation programme under grant agreement No 101056777

During all campaigns, the thresholds to start and stop a measurement were set as low as possible and regularly adjusted throughout the day to minimize the number of missed L-vehicle passes. It is therefore not guaranteed that the sound pressure level drops below the threshold in between vehicles in a traffic flow. Shorter recordings containing only the sound of a single L-vehicle passing the measurement site were extracted from the raw recordings before further processing. These recordings need to be short enough to allow isolating a single vehicle sound signature in a traffic flow, but also long enough to still recognize the L-vehicle sound signature. A fixed window size of 3 s was selected as a compromise. The selection of the relevant window from the raw recordings was done largely automatically, centered around the maximum sound pressure level computed in 100 ms windows after band-pass filtering the signal to the 50 Hz – 500 Hz band. All 3 s recordings were checked and recordings polluted by talking in the background were removed from the database. If a cropped recording contained more than 1 LV signature, it was attempted to manually adjust the 3 s window to improve separation with preceding and trailing vehicles. Recordings for which this did not result in a clear recording with a single LV signature, were discarded from further analysis. Furthermore, additional 3 s segments containing the signature of less loud L-vehicles, ignored by the automatic extraction, were manually extracted from the dataset to maximize the available data.

The identification of the L-vehicles is done by synchronization with the Opus RSD 6000 measurements. A 2 s tolerance is used in the synchronization process to automatically detect, for each RSD 6000 measurement of an L-vehicle, all sound recordings which could correspond to it based on the timestamps. For various reasons, not all RSD 6000 measurements have a corresponding sound measurement and not all recordings of L-vehicle sound could be associated with confidence to an RSD 6000 measurement. In case of ambiguity (e.g., when vehicles are driving close together) or L-vehicles missed by the RSD 6000, the L-vehicle and its technical information is considered unknown. Only the signal of the first microphone of the array is used in the analyses, but the signals of all 5 microphones are available in the dataset for future research.

2.3 Measurement sites and instrument set-up

The tampering in-field surveys were conducted in three cities/regions in three EU countries in 2024:

- Leuven, Belgium (13-16 May); two measurement sites. Leuven was selected to host the first survey already when the LENS grant application was written and for several reasons:
    - LENS partner KU Leuven, heavily involved in the LV noise tampering detection work in LENS, is located in Leuven and could provide local support in the survey in many ways.
    - The city of Leuven had expressed interest in the surveys at an early stage and support from the local city police in the roadside inspections could be provided.
    - During terms, Leuven holds about 50,000 university students, which results in a substantial traffic of mainly small L-vehicles in the city for food deliveries.
    - The main site for the survey, a free field site along a city trunk road with speed limit 50 km/h and a moderate inclination, which made it a good site for the roadside measurements. The other site was located in the city center and was selected mainly for the high load of small LVs delivering food to students residing just outside the city center.

This project has received funding from the European Union's Horizon Europe research and innovation programme under grant agreement No 101056777

- Rueil Malmaison and Dampierre-en-Yvelines in the Paris region, France (16-21 September); two measurement sites. The Paris region was selected since it's one of the most populated areas in Europe with extensive LV traffic and LENS partner IFPEN has its office in Rueil Malmaison close to the selected measurement site. The site in Dampierre-en-Yvelines was along a scenic route with a lot of larger LVs travelling there in weekends. It's a famous site, lots of complaints from local residents and often checks by law enforcement. Both sites had a moderate inclination and typical urban driving conditions, with occasionally quite heavy traffic for the Rueil Malmaison site.
- Barcelona, Spain (14-17 October); one measurement site. Barcelona was not an option for the tampering in-field surveys until about 18 months into the project (see the introduction of this chapter). Thanks to Spanish LENS partner IDIADA associated with the PTI operator Applus+, LENS subcontractor Opus RSE located in Madrid and the interest and support from Barcelona city, this site met most of the criteria applicable to the tampering in-field survey.

Images and coordinates of all the measurement sites are given in the Appendix and the speed and acceleration profiles for each site are presented in Figure 15.

The instrumental set-up was principally the same for all measurement sites, with only the order of the instruments varying from site to site. In most cases, vehicles first passed the microphone array, then the point sampling instruments, and finally the Opus RSE RSD 6000 remote sensing system – see Figure 8. Only on the second measurement site in Leuven, this order was reversed.

Figure 8. Typical instrumental set up in the LENS tampering in-field survey: 1. Opus RSD 6000 dual remote sensing system: 1a. source/detector module, 1b. lateral reflective mirror, 1c. speed and acceleration measurement bars, 1d. automatic license plate readers; 2. TU Graz point sampling system: 2a. van hosting measurement instruments for PN, BC, NO_x, and CO_2, 2b. air sampling inlet to instruments in the van, 2c. stands for triggering of passing vehicles and Schlieren imaging; 3. KUL array of noise measurement microphones.

This project has received funding from the European Union's Horizon Europe research and innovation programme under grant agreement No 101056777

2.4 Roadside inspections

Roadside inspections in conjunction to the roadside noise and pollutant emission measurements were only carried out in Leuven and Barcelona. The intended roadside inspections for the Paris region campaign in mid-September, could regretfully not be carried out due to the lack of police resources following the Paris 2024 Summer Olympic and Paralympic games in Paris, arranged in August and September, respectively.

All the data collected in the roadside inspections can be found in the Appendix.

2.4.1 Leuven roadside inspections

In the Leuven campaign, roadside inspections were carried at both sites and on all the four days that the roadside noise and pollutant emission measurements were carried out, i.e., 13-16 May (see Figure 9). L-category vehicles passing the roadside measurement instruments were systematically pulled over to the roadside by the Leuven city police some 100 meters downstream of the measurement site to be subject to an inspection. The police checked that the vehicle documents were in order and an L-category vehicle expert from TU Graz carried out the following actions:

- a low idle emission test of CO and HC;
- on the last day of the measurement campaign, a stationary noise test;
- documented the vehicles' technical (make, model, engine capacity and power, 2- or 4-stroke, model year, Euro class and odometer reading);
- made and notified an assessment of whether the vehicle should be considered tampered - or modified in some other notable way - or not, through a visual inspection;
- it should be noted that a roller bench test was not used, therefore it was not possible to assess whether engine speed restrictors had been removed or tampered with or not.

In all, 165 L-category vehicles were pulled over and inspected in the Leuven campaign.

Figure 9. A roadside inspection taking place in the Leuven measurement campaign.

This project has received funding from the European Union's Horizon Europe research and innovation programme under grant agreement No 101056777

2.4.2 Barcelona roadside inspections

In the Barcelona campaign, due to limitations of capacity of the Barcelona city police, roadside inspections could only be carried out on two of the four days that the roadside noise and pollutant emission measurements were carried out (15 and 17 October – see Figure 10). Here, L-category vehicles were pulled over by the Barcelona city police to the roadside some 100 m upstream of the roadside measurement instruments.

PTI experts from the Barcelona based global company Applus+ (https://www.applus.com/global/en/) carried out the inspections of the LVs pulled over. The testing and inspections followed basically the same procedure as for Leuven, apart from that in Barcelona all the LVs pulled over were subject to a stationary noise test.

Figure 10. A roadside inspection taking place in the Barcelona measurement campaign.

In all, 94 L-category vehicles were pulled over and inspected.

This project has received funding from the European Union's Horizon Europe research and innovation programme under grant agreement No 101056777

3 Results

3.1 Pollutant emissions

3.1.1 Opus RSD 6000 measurements

3.1.1.1 Measurements overview

The overall Opus RSD 6000 hit rate (i.e., cases where all pollutant emission data are valid) varies across measurement sites – see Table 1. Barcelona has the lowest hit rate at 7%, while Leuven reports the highest at approximately 46%. It should be noted that hit rates differ by pollutant; for instance, NOx has the lowest hit rate among them, ranging from 8% in Barcelona to 55% in Leuven – see Table 2.

The high Opus RSD 6000 hit rate in Leuven can be attributed to a number of factors:

- Not very dense traffic at the main measurement site;
- The main site had the highest road grade among all measurement sites;
- Due to the low number of LVs passing the site, the local city police were driving around in the nearby area and when noticed an LV the driver was asked to escort the police to the measurement site and pass by the instruments with a good acceleration.

In both the Paris (mainly the Rueil Malmaison site) and the Barcelona sites, it was frequently very dense traffic, which reduced the hit rates due to overlapping exhaust plumes and vehicle generated noise (from all kinds of vehicles, not only LVs) and vehicles passing so close to each other that the instrument could not separate these vehicles.

Table 1. Opus RSD 6000 measurements overall hit-rate.

Site	Total counts	Valid measurement counts[1]	Ratio of valid data[1]
Barcelona	3139	213	6.8%
Paris	1776	281	15.8%
Leuven	457	208	45.5%

[1]Values refer to when all measured pollutants, i.e., CO, HC, NO and NO_2, were valid.

Table 2. Opus RSD 6000 measurements hit rate per pollutant.

		CO	NO	NO_2	NO_X	HC	All valid
Paris	Valid count	356	357	303	300	355	281
	Hit rate	20.0%	20.1%	17.1%	16.9%	20.0%	15.8%
Leuven	Valid count	280	286	258	252	284	208
	Hit rate	61.3%	62.6%	56.5%	55.1%	62.1%	45.5%
Barcelona	Valid count	265	279	259	255	266	213
	Hit rate	8.4%	8.9%	8.3%	8.1%	8.5%	6.8%

In total, 2662 unique LVs were measured by the Opus RSD 6000 instrument during the three campaigns, of which 173 in Leuven, 767 in Paris and 1722 in Barcelona.

This project has received funding from the European Union's Horizon Europe research and innovation programme under grant agreement No 101056777

3.1.1.2 Fleet composition of LVs measured

For all valid vehicle emission records from the three field campaigns, 79% of them have a known Euro class. As seen by Figure 11, Euro 3, 4 and 5 have very equal shares when all measurement campaigns are considered, but there are substantial differences in the Euro class distribution between campaigns.

In terms of engine displacement, 98% of the vehicles have known engine displacement data. They are grouped into three size categories in Figure 12 (≤ 250 cc, 250-750 cc and ≥750 cc). In total the shares of these three size classes are very equal, but the shares differ substantially between the three city campaigns. For instance, Leuven had a very high share of small LVs, whereas Paris had high shares of the heavier categories.

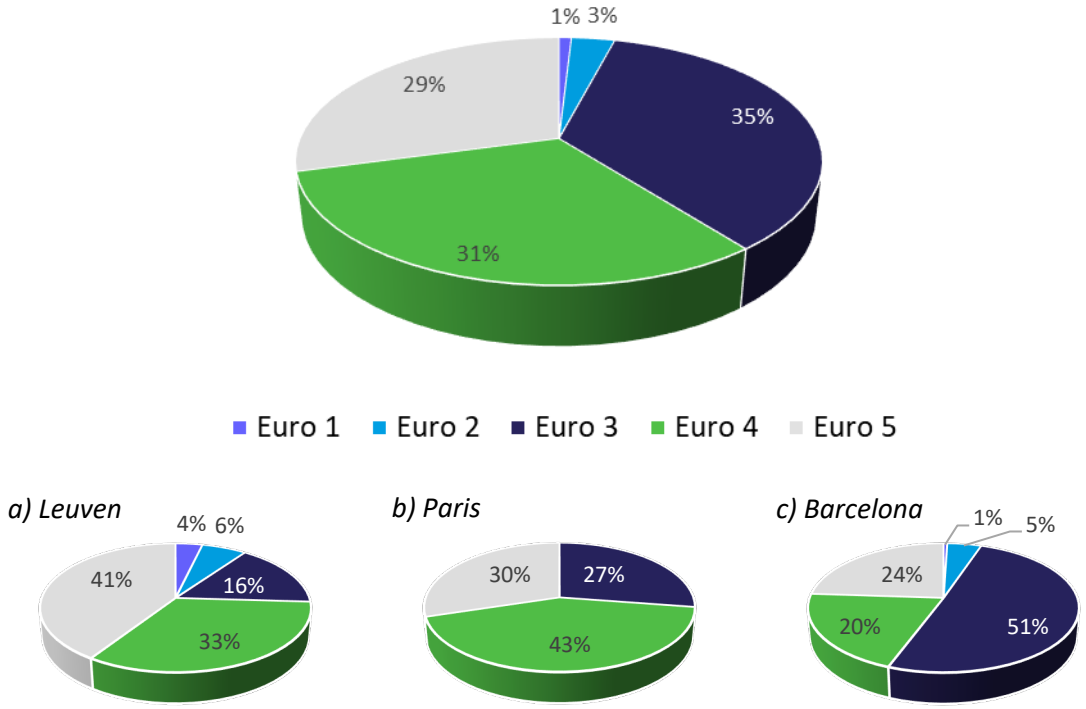

Figure 11. Distribution of LVs (with all valid emission data) by Euro class. Top chart all campaigns, a) Leuven, b) Paris, c) Barcelona.

This project has received funding from the European Union's Horizon Europe research and innovation programme under grant agreement No 101056777

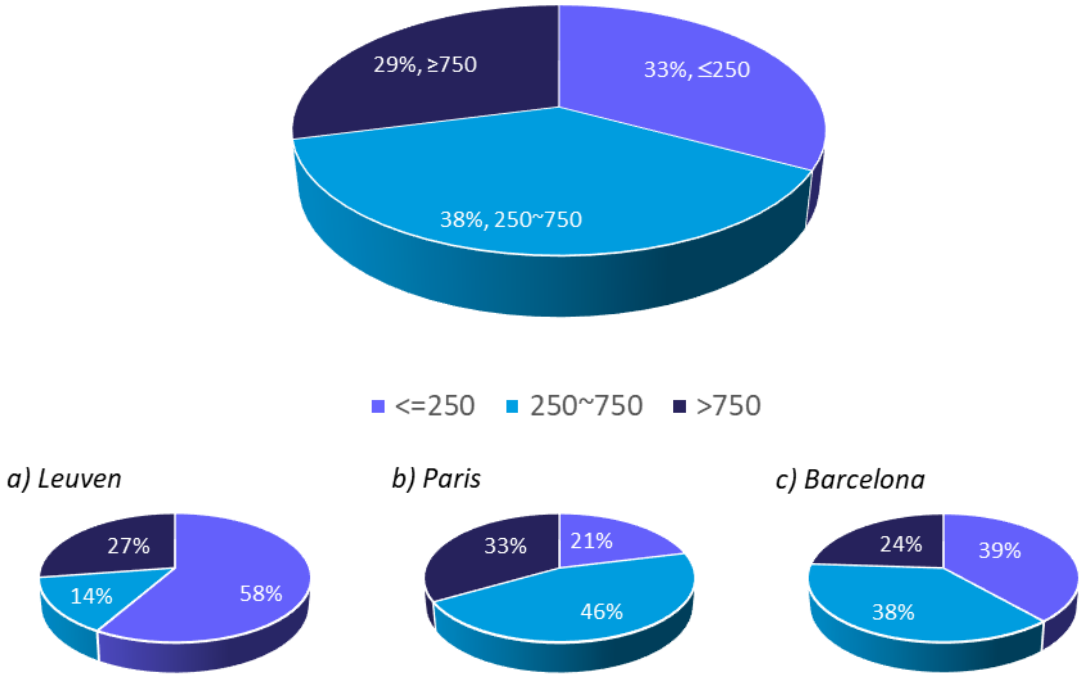

Figure 12. Distribution of LVs (with all valid emission data) by engine displacement groups. Top chart all campaigns, a) Leuven, b) Paris, c) Barcelona.

3.1.1.3 Average emissions by Euro class

The average emissions of CO, HC, NO_X and PM in g/kg fuel (Figure 13) show a decreasing trend as the Euro class increases from Euro 2 to Euro 5, although the trend is not as pronounced for NOx as for the other pollutants. The decline in average emissions becomes particularly evident with the introduction of Euro 5: CO, HC, and PM levels are down by 80-90% from Euro 2 to Euro 5, and NOx levels by 60% from Euro 3 to Euro 5.

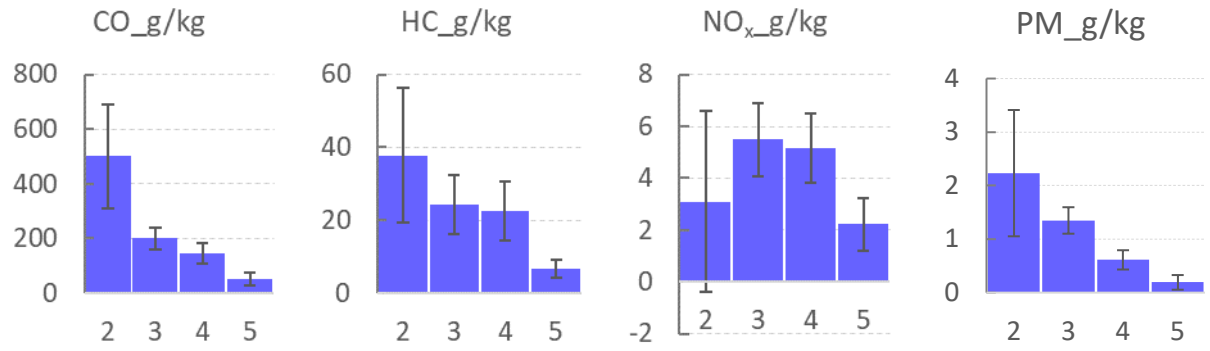

Figure 13. Average emissions of regulated pollutants (in g/kg fuel) by Euro class.

These emissions drops are similar to the reductions in the Euro limits from Euro 2 to Euro 5 and Euro 3 to Euro 5, respectively, presented in Table 3.

This project has received funding from the European Union's Horizon Europe research and innovation programme under grant agreement No 101056777

Table 3. Euro limit drop (in %) for LVs from Euro 2 to Euro 5 (CO and HC) and from Euro 3 to Euro 5 (NO_X), respectively.

	Euro limit drop	
	Euro 2 → 5	Euro 3 → 5
CO	-91%	
HC	-93%	
NO_X		-60%

3.1.1.4 Average emissions by engine displacement

Figure 14 shows the average LV emissions in g/kg fuel by engine size (engine displacement). It is clear that vehicles in the largest size class (engine displacement >750 cc) exhibited substantially lower emissions of all pollutants compared to the other two size classes. The highest average emissions for all pollutants is observed for the LVs with mid-size engines

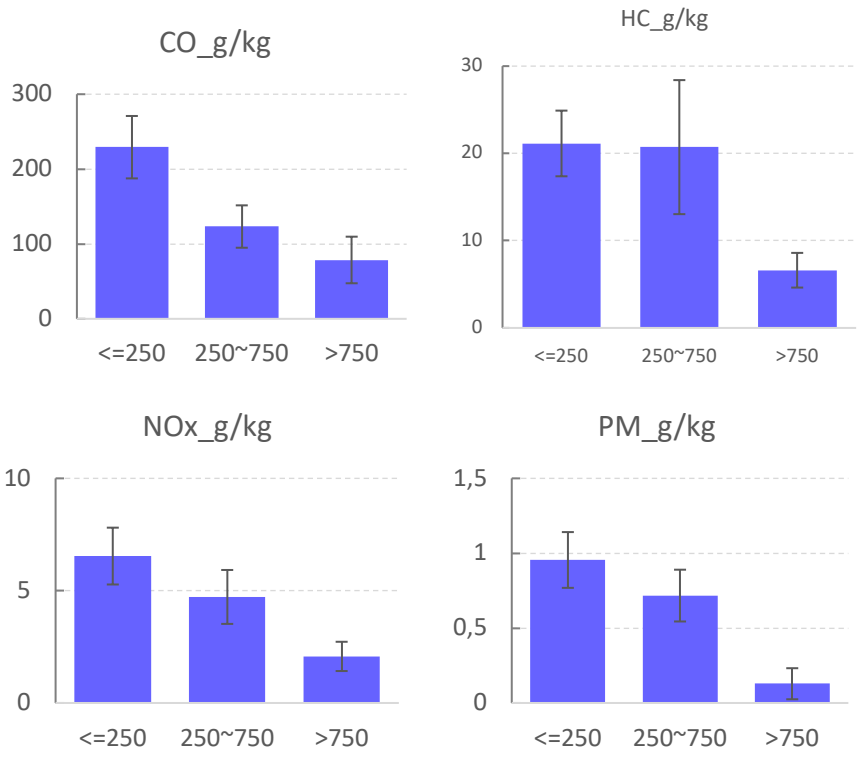

Figure 14. Average emissions (in g/kg fuel) of regulated pollutants by engine displacement (cm^3) split into three groups: ≤250 cm^3, 250~750 cm^3 and >750 cm^3 for all measured LVs (all Euro classes).

This project has received funding from the European Union's Horizon Europe research and innovation programme under grant agreement No 101056777

In Figure 15, the statistics for speed and acceleration are given for the L-vehicles – split into the three engine displacement categories – measured in the three campaigns.

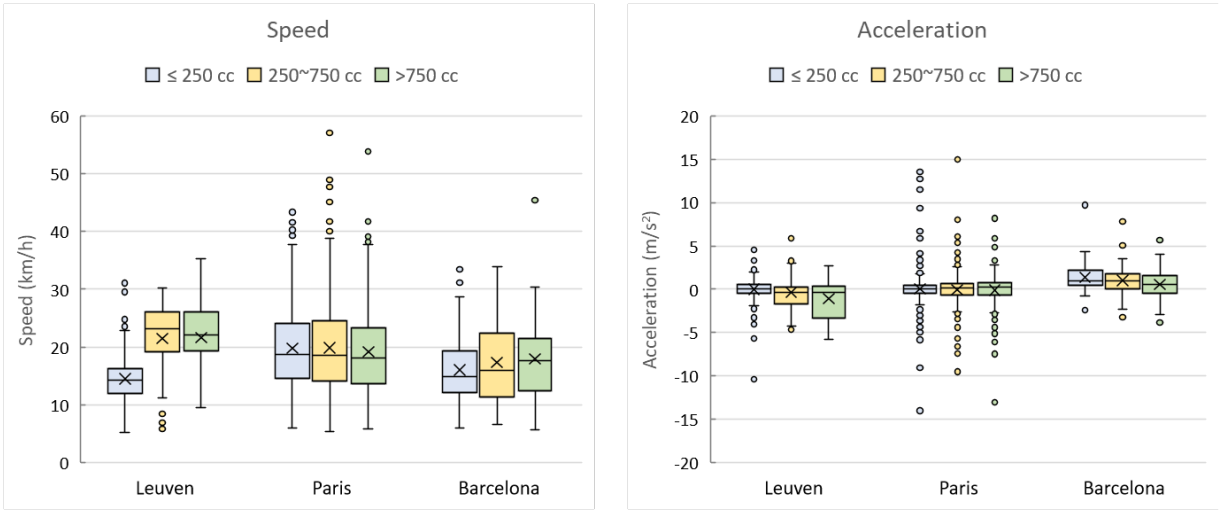

Figure 15. Speed and acceleration data by engine size for the L-category vehicles measured in the three campaigns.

As can be seen from Figure 15, measured L-vehicle speed and acceleration were mostly in the range 15-25 km/h and 0-2 m/s^2, respectively.

3.1.1.5 Emissions as a function of driving conditions (VSP)

An attempt was also made to study the measured average emissions as a function of driving conditions – speed, acceleration and vehicle specific power (VSP). Regretfully, by breaking down the measured average emissions into speed, acceleration and VSP bins and simultaneously also into Euro class or engine size, makes the statistics very poor and no clear trends could be seen and any conclusions could not be drawn. Much larger sample numbers would be required for this.

This project has received funding from the European Union's Horizon Europe research and innovation programme under grant agreement No 101056777

3.1.1.6 Emission distributions by Euro class

Figure 16 shows the emission distributions for CO, HC, NO_X and PM by Euro class as box plots. It may be worth notifying that for HC, Euro 3 and Euro 4 vehicles exhibit a much wider range of emissions values compared to Euro 5 vehicles.

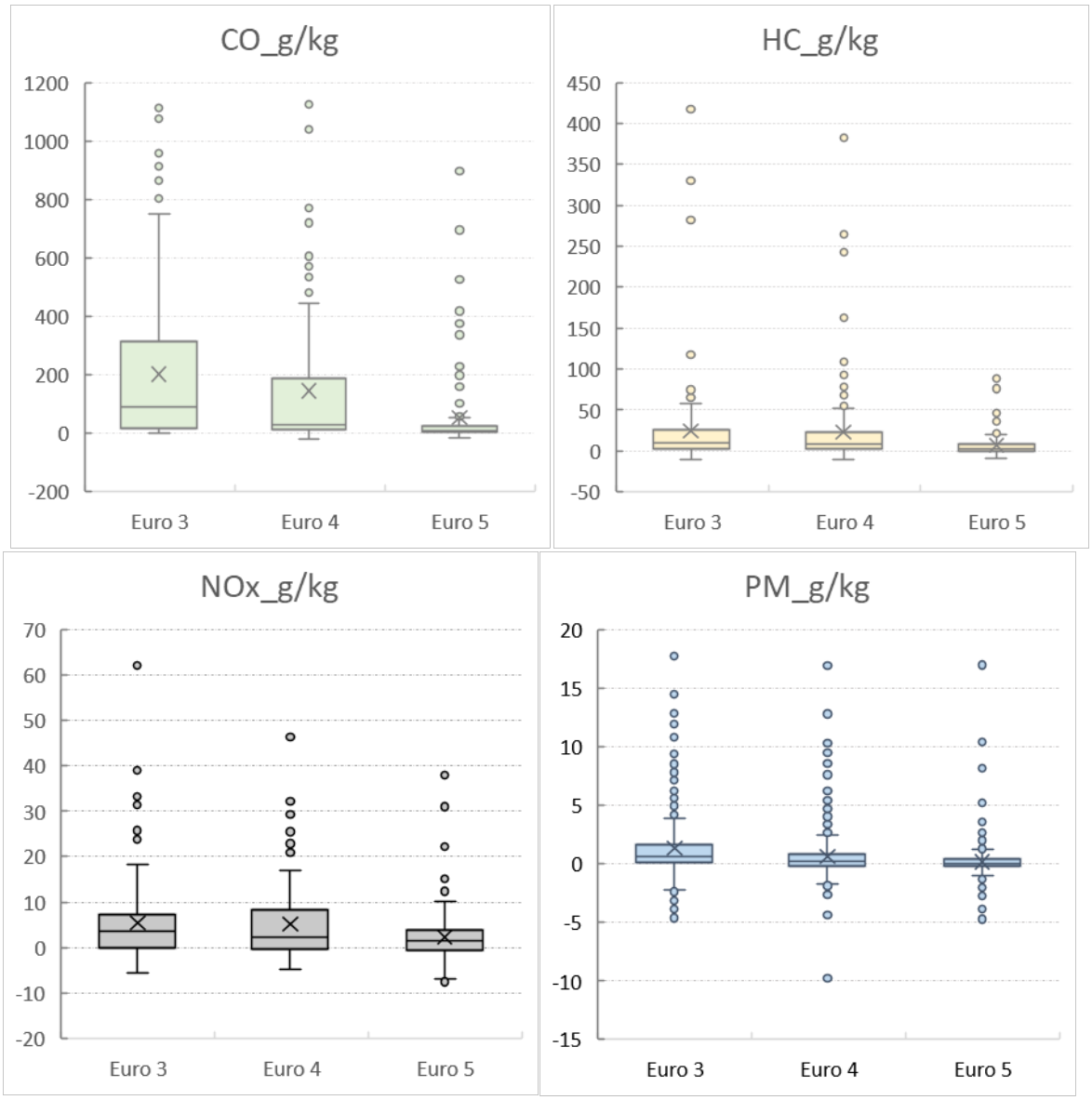

Figure 16. Box plot of regulated emissions in g/kg fuel. The box represents the middle 50% of the values (from the 25th to the 75th percentile), the line inside the box is the median, crosses are averages and circles are outliers.

This project has received funding from the European Union's Horizon Europe research and innovation programme under grant agreement No 101056777

3.1.2 TU Graz measurements

The evaluation of the PS results turned out to be very challenging for LVs. The detection of tampered category-L vehicles in traffic is not reliably possible by this technique. The results from Schlieren imaging were satisfactory, allowing a visualization of the exhaust spread. This technique does not allow the detection of tampered vehicles and was not expected to.

3.1.2.1 Pollutant emissions

The point sampling approach was found to be very challenging for LVs. The main reason for this is probably in the low exhaust mass flow of the comparably small combustion engines. Although the pollutant concentration in the exhaust can be high, the amount of substance emitted is still low for single vehicles for the given amount of exhaust. With the sampling position roadside, at the edge of the lane with an approximate broadness of 2.75 m, the pollutant concentration does not exceed background concentration for most cases. Additionally, aggravating circumstances occur regularly, like several LVs driving close to each other or increased background due a pass of a high emitting car or heavy-duty vehicle. The capture rate for the PS technique was found to be 2 to 5 times lower compared to open-path RES systems (e.g. the Opus RSD 6000 instrument) for passenger cars. But because of the comparably high accuracy, especially for particle measurements, it emerged as a feasible technique for high-emitter detection [21]. However, for LVs it could not be proven that high emitters can be detected reliably.

Table 4. Evaluation of the Leuven campaign

Total Valid PS Measurements	11
BC Measurement Valid	5
PN Measurement Valid	8
Both Valid	2

Evaluation of the measurement campaign in Leuven gave only 11 valid PS measurements (Table 4), as evaluation of the measurement is only possible if both the measurement of the pollutant and CO_2 are successful. A CO_2 level was considered valid if a value of 3σ above background was detected, which was the case for 10.5 % of passes. The Opus RSD 6000 counted 457 vehicles and achieved 280 valid measurements, which corresponds to a capture rate of 2.4 % for the PS in Leuven, which is 3.9 % of the valid measurements of the RSD 6000.

The difficulty described can be seen in Figure 17, where exemplary data from the Leuven campaign is plotted. The left column shows an ideal valid event for a passing LV, with signal levels clearly above noise, but actually very low. In the right column, an exemplary event is shown to illustrate how most detected passes with a valid CO_2 signal look like.

This project has received funding from the European Union's Horizon Europe research and innovation programme under grant agreement No 101056777

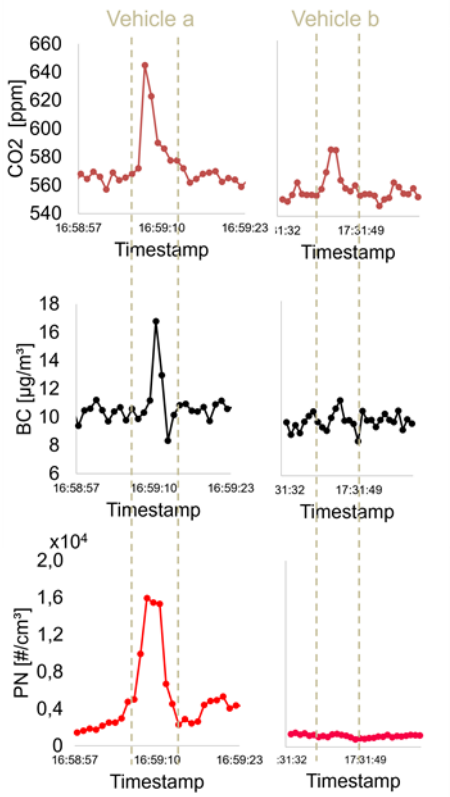

Figure 17: Exemplary raw data from the Leuven campaign. The dashed vertical lines indicate a vehicle pass.

The data analysis was done manually, as the automated approach described in D5.2 does not reliably evaluate events at such low signal levels. Originally, it was developed in the CARES project [22], where it was used to evaluate the large amounts of PS data. An adaptation to the LENS PS data failed, as the vehicle passes of LVs do not cause distinct peaks regularly, as it is the case for passenger cars.

The light barrier operated fully satisfactory, while the AI-based evaluation algorithm of the ANPR system was not trained sufficiently during the Leuven campaign and detected fully automated 152 numberplates of LVs. However, not evaluated, but triggered images from the Leuven campaign have been used as training data and improved the operation of the ANPR system substantially for the other campaigns. Details have been published in a journal paper by Imtiaz et al. [11].

Similar data was obtained from the Paris and Barcelona campaigns, whereas the number of detected vehicle passes was substantially higher compared to Leuven. While a manual evaluation of all events was done for the Leuven data, this approach was assessed as unreasonable for the Paris and Barcelona data. The automated data evaluation extracts from the data successfully vehicle passes of passenger cars and HDV, while LVs did not cause any detectable event. It must be stated that this is not due to an inadequately designed algorithm or to the sensitivity of the instruments used. The measurement task in relation with PS relates to the measurement of ambient diluted exhaust, at least one meter away from the source, while several emitters might pass with several seconds of separation. The area of exhaust spread is exposed to weather, wind and is generally within road traffic. The approach is very challenging with the used experimental setup with one roadside sampling position. There is room for improvement by, e.g., using several sampling positions, the choice of closed

This project has received funding from the European Union's Horizon Europe research and innovation programme under grant agreement No 101056777

measurement locations as tunnels, or, ideally, specially designed street sections which are shielded from weather and support a defined flow of the spreading exhaust by, e.g., a ventilation system.

3.1.2.2 Schlieren imaging

Results are in preparation for publication. As this report is public, we do not include results which are not published yet. Everything presented here was prepared dedicated to this report. Currently, a manuscript is under review at SAE Journal of Engines (Imtiaz H.H. et al., 2025, *Reconstruction of Density Fields of Category L-Vehicles Exhaust Plumes using Windowed Fourier Transform based Geometrical Phase Analysis and Optical Flow and Comparison with State-of-the-art*, submitted to SAE International Journal of Engines) and a manuscript by Imtiaz et al. is in preparation for submission.

During the emission measurement campaign in Leuven, Belgium, various categories of L-vehicles were tested. The vehicles moved from left to right between the Gas Schlieren Imaging Camera and a pattern board, as illustrated in the setup. The distance between the camera and the pattern board was approximately 3 to 5 meters.

The Schlieren images of the exhaust plumes were captured for qualitative analysis, while the 2-D line-of-sight integrated density fields were reconstructed for quantitative analysis of the exhaust plumes from L-vehicles. By analysing these density fields, we can identify the areas with the highest density of exhaust plumes. We can also identify why vehicle exhausts were not captured and determine the location of the exhaust in relation to the remote emission sensing systems. Also, this data will help design more innovative and efficient remote emission sensing systems. It aims to improve the capture rate of emissions by optimizing the positioning of the sampling line for point sampling-based remote sensing systems and the placement of the laser for absorption spectroscopic-based remote sensing systems.

Figures 19 and 20 display the Schlieren images of the exhaust plumes from a heavy L-vehicle and a smaller L-vehicle, respectively. The specifications of the vehicles are detailed in Table 5.

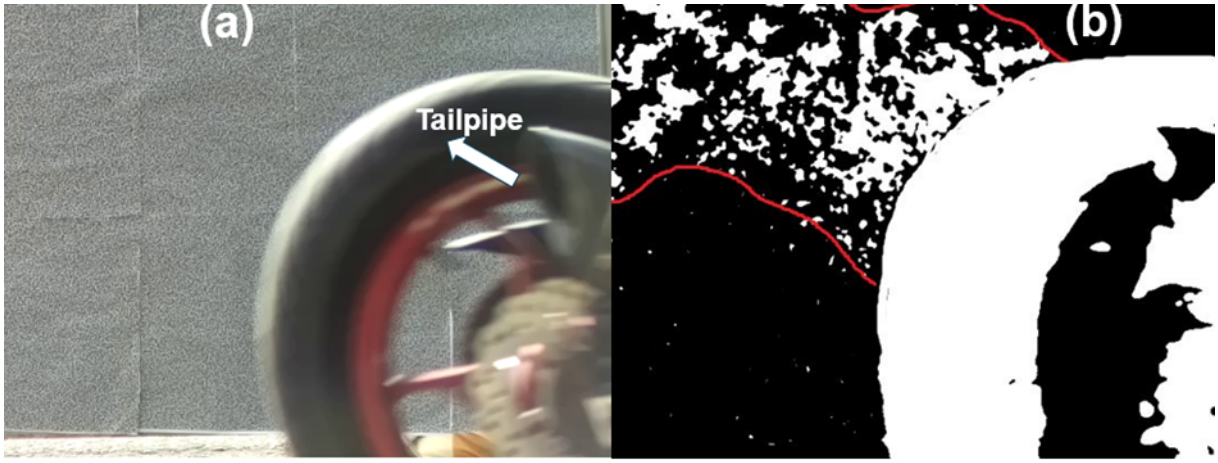

Figure 18. Heavy L-vehicle -- (a) Original Frame, (b) Schlieren Image.

This project has received funding from the European Union's Horizon Europe research and innovation programme under grant agreement No 101056777

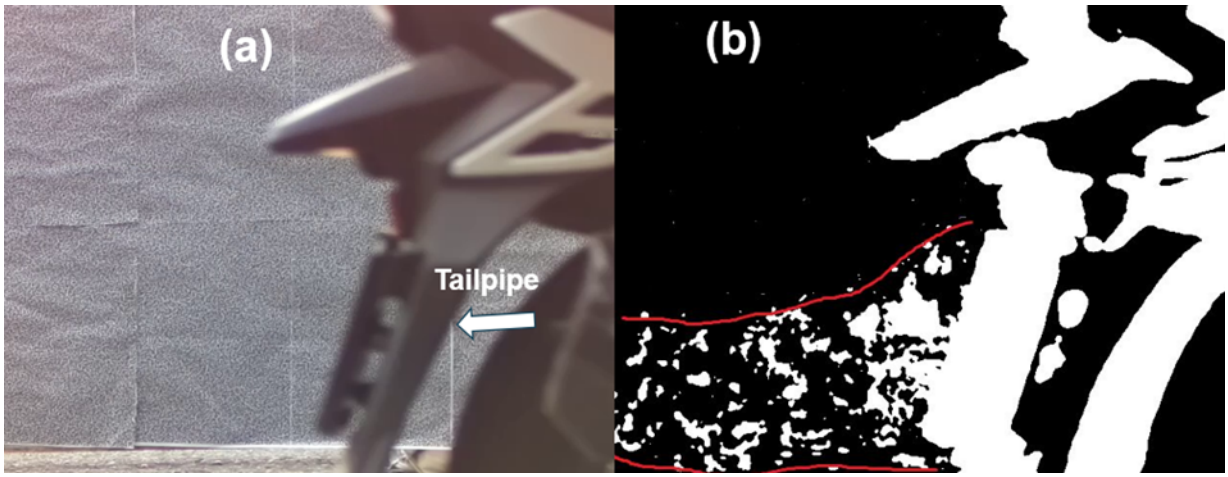

Figure 19. Small L-vehicle -- (a) Original Frame, (b) Schlieren Image

Table 5. Specifications of the vehicles appearing in Figure 18 and Figure 19.

L-Vehicle	Engine displacement (cc)	Engine	Model year	CO_2 emissions (vol-%)	NO_2 (ppm)	HC (ppm)
(1) Bike	1200	4-stroke	2008	15.1	368	183
(2) Scooter	50	4-stroke	2023	14.6	22	579

The reconstructed density fields of exhaust plumes from two types of L-vehicles are presented in Figure 20 and Figure 21. The values are represented as the ratio of calculated density to background density in kg/m³ for improved comparability. The frames illustrating the positions of the vehicles' tailpipes are provided to explain the setup and categorize the types of L-vehicles. The specifications of these vehicles are detailed in Table 7. More results of reconstructed density fields of exhaust plumes of category L-vehicles will be published in the submitted article "Reconstruction of Density Fields of Category L-Vehicles Exhaust Plumes for Remote Emission Sensing Applications."

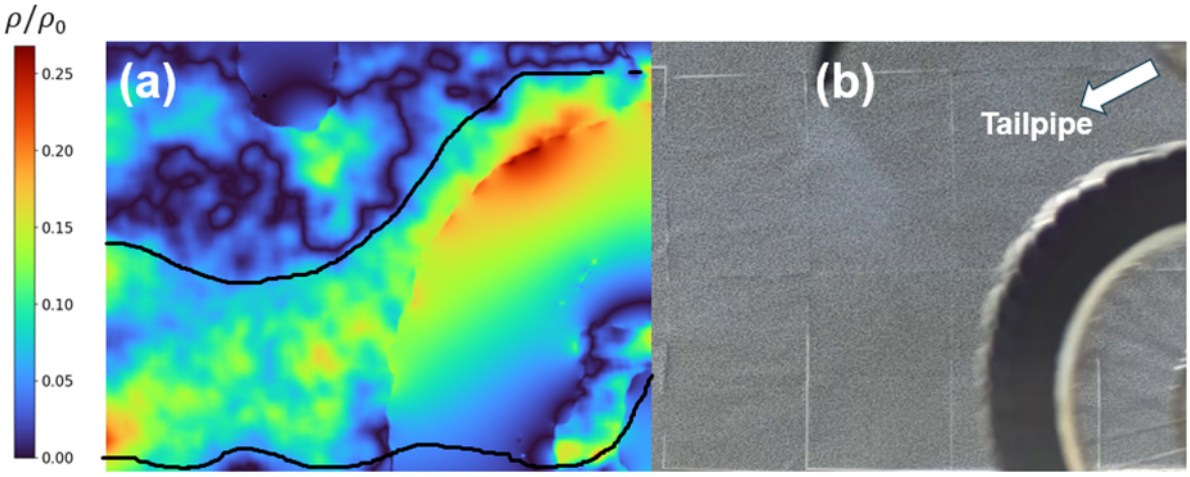

Figure 20. Normal sized 2-stroke L-vehicle -- (a) Reconstructed Density Field, (b) Original Frame.

This project has received funding from the European Union's Horizon Europe research and innovation programme under grant agreement No 101056777

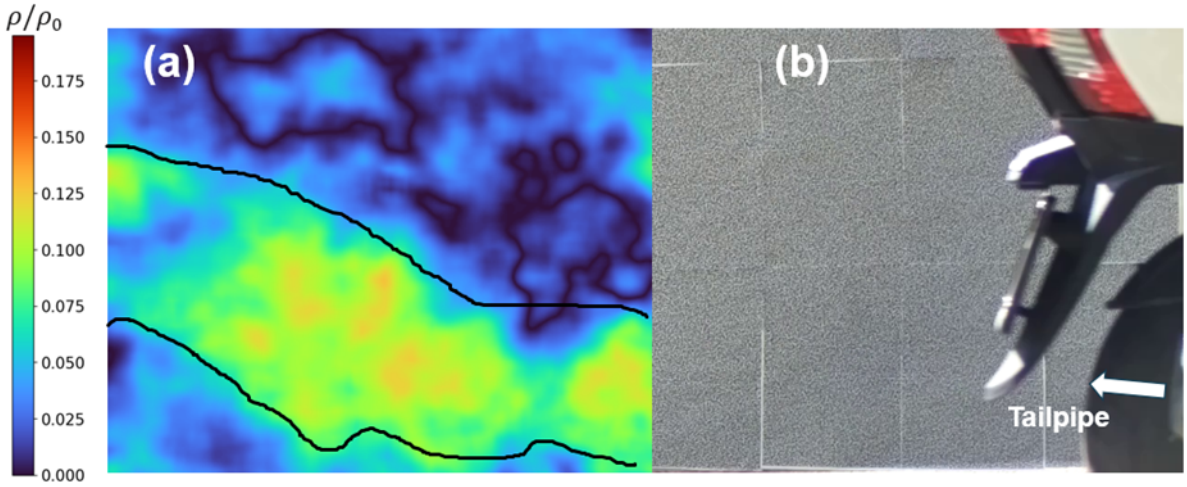

Figure 21. Normal sized 4-stroke L-vehicle -- (a) Reconstructed Density Field, (b) Original Frame.

Table 6. Specification of vehicles shown in Figure 20 and Figure 21.

L-Vehicle	Engine Displacement (cc)	Engine	Model year	CO_2 Emissions (%)	NO_2 (ppm)	HC (ppm)
(3) Bike	125	2-stroke	2006	9.34	207	16384
(4) Bike	125	4-stroke	2016	14.5	47	1462

3.1.3 IVL EEPS point sampling measurements

The EEPS point sampling devices were located at the same measurement position as the black carbon PM measurement (BCT) instrument and the PN-counter. Using this intrument it was possible to evalaute several drive by events in contrast to the used BCT instrument and the PN-counter. This is because the detection limit of the BCT is at 1.12 µg/m^3 (3 σ , 1 s), and thus too high for the small amounts of soot emitted by a passing LV. The PN-counter on the other hand is capable to detect ultrafine particles down to concentrations of ~4000 #/ccm, while ambient concentrations in urban areas are a multiple of that. Unfortunately, increases of the measured concentrations in the period of a passing LV could not be clearly identified as vehicle passes, according to the peak criteria applicable for passenger cars. This was due to the measured changes in background concentrations using the PN-counter predominate the contribution of most passing LVs. The EEPS on the other hand measures across the full size distribution, and includes the volatile fraction. Although, it must be stated that the smaller exhaust flows from LVs, and hence more diluted plumes made it challenging also to evaluate the EEPS data where the analysis of every single event had to be done manually.

3.1.3.1 Fleet composition

In total, 86 LV passages were measured according to the criteria described in Figure 6, and almost half of those were Euro 3 LVs (43%, Figure 22), followed by Euro 5 (27%), Euro 4 (20%), Euro 2 (8%) and Euro 1 (2%). For all Euro classes, the most common engine displacement was ≤ 250 cc, but for Euro 4 class the LVs were more evenly distributed between the three engine displacement categories shown in Figure 22. This fleet composition is similar to the fleet of valid measurements of the Opus

This project has received funding from the European Union's Horizon Europe research and innovation programme under grant agreement No 101056777

RSD 6000 data with respect to Euro class, whereas the larger engine displacement categories are less represented in the EEPS data.

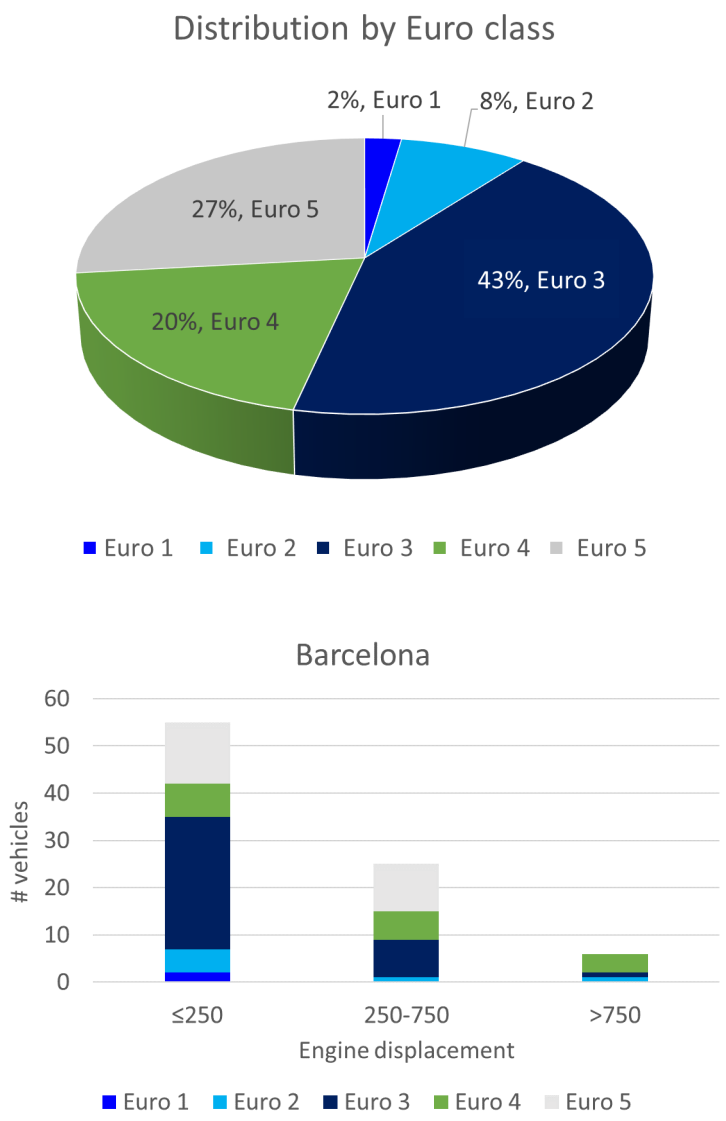

Figure 22. LV distribution by Euro class and by engine displacement of the EEPS measurements in Barcelona.

In Figure 23, the EFs of PN, PN_{23} and PM in g/kg fuel are shown and there is a general trend of decreasing emissions from Euro class 1 to 5. However, the number of vehicles is low, specifically in Euro class 1 and 2. For Euro 2 there is a clear trend of increasing emissions, both PN and PM, with decreasing engine displacement. For the other Euro classes this relationship was not obvious.

This project has received funding from the European Union's Horizon Europe research and innovation programme under grant agreement No 101056777

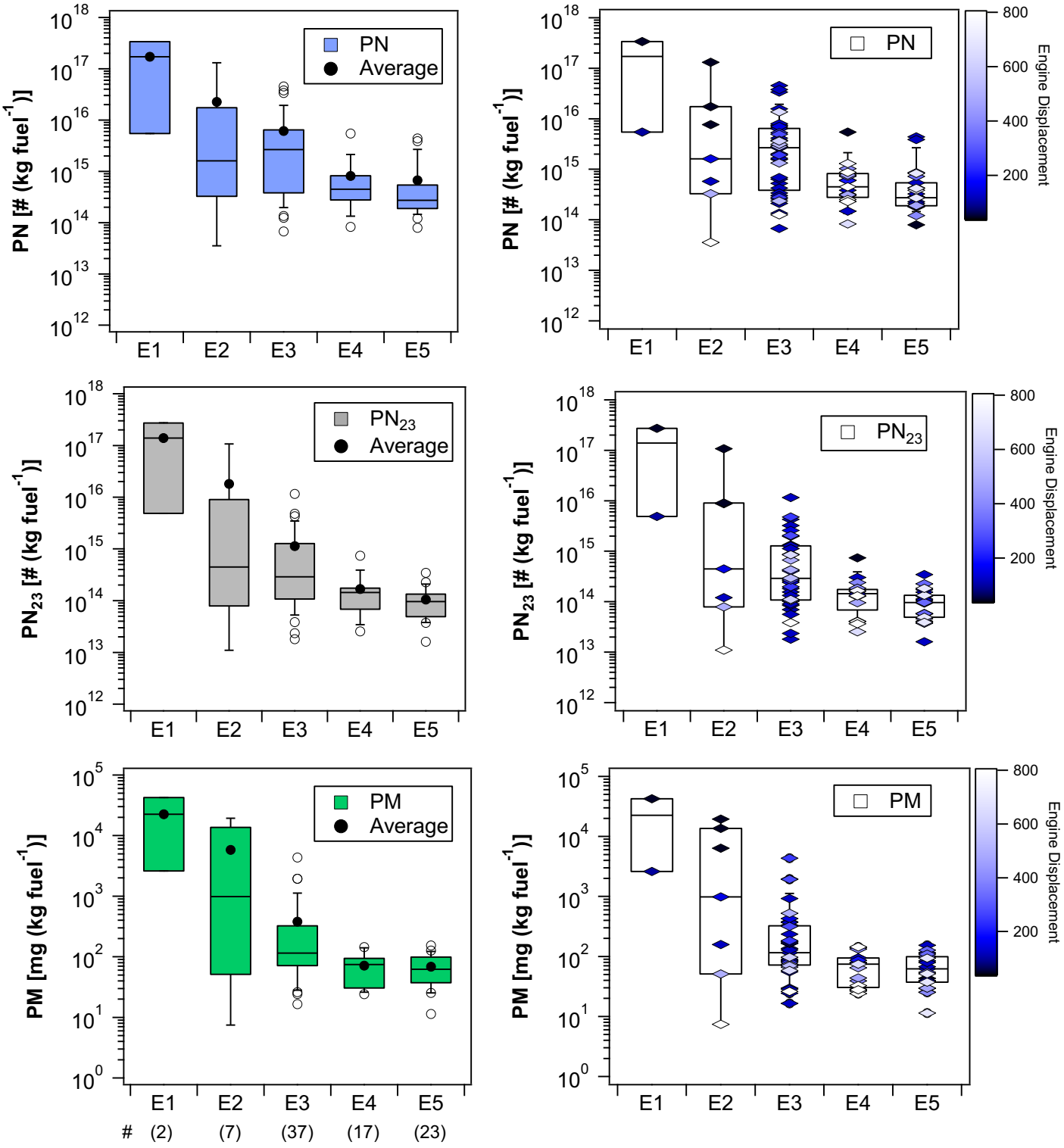

Figure 23. Box plots of the EF_{PN} (a, b), EF_{PN23} (c, d) and EF_{PM} (e, f) as a function of Euro class (E). The box represents the 25th and 75th percentiles, and the whiskers the 10th and the 90th percentiles. Horizontal lines are medians. White circles are >90th and <10th percentiles. In the figures to the right all data points are included as a function of engine displacement.

This project has received funding from the European Union's Horizon Europe research and innovation programme under grant agreement No 101056777

As presented in the results there is a challenge with the smaller exhaust flows from LVs and hence more diluted plumes compared to other vehicle types. However, if the emissions are high even at very diluted conditions (i.e., small elevation of CO_2) high emitters can be identified, as shown in Figure 5. In order to increase the hit rate, important factors are good temporal separation between vehicle passages, assuring high engine load while passing, ensuring passage as close to the measurement set-up as safety permits.

3.2 Noise

3.2.1 Measurements overview

The noise measurements operated independently from the other instruments and recordings were triggered based on the instantaneous sound pressure level. Table 7 gives an overview of the number of noise measurements performed in the different campaigns (see section 3.2 and appendix) and the total number of LVs considered in the campaigns. As LVs tend to drive close together in dense traffic situations and the number of vehicles' signatures captured in a recording is not always clear, the numbers in the table are an underestimation of the actual number of LVs passing the noise measurement system.

Table 7. Overview of the noise measurement database

	Leuven Site 1	Leuven Site 2	Paris (Rueil Malmaison)	Paris (Dampierre-en-Yvelines)	Barcelona	Total
Total number of raw sound recordings	1899	309	3134	264	3531	9137
Total number of LV sound signatures	184	67	823	155	920	2149
Number of single LV preprocessed recordings	145	23	512	81	893	1655
Number of single LV preprocessed recordings linked to an RSD 6000 measurement, of which:	131	20	310	50	664	1175
Number of preprocessed recordings linked to an identified LV	88	9	204	35	459	795
Number of preprocessed recordings linked to an identified inspected LV	88	9	0	0	40	137

This project has received funding from the European Union's Horizon Europe research and innovation programme under grant agreement No 101056777

Table 7 also provides the number of preprocessed 3 s recordings containing a single LV sound signature, available for further analysis, for each measurement site. The identification of LVs is done via the ANPR camera of the RSD 6000 instrument. As mentioned in the table, only a fraction of the noise recordings could – after synchronization of the systems – be linked to a unique vehicle passage recorded by at least one of the Opus RSD 6000 instruments. The table also reports the number of these vehicles for which technical information could be retrieved and the number of these recordings which could be linked to an inspected vehicle.

3.2.2 Fleet composition

Because of the independent measurement systems, the composition of the fleet corresponding to the preprocessed noise recordings is slightly different from the composition reported in earlier sections. The charts in Figure 24 give an overview of the composition of the part of the fleet for which preprocessed noise recordings are available in the database and which could be linked to an identified vehicle. Besides the data reported in the graphs, there is also a significant number of vehicles for which the noise recordings could not be linked with high confidence to an Opus RSD 6000 measurement or for which no vehicle information could be retrieved based on the license plate and/or vehicle inspections. Taking both measurement sites together, the fleet composition for Leuven and Paris is in line with the fleet composition reported in section 3.1.1.2 for all Opus RSD 6000 measurements. For Barcelona however, the share of light L-vehicles with an engine displacement below 250 cc is significantly higher than in the statistics for all OPUS RSD 6000 measurements, indicating that the data loss due to the synchronization process was not uniform over the different categories.

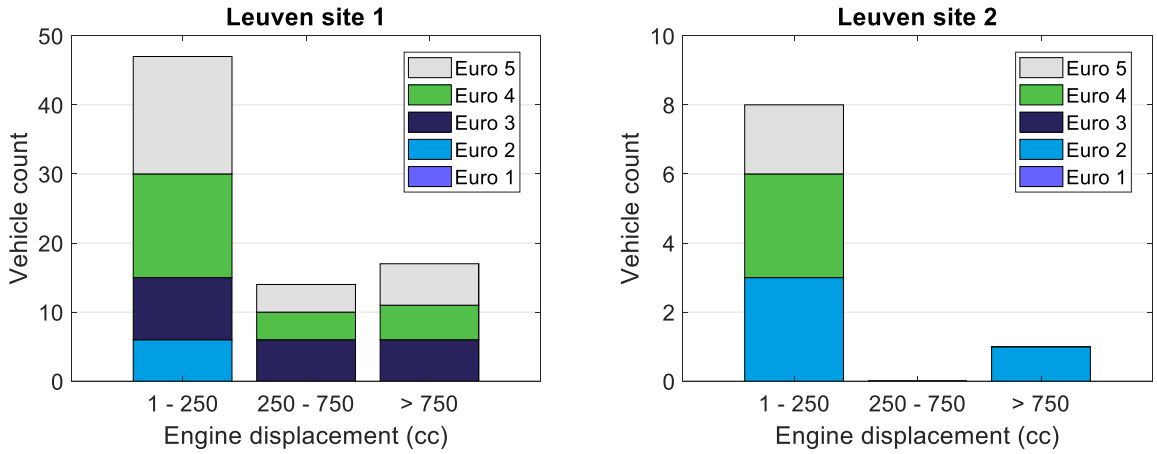

This project has received funding from the European Union's Horizon Europe research and innovation programme under grant agreement No 101056777

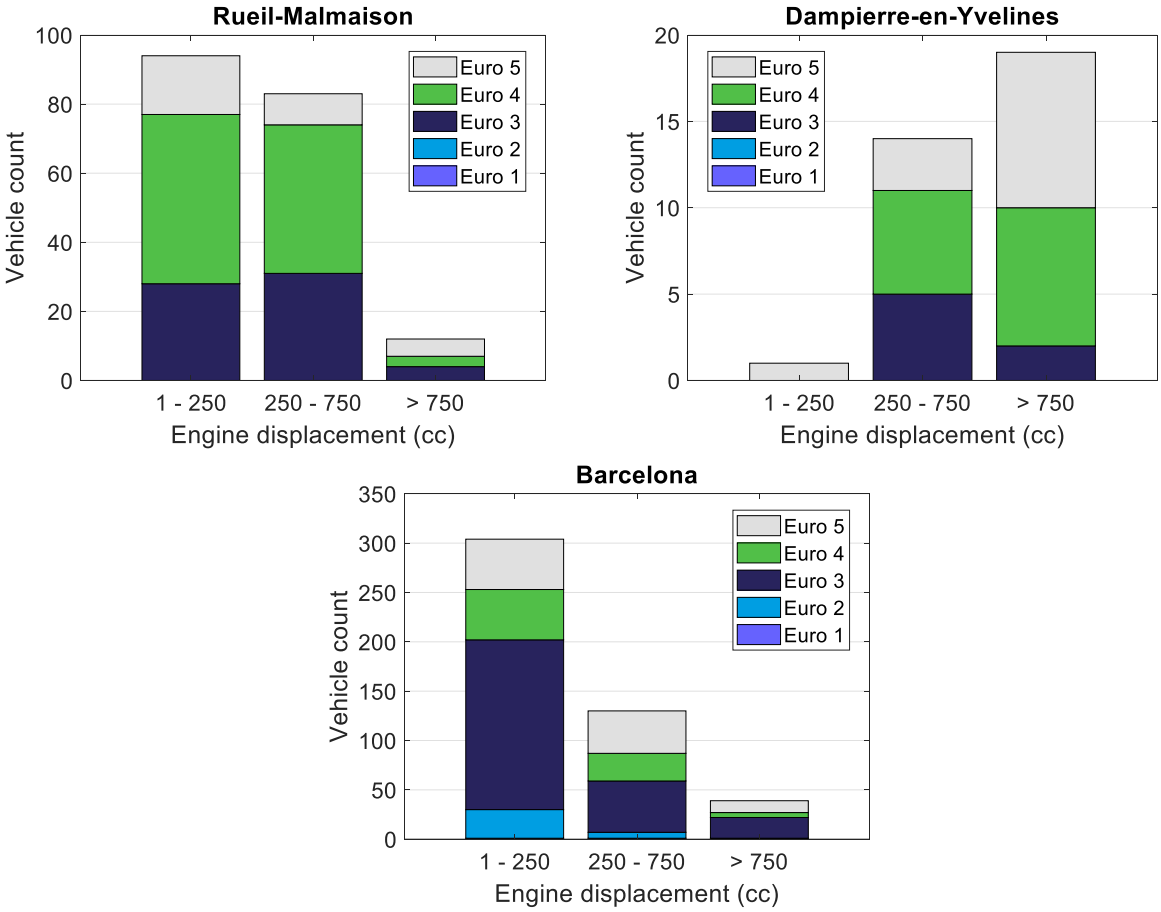

Figure 24. Composition of the fleet corresponding to the preprocessed single LV noise recordings linked to an identified LV at all measurement sites.

3.2.3 Sound pressure level

Figure 25 presents the distribution of the maximum instantaneous A-weighted sound pressure level (LAFmax) for all preprocessed single LV sound recordings at each measurement site. This is the metric used in the type approval regulations for LV noise and used in legislation on noise radars. The results are presented as violin plots, representing the kernel density estimate of the probability density function. A boxplot of the measurement data is overlaid to indicate the statistics of the dataset. Only the outliers of the distribution are indicated as individual points on the graphs.

This project has received funding from the European Union's Horizon Europe research and innovation programme under grant agreement No 101056777

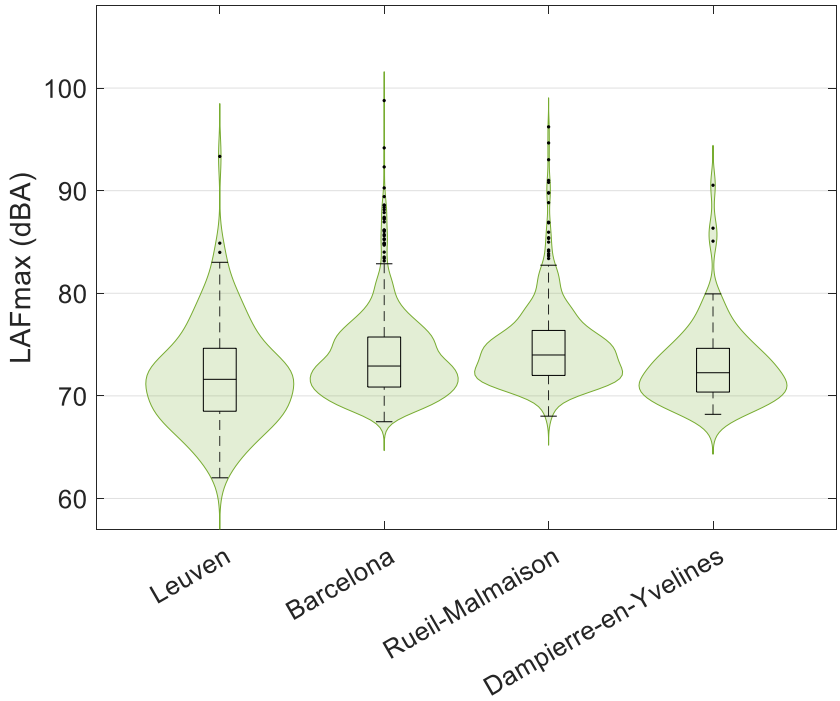

Figure 25. Maximum A-weighted sound pressure level (LAFmax) considering all preprocessed single LV recordings at each measurement site.

The median levels are 1 to 2 dB(A) higher at the urban sites (Barcelona: 72.9 dB(A) and Rueil-Malmaison (Paris): 74.0 dB(A)) than at the sites with less dense traffic (Leuven: 71.6 dB(A) and Dampierre-en-Yvelines (Paris): 72.3 dB(A)). These differences can most likely be attributed to the lower background noise level at the latter sites. For all sites, the inter-quartile range (IQR) covers a range of 4 to 6 dB(A). The distributions for most sites deviate from the expected normal distribution and exhibit a heavy tail towards higher noise levels, with a large number of outliers in that direction.

The charts in Figure 26 show the distribution of the maximum A-weighted sound pressure level (LAFmax) as a function of Euro class, considering only noise recordings linked to an identified vehicle at each measurement site. These results can't be compared to the limits imposed by the type approval regulations because of differences in measurement setup, driving conditions, road surface, etc. but provide an indication of the differences in noise levels between older and newer LVs.

For all measurement sites, it can be observed that there is a large overlap between the distributions of the different classes. The median levels for most classes at each site are comparable and within 1 dB(A) of each other. The only exceptions are the classes containing a small number of vehicles and the Euro 3 class in Leuven, for which the median is surprisingly 3 dB(A) lower than the other categories at that site. The absence of a clear downward trend can be explained by several important factors, such as the mixed fleet considered in these figures and the driving conditions. With an average velocity around 25 km/h at all measurement sites, it is clear that most vehicles were not tested at their most noise critical conditions. Looking at the maxima (excluding outliers) of the boxplots, the lowest levels are observed for the Euro 5 category at all measurement sites. Most of the outliers towards higher sound levels can be attributed to specific driving behavior that causes high instantaneous noise levels.

This project has received funding from the European Union's Horizon Europe research and innovation programme under grant agreement No 101056777

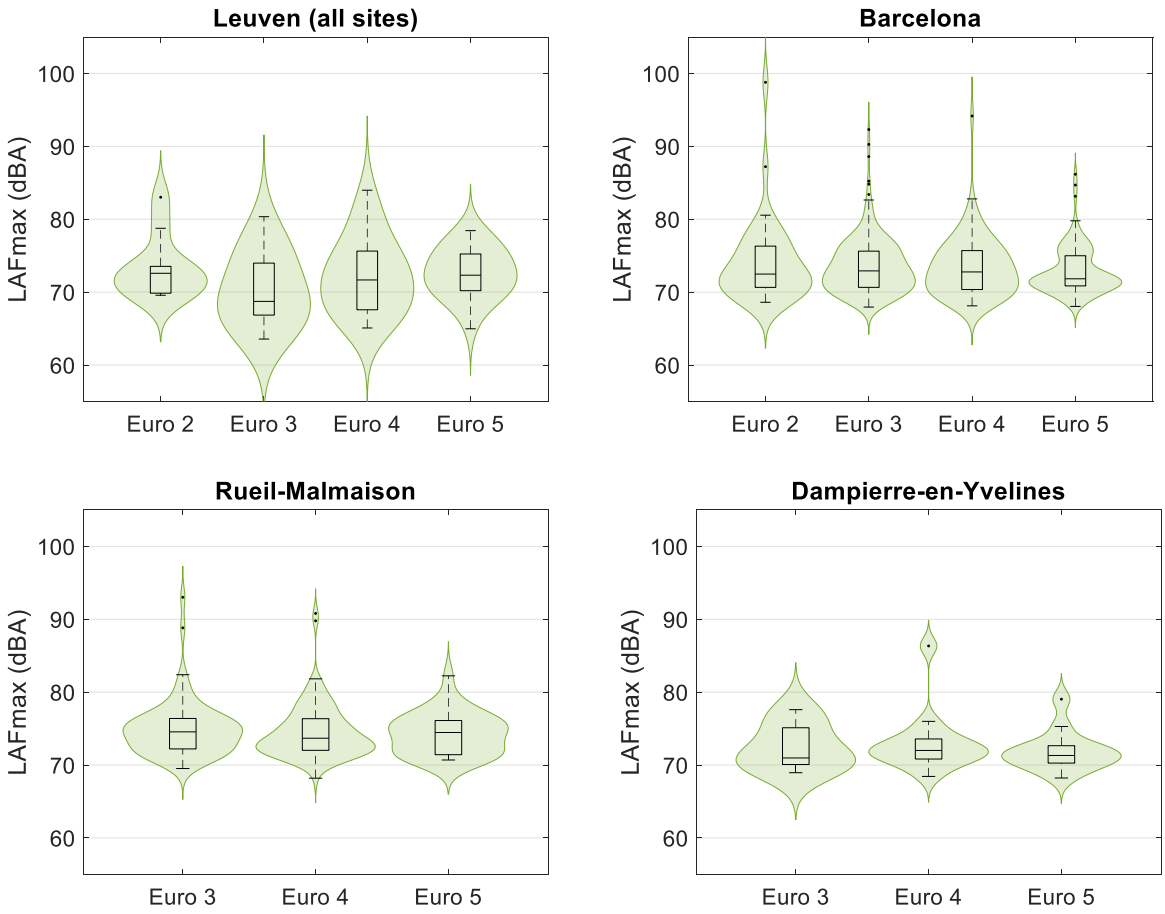

Figure 26. Maximum A-weighted sound pressure level (LAFmax) as a function of Euro class, considering all preprocessed single LV recordings linked to an identified LV at each measurement site

Figure 27 visualizes the maximum A-weighted sound pressure level (LAFmax) as a function of engine displacement, considering only noise recordings linked to an identified vehicle at each measurement site. Although different noise limits apply to different LV categories in the type approval regulations, a large overlap between the distributions for all classes can be observed at all measurement sites. For Paris and Barcelona, the difference between the median levels for all categories is negligible (less than 1 dB(A)). In Leuven, the same holds for the smallest LV categories, but the median level for the >750 cc category is 2 dB(A) higher. This is most likely due to differences in driving conditions. In Leuven, drivers were asked by the police to accelerate while driving by the microphones, whereas LV drivers at other sites often slowed down to look at the instruments. Additionally, in Leuven a significant share of the >750 cc category corresponds to repeated measurements of the motorbikes of the police supporting the measurement campaign with different driving conditions than the regular traffic. Also many of the outliers can be related to noisy driving conditions. For example, the highest level (98.8 dB(A)) measured in the Barcelona campaign corresponds to a motorcycle doing what is referred to as an “rpm burst” in LENS D6.1 [23] in front of the microphones.

This project has received funding from the European Union's Horizon Europe research and innovation programme under grant agreement No 101056777

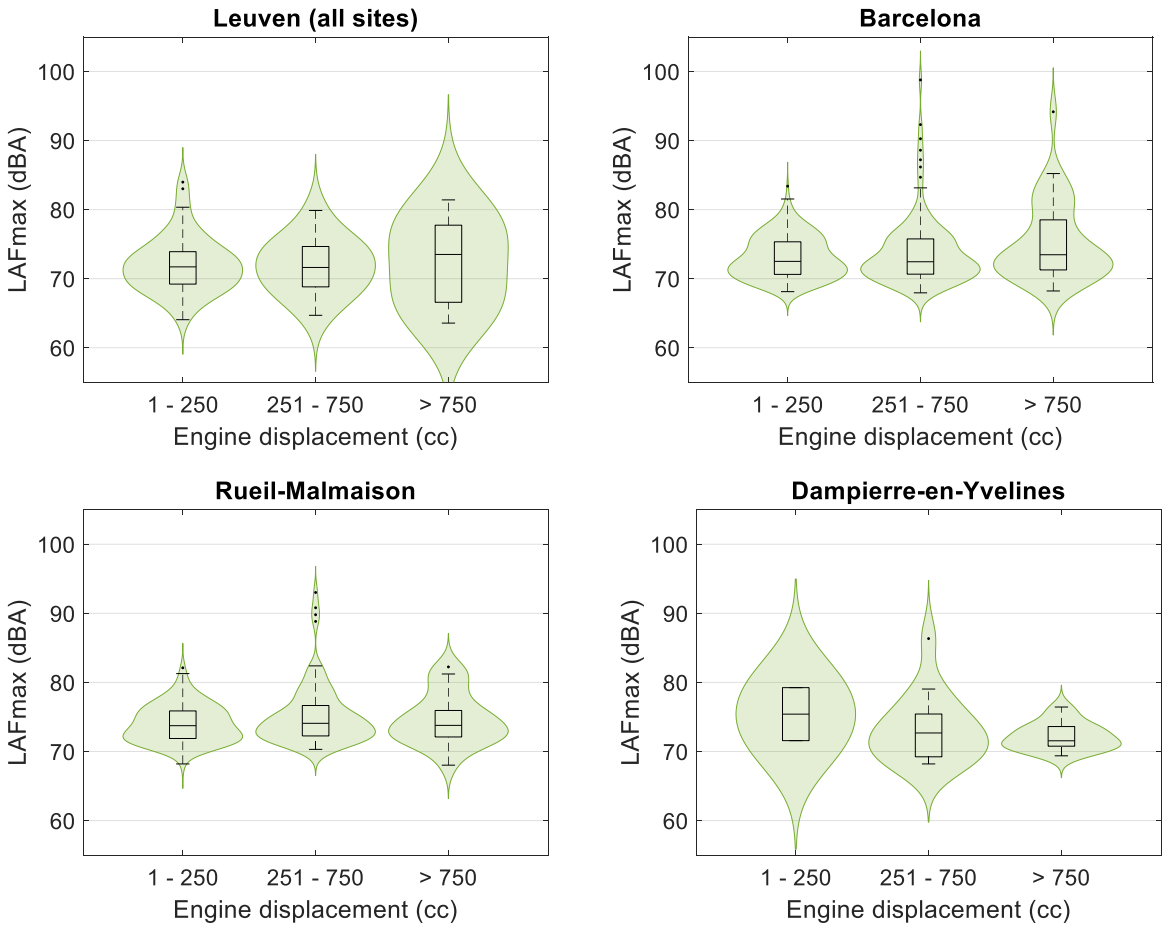

Figure 27. Maximum A-weighted sound pressure level (LAFmax) as a function of engine displacement, considering all preprocessed single LV recordings linked to an identified LV at each measurement site

The A-weighting filter, which is most commonly used for expressing noise levels, was originally designed to correct for the frequency dependence of the human hearing for low amplitude sounds. The C-weighting filter is more appropriate for higher sound pressure levels and suppresses the influence of the low frequency content of the sound much less than the A-weighting filter. Because of the importance of low frequencies in the perception of LV sound, especially at low engine RPM, Figure 28 presents an overview of the measured maximum C-weighted sound pressure levels (LCFmax) for all preprocessed single LV recordings at all measurement sites. Compared to Figure 25, the levels have clearly increased by several dB due to the increased contribution of the low frequency content of the noise signals. Additionally, also the ranking of the median levels across sites has changed and the highest median level is now observed for the rural site in Paris (83.1 dBC). This large difference is due to the fleet composition at this site, with a larger share of heavier LVs typically producing more low frequency sound. For the measurement sites in Leuven, it can be observed that the IQR has increased from 6 dB(A) to 10 dBC. This is most likely due to the large number of recordings corresponding to a motorbike of the supporting police, for which the driving conditions varied more than the other LVs.

This project has received funding from the European Union's Horizon Europe research and innovation programme under grant agreement No 101056777

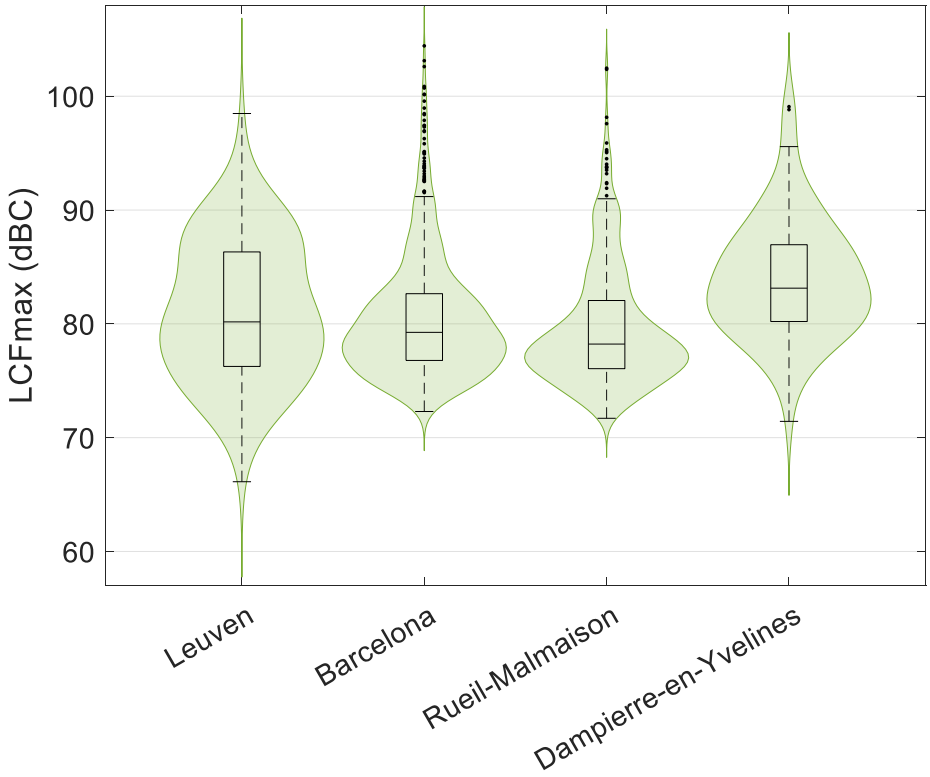

Figure 28. Maximum C-weighted sound pressure level (LCFmax) considering all preprocessed single LV recordings at each measurement site.

The distribution of the C-weighted sound pressure level as a function of engine displacement in Figure 29 confirms that the observations above for the overall fleet are mostly linked to larger LVs and that, as a result, the fleet composition plays a significant role in the difference between Figure 25 and Figure 28.

This project has received funding from the European Union's Horizon Europe research and innovation programme under grant agreement No 101056777

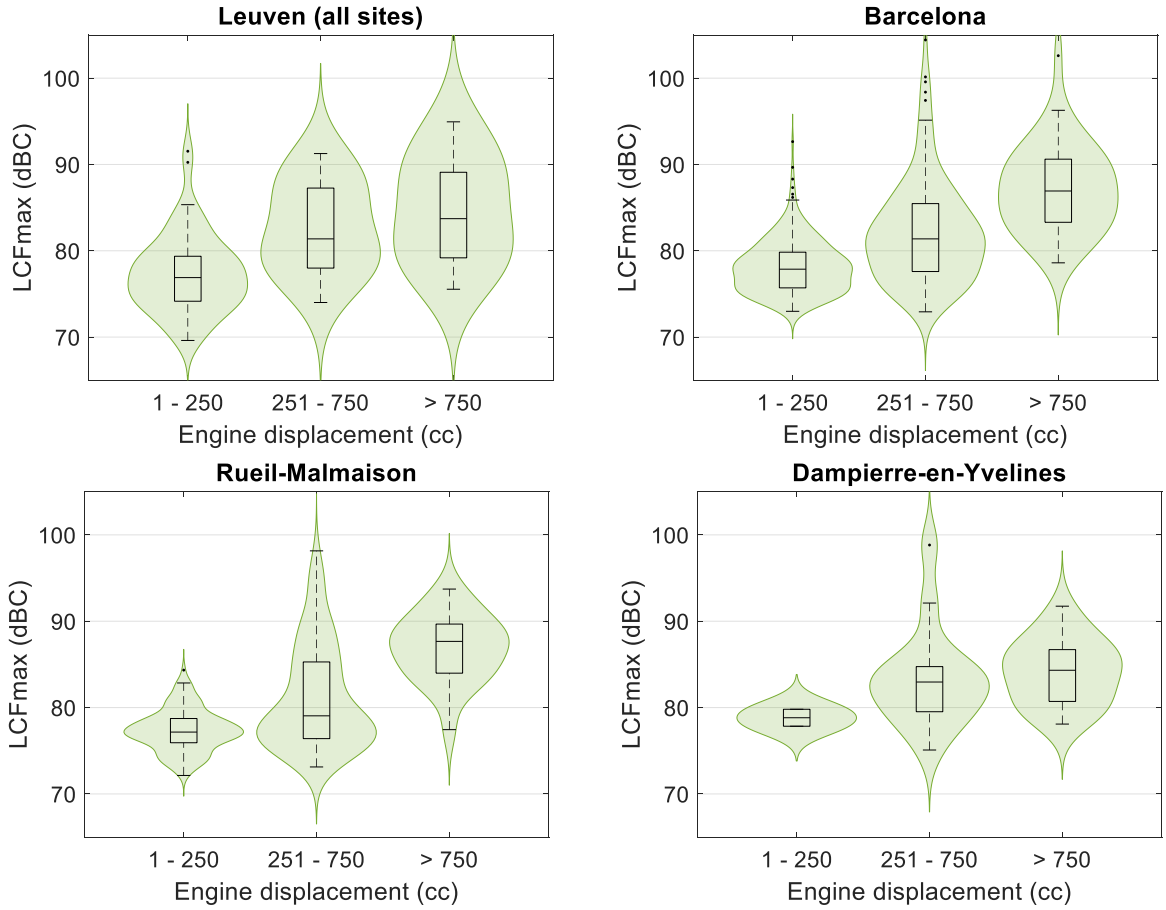

Figure 29. Maximum C-weighted sound pressure level (LCFmax) as a function of engine displacement, considering all preprocessed single LV recordings linked to an identified LV at each measurement site

3.2.4 Perception of LV sound: psychoacoustic metrics

Besides noise levels, also the perception of the sound character plays an important role in the perceived annoyance due to LV noise. A number of common psychoacoustic metrics have been analyzed. These metrics quantify perceptional characteristics of a sound signal and have been computed with the open source MATLAB toolbox SQAT [24].

The perception of LV sound signatures strongly depends on the tonal components present in the sound signals. Distinct audible tones and modulation phenomena, caused by interaction between different tonal components, are important drivers for the human perception of the sound character and can be quantified by psychoacoustic metrics such as tonality, roughness and fluctuation strength:

- Tonality, expressed in tonality units (t.u.), is a measure for the importance of audible tones in a sound signal. Alternative metrics to quantify the importance of such tones include the prominence ratio, tone-to-noise ratio, etc.
- Roughness, expressed in asper, is a measure for fast modulation present in the signal, with a modulation frequency between 20 Hz and 300 Hz. Such modulation is not perceived as actual loudness fluctuations but leads to a rough sound character.

This project has received funding from the European Union's Horizon Europe research and innovation programme under grant agreement No 101056777

- The fluctuation strength, expressed in vacil, is a measure for modulation with a frequency between 0 and 20 Hz. Such slow modulation is perceived as a sound with a fluctuating loudness.

The roughness is computed using the method developed by Daniel and Weber [25] using windows of 200 ms with 50% overlap on the complete 3 s recording for each LV. The maximum roughness value obtained for the 3 s recording for all identified LVs is considered in the charts in Figure 30 below. A large overlap between the distributions and skewed distributions, with a heavy tail and many outliers towards higher roughness values can be observed. For Leuven, Barcelona and the urban site in Paris (Paris site 1), the median roughness is around 0.3 asper for the two smallest LV categories and slightly higher (between 0.3 and 0.35) for the >750 cc category. For the urban site in Paris, the median roughness for the 251cc – 750cc and >750cc categories is clearly higher and around 0.46 asper for both. This increase could be due to tampering (see section 3.3.3.2), although also driving conditions are expected to play a role. Tampering often leads to more pronounced tonal components in the noise spectrum, which are the driving factors for the roughness. Although no LV inspections took place at this site, it is believed that a significant share of the LVs at Paris site 2 was tampered. The distribution of the 1cc – 250cc category at this site is included in the graph for completeness but contains too few vehicles to draw meaningful conclusions.

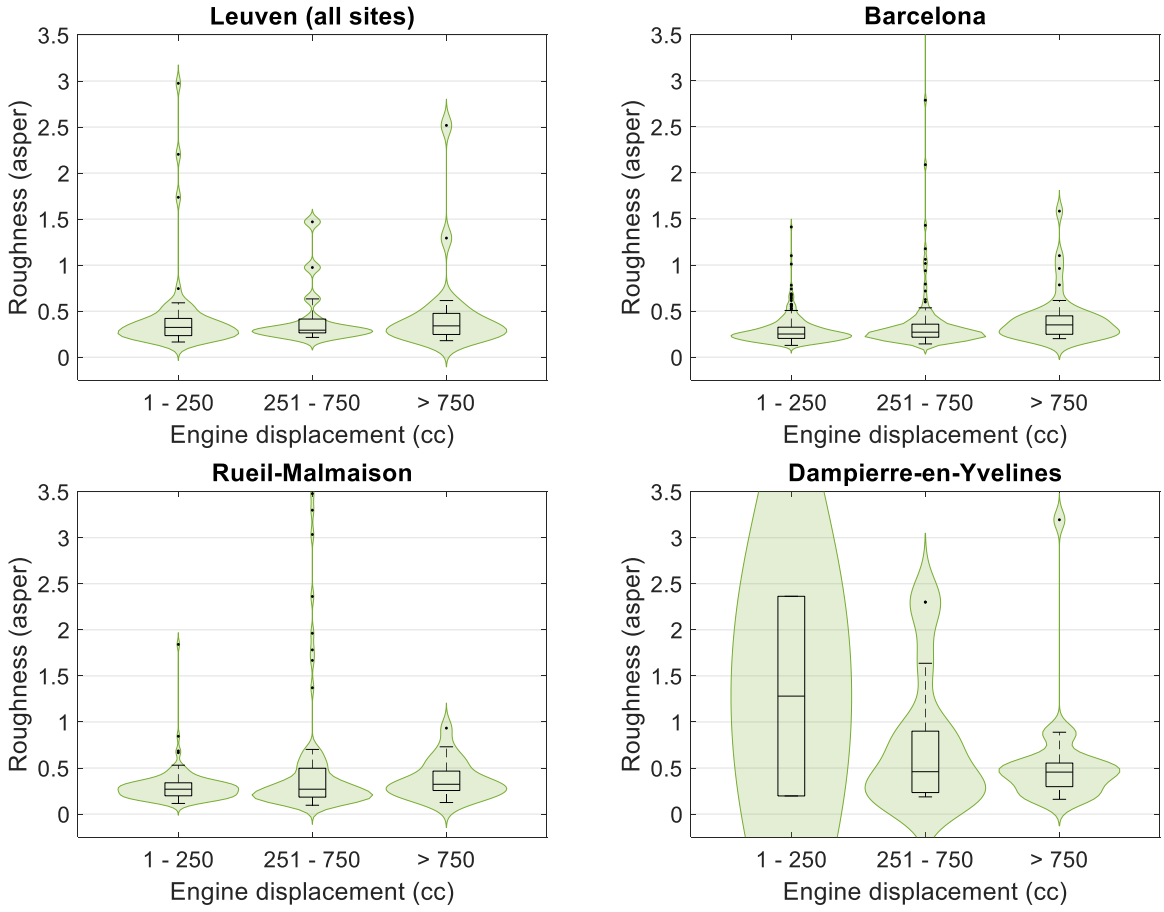

Figure 30. Maximum roughness as a function of engine displacement, considering all preprocessed single LV recordings linked to an identified LV at each measurement site.

This project has received funding from the European Union's Horizon Europe research and innovation programme under grant agreement No 101056777

The fluctuation strength is computed with the method developed by Osses et al. [26] using 2 s windows with 90% overlap. Also here, the maximum value obtained within the 3 s recording for each LV is included in the figures below. Larger LVs often by design have a sound character where low frequency modulation can clearly be perceived. This is realized by design choices, including the engine configuration, uneven firing rate and the design of the exhaust system. LVs in this category are therefore on average expected to reach higher values for the fluctuation strength for comparable driving conditions. In Figure 31, it can be observed that the median fluctuation strength indeed slightly increases towards the larger LV categories for all measurement sites. However, most LVs exhibit a low fluctuation strength, below 0.5 vacil.

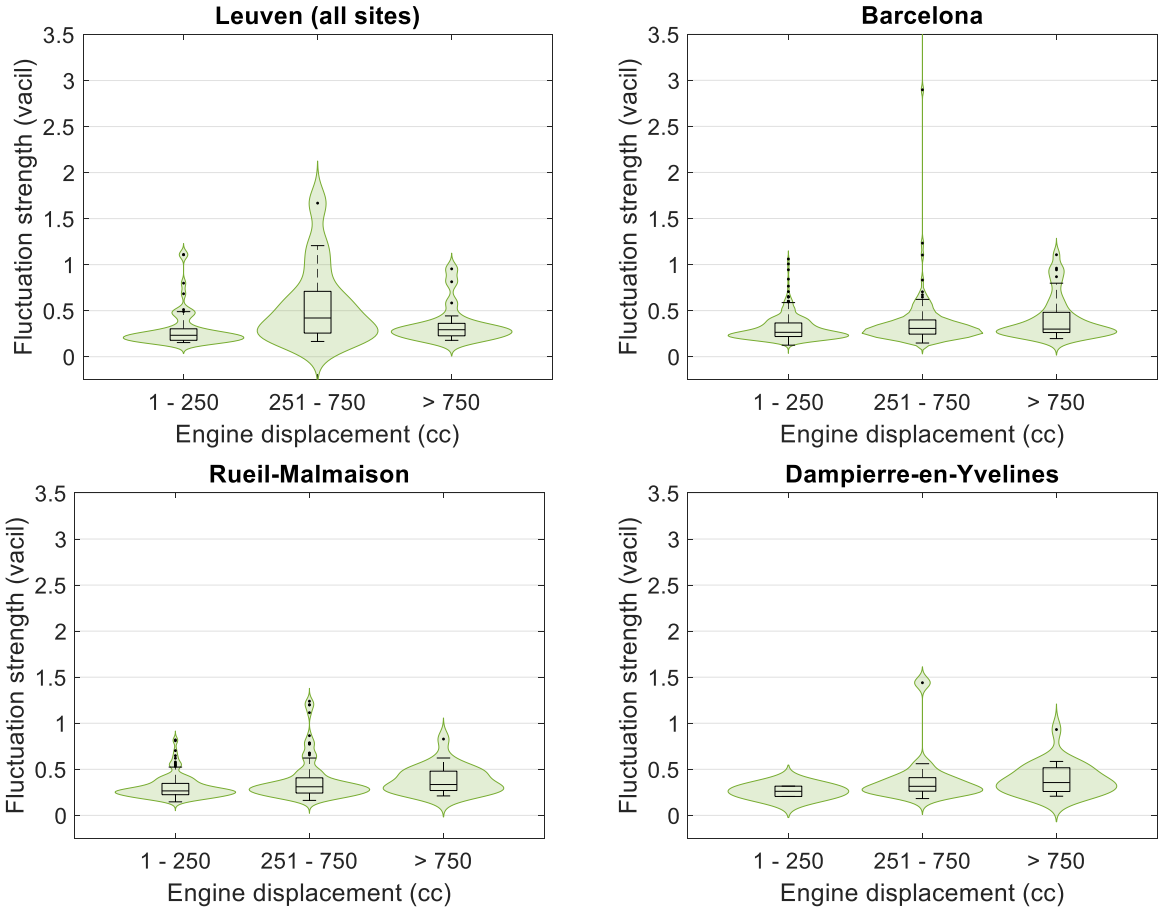

Figure 31. Maximum fluctuation strength as a function of engine displacement, considering all preprocessed single LV recordings linked to an identified LV at each measurement site.

Finally, also the tonality of the LV sound signatures has been computed using the method developed by Aures [27] using 160 ms windows and 50% overlap. Also here, the maximum value obtained within the 3 s recording for each LV is included in Figure 32. Although LV sound signatures contain a large number of tonal components originating from the engine, transmission, etc., these components are typically not audible as tones but rather contribute to the above modulation phenomena. As a consequence, a low tonality is observed for all measurement sites and vehicle categories in Figure 32. It should be noted that electric vehicles typically have sound signatures with significantly higher

This project has received funding from the European Union's Horizon Europe research and innovation programme under grant agreement No 101056777

tonality. However, the number of electric LV sound signatures measured in the campaigns was too low to derive significant conclusions on this.

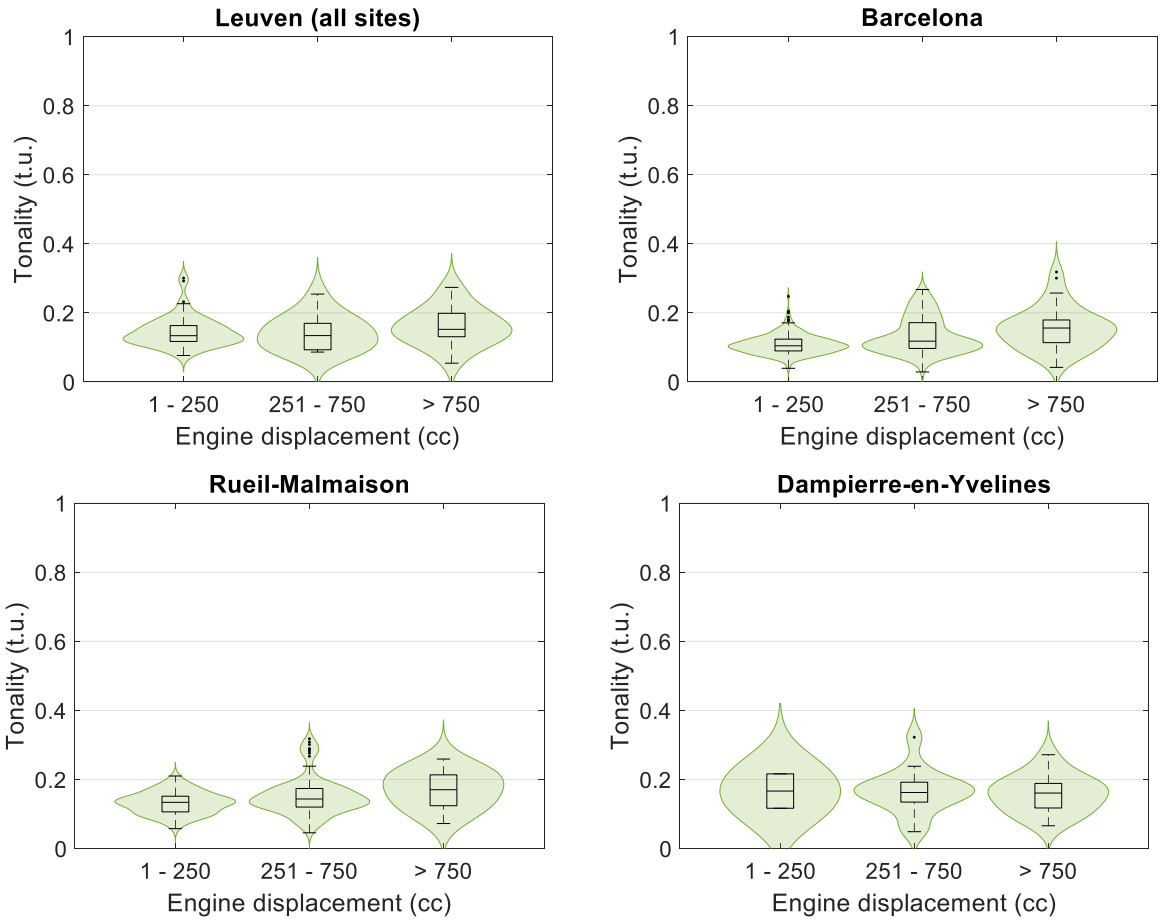

Figure 32. Tonality as a function of engine displacement, considering all preprocessed single LV recordings linked to an identified LV at each measurement site.

This project has received funding from the European Union's Horizon Europe research and innovation programme under grant agreement No 101056777

3.3 Tampering analysis

3.3.1 Roadside inspections

All the data collected in the roadside inspections in Leuven and Barcelona can be found in the Appendix.

The fleet composition (with regard to Euro class and engine size) of the LVs inspected at the roadside is shown in Figure 33and Figure 34. Since LVs generally were pulled over in a random manner, these compositions resemble very much the fleet composition given in Figure 11 and Figure 12, e.g., the much larger share of the smallest engine size categories in Leuven compared to in Barcelona.

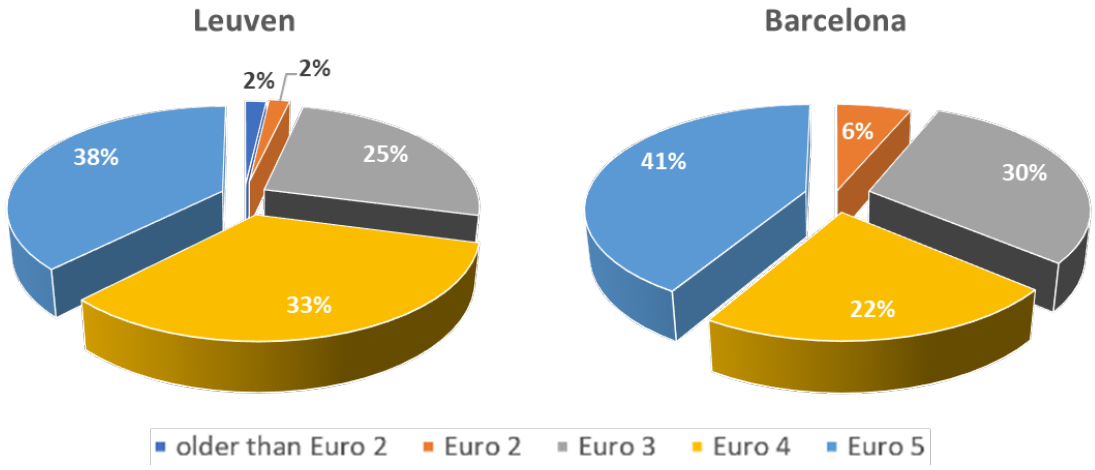

Figure 33. Euro class distributions for the LVs inspected at the roadside in Leuven and Barcelona, respectively.

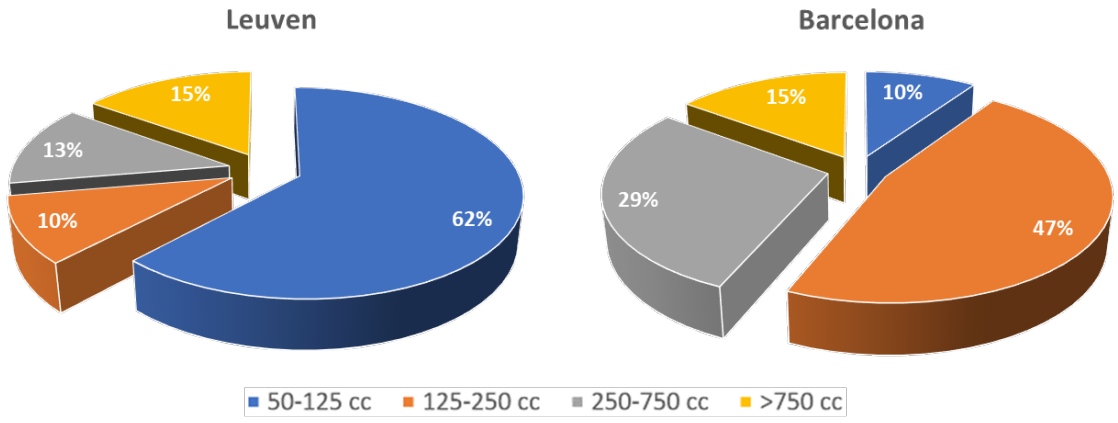

Figure 34. Engine displacement distributions for the LVs inspected at the roadside in Leuven and Barcelona, respectively.

This project has received funding from the European Union's Horizon Europe research and innovation programme under grant agreement No 101056777

The results from the roadside inspection idle emission tests (CO and HC) are presented in Figure 35 as average emissions by Euro class. The trend of decreasing idle emissions with increasing Euro standard is very similar to the trends in measured on-road emissions and the Euro emission limit as given by Figure 15 and Table 4 in section 3.1.1.3.

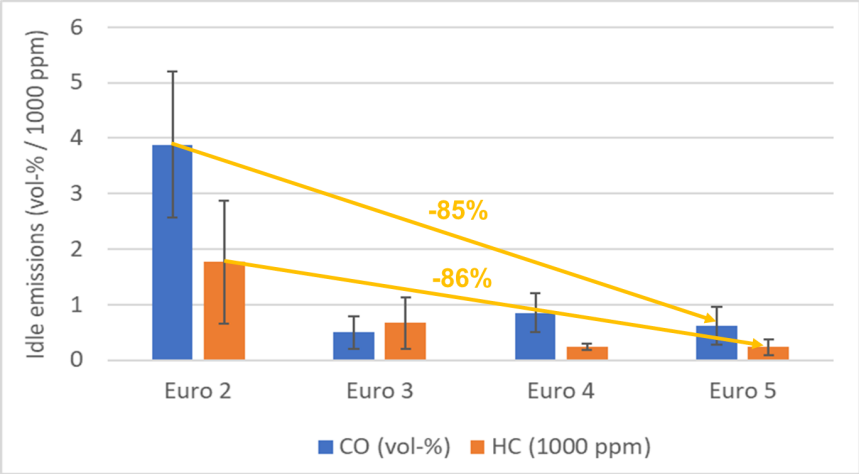

Figure 35. Average idle emissions of CO and HC by Euro class according to the roadside inspection idle tests carried out in Leuven and Barcelona.

The trends of idle CO and HC emissions by Euro class, split up in the three engine size fractions ≤250 cc, 250-750 cc and ≥750 cc, are presented in Figure 36. Note the big differences in idle emission levels between the smallest and the bigger engines, particularly for HC.

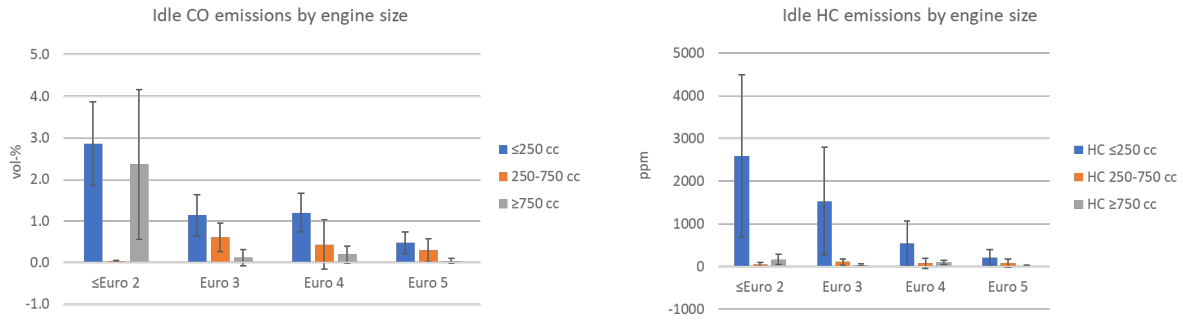

Figure 36. Average idle emissions of CO and HC by Euro class and engine size (displacement volume cm^3) according to the roadside inspection idle tests carried out in Leuven and Barcelona.

In Figure 37 and Figure 38 the shares of modified/tampered LVs, along with the shares of the different modification/tampering approaches for Leuven and Barcelona, respectively, are given. The overall modification/tampering share is very similar in the two cities – slightly above 10%.

This project has received funding from the European Union's Horizon Europe research and innovation programme under grant agreement No 101056777

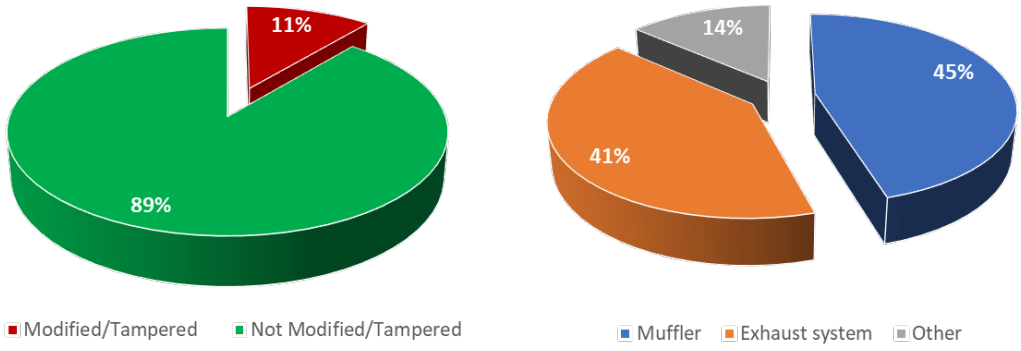

Figure 37. Share of modified/tampered LVs (left) and shares of the different types of modification/tampering in Leuven.

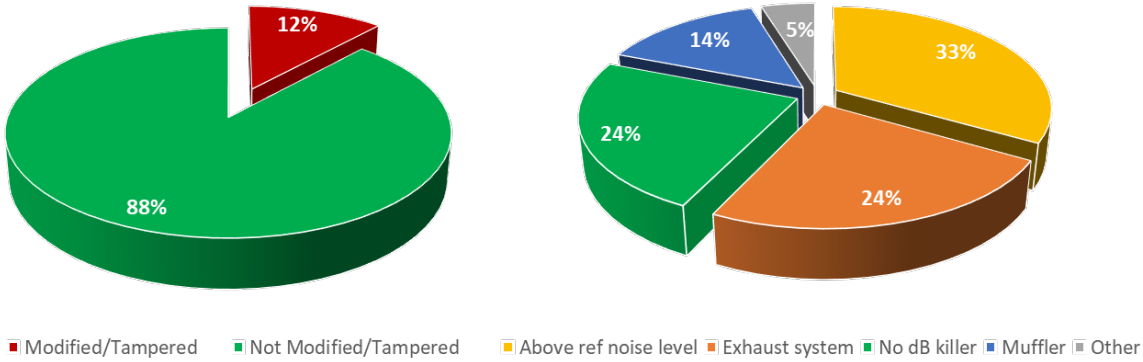

Figure 38. Share of modified/tampered LVs (left) and shares of the different types of modification/tampering in Barcelona.

Some characteristics of the modified/tampered LVs compared (group A) to the non-modified/non-tampered LVs (group B) were:

- There was a higher share of 2-stroke engines in group A than in group B: 23% vs 3%, respectively. Note though that the share of 2-stroke engines in the inspected fleet was only about 10%, i.e., 90% were 4-stroke engines.
- The average vehicle age for group A was about two years older than for group B.
- The average engine displacement (engine size) was substantially higher for group A compared to group B (446 cc vs 285 cc), i.e., LVs with larger engines are more commonly modified/tampered (Figure 39).
- Looking at the share of modified/tampered LVs by Euro class (Figure 40), Euro 2 LVs seem to be the most frequently modified/tampered ones. The muffler and the exhaust system seems to be subject to the most frequent modifications/tampering.
- Although there was not a significant difference mileage (22,800 vs 23,600 km) between the two groups, there were some differences in vehicle mileage distribution - cf. Figure 41. LVs with very low mileages and very high mileages appear to be less modified/tampered.

This project has received funding from the European Union's Horizon Europe research and innovation programme under grant agreement No 101056777

-

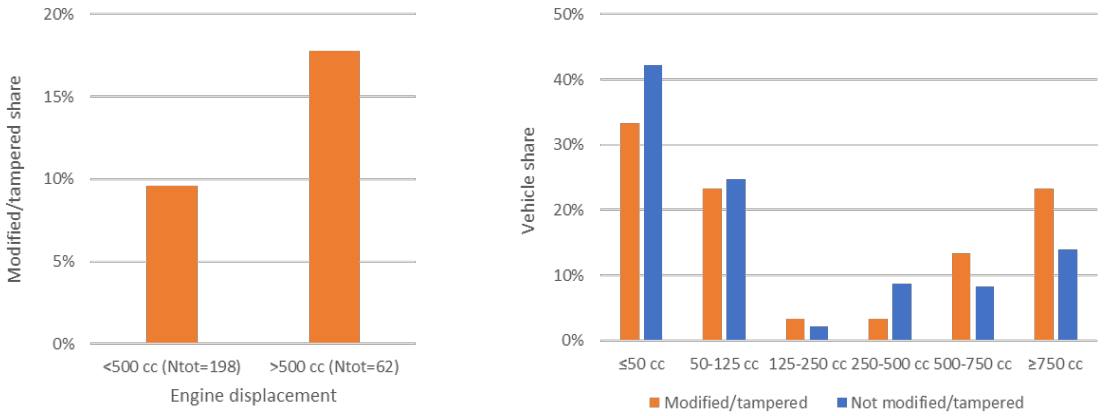

Figure 39. Shares of LVs by engine size for modified/tampered and not modified tampered vehicles, respectively, according to the roadside inspections in Leuven and Barcelona.

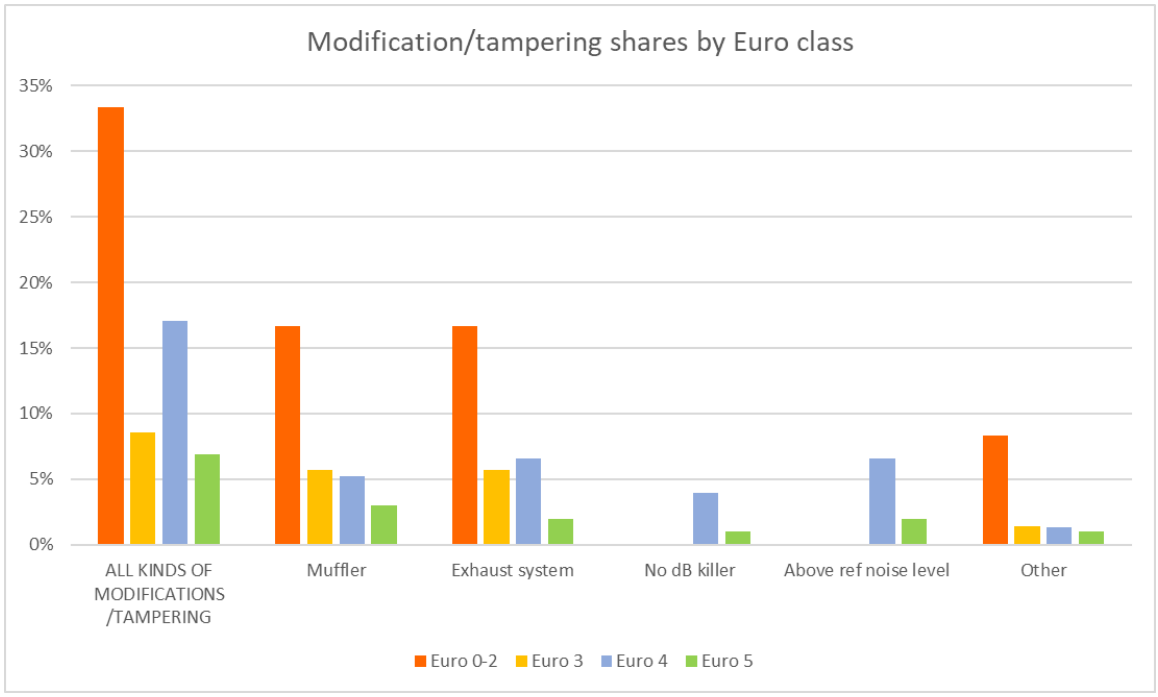

Figure 40. Shares of modified/tampered and not modified/tampered LVs by Euro class (left) and mileage range (right), respectively, according to the roadside inspections in Leuven and Barcelona.

This project has received funding from the European Union's Horizon Europe research and innovation programme under grant agreement No 101056777

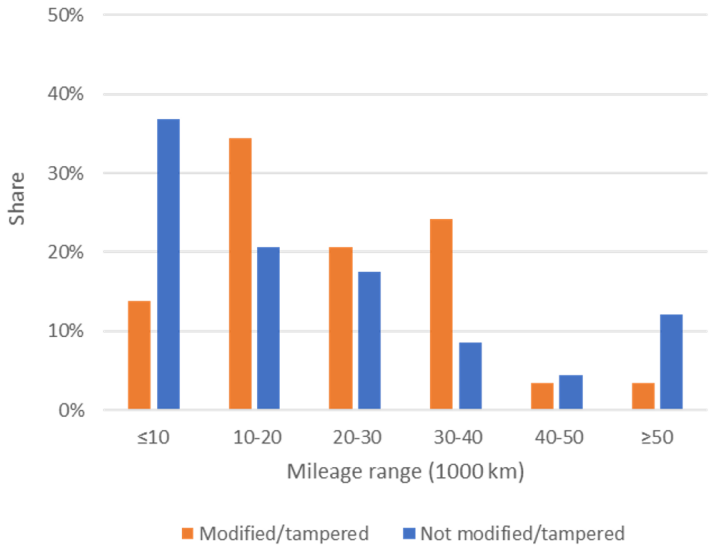

Figure 41. Shares of modified/tampered and not modified/tampered LVs by mileage range, according to the roadside inspections in Leuven and Barcelona.

Figure 42 shows the impact of tampering on idle CO and HC emissions, which is quite substantial, especially for HC emissions.

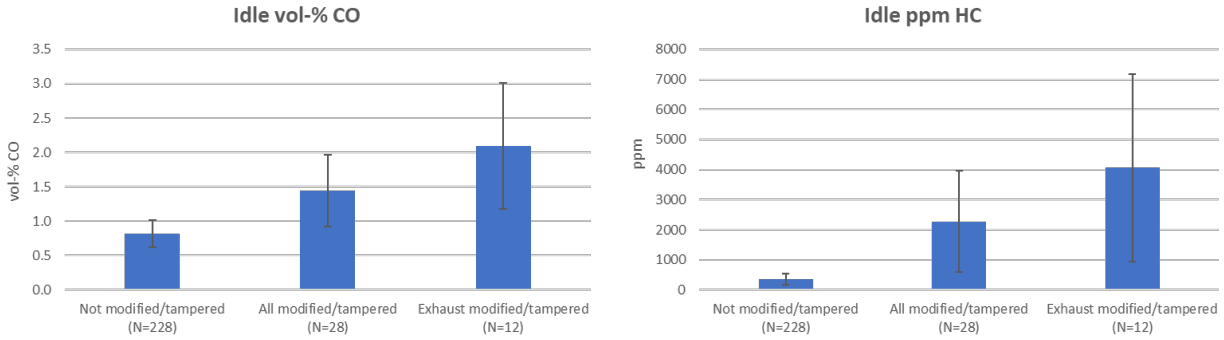

Figure 42. Impact of modification/tampering on CO and HC idle emissions according to the roadside inspections in Leuven and Barcelona.

Figure 43 shows the distribution of the measured sound pressure levels in the stationary noise test during the vehicle inspections in Leuven and Barcelona. On top of the distribution, markers are added to indicate the vehicles labeled as tampered. Triangles indicate tampering with the exhaust system (blue) or muffler and/or dB killer (red). For all vehicles which didn't pass the stationary test due to a measured level exceeding the reference level, a gray circle is added. It can be seen that most outliers in the distributions (marked as black dots) are tampered vehicles and that most noise tampered vehicles (muffler and/or dB killer) can be found above the 75% percentile of the distributions. For vehicles with tampered exhausts, there is no clear trend. It should also be noted that the stationary noise test doesn't impose an absolute limit but compares the measured noise level to a reference value measured by the manufacturer for this specific vehicle. Not passing the test therefore doesn't say much about the LVs absolute noise level and its position in the distribution considering the entire fleet.

This project has received funding from the European Union's Horizon Europe research and innovation programme under grant agreement No 101056777

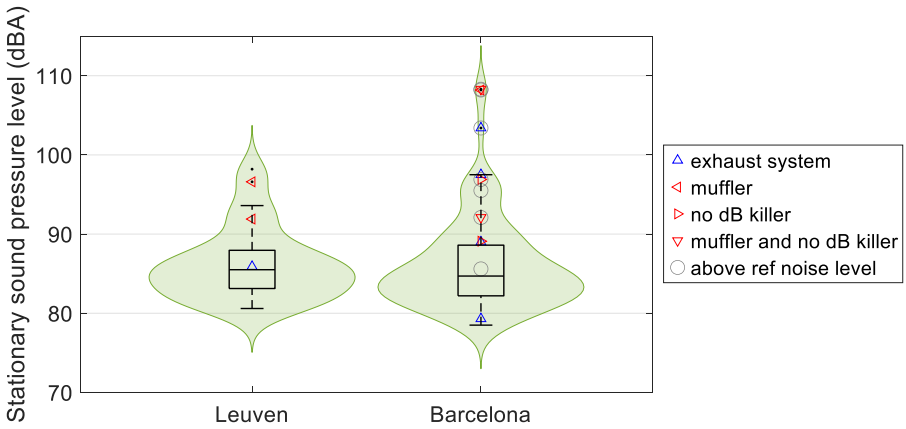

Figure 43. Distribution of the stationary noise level (dB(A)) measured on the LVs inspected at the roadside in Leuven (29 LVs) and Barcelona (94 LVs). Noise levels of tampered LVs are indicated with markers. Triangles indicate tampering with the exhaust system, muffler and/or dB killer. A circle is added for all vehicles that didn't pass the stationary noise test.

3.3.2 Tampering analysis based on measured on-road emissions

Figure 44 shows the substantial impact of modification/tampering on on-road CO, HC and PM emissions. Fuel-specific CO and HC emissions from exhaust system modified/tampered LVs are a factor of about 5 and 7 higher, respectively, than non-modified/non-tampered LVs, and for PM the corresponding increase is nearly one order of magnitude. On the contrary, for on-road NO_X emissions no clear impact is seen.

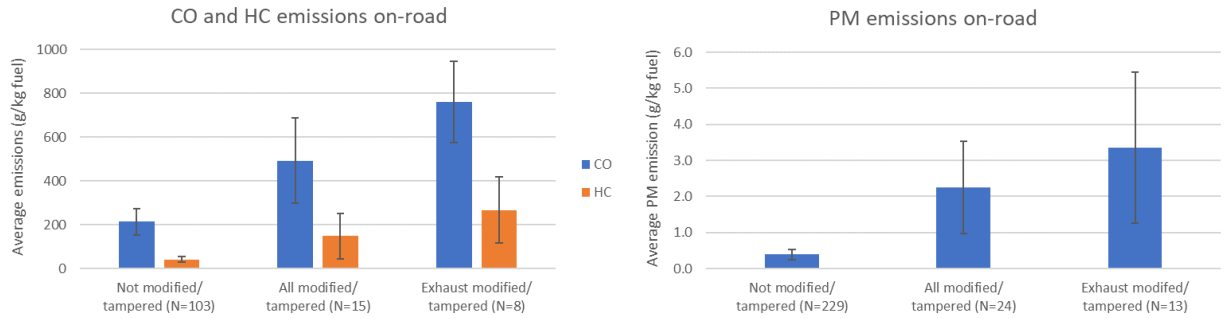

Figure 44. Impact of modification/tampering on CO and HC on-road emissions (in g/kg fuel) for the LVs inspected at the roadside inspections in Leuven and Barcelona.

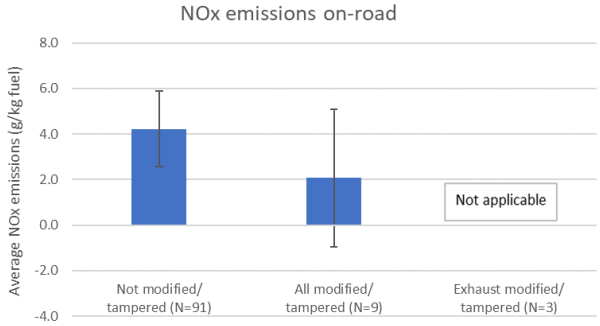

Figure 45. Impact of modification/tampering on NO_X on-road emissions (in g/kg fuel) for the LVs inspected at the roadside inspections in Leuven and Barcelona.

This project has received funding from the European Union's Horizon Europe research and innovation programme under grant agreement No 101056777

3.3.3 Tampering analysis based on roadside noise measurements

3.3.3.1 Overview of the roadside noise dataset for inspected vehicles

Since, as explained in section 3.2, the composition of the noise dataset is different from the composition of the Opus RSD 6000 dataset, the composition of the dataset with respect to tampering is presented in Figure 46. Considering all noise recordings associated to an inspected vehicle, vehicles confirmed as tampered account for 11.1% of the recordings for the Leuven campaign and 17.5% for the Barcelona campaign. For both measurement sites where vehicle inspections took place, noise recordings are available for only a handful of vehicles labeled as tampered. This implies that all conclusions below should be interpreted with the necessary caution given the small sample sizes.

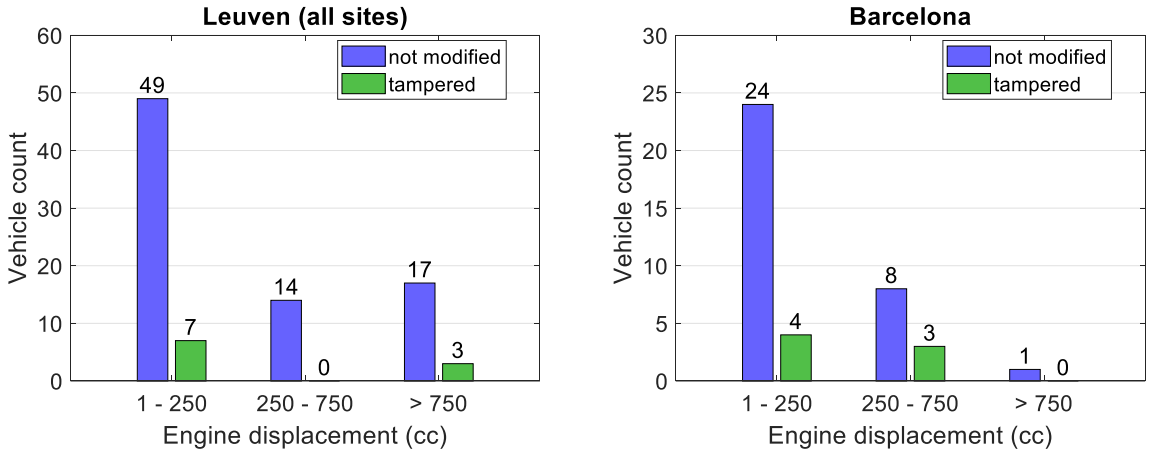

Figure 46. Overview of the fleets of inspected LVs for which preprocessed roadside noise recordings are available.

3.3.3.2 Influence of tampering on roadside noise levels

Figure 47 shows the distribution of the measured maximum A-weighted sound pressure level (LAFmax) for the complete fleet of LVs which have been inspected and labeled as either not modified or as tampered (see section 3.3.1). For Leuven, there is a clear difference between the distributions of the A-weighted sound pressure level for the fleets of tampered and not tampered LVs. The median is around 8 dB(A) higher for tampered LVs. Also for Barcelona, a clear increase of the median by around 4 dB(A) can be observed. However, in contrast to the common belief that tampered vehicles are by definition louder, there is a large overlap between the distributions of tampered and non-tampered vehicles for this measurement site. This can have multiple causes, such as differences in types of tampering, vehicle types and driving conditions. In fact, it was observed during the measurements that many LVs suspected of tampering tended to release the throttle when spotting the instruments and drove more carefully past the measurement site in Paris and Barcelona. In Leuven this was not the case thanks to the police support. Although valid speed and acceleration measurements are available in the Opus RSD 6000 measurement database for only a subset of the considered vehicles, Figure 48 illustrates this influence of human behavior on the considered driving conditions and the measurement results.

This project has received funding from the European Union's Horizon Europe research and innovation programme under grant agreement No 101056777

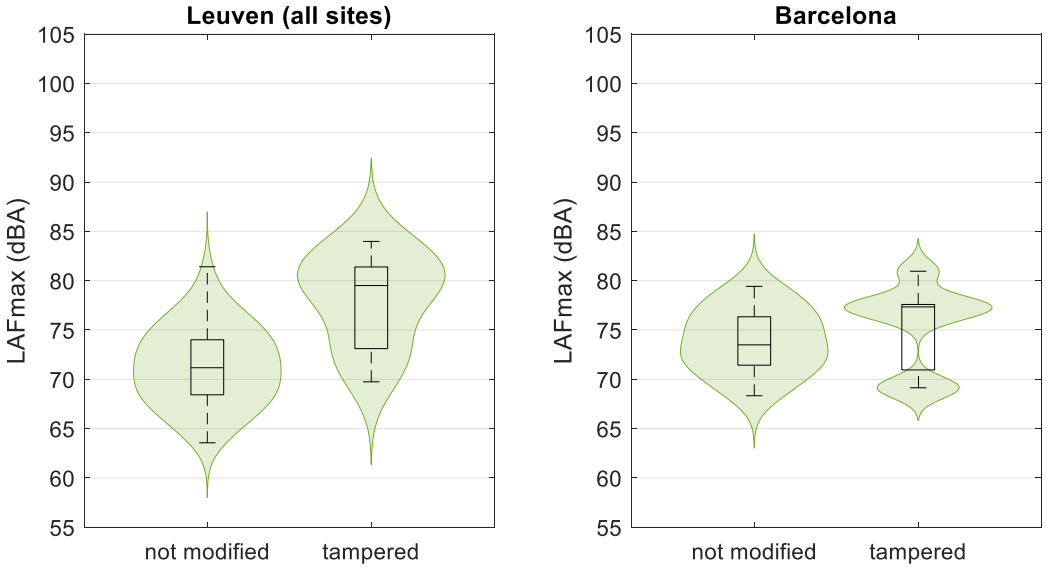

Figure 47. Maximum A-weighted sound pressure level (LAFmax) for all noise recordings corresponding to an inspected LV.

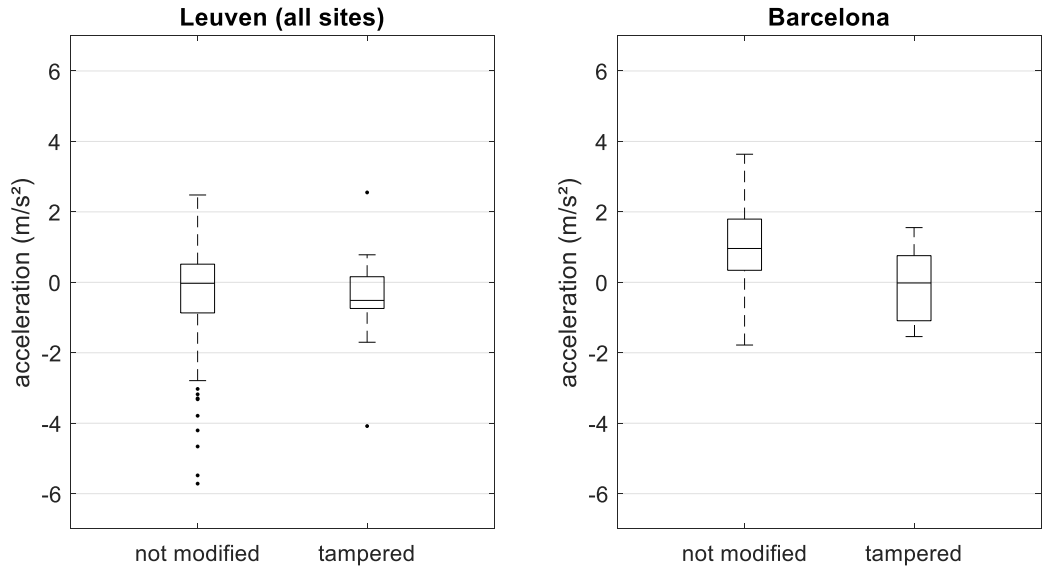

Figure 48. Acceleration measured by the Opus RSD 6000 for LVs considered in Figure 51.

As can be seen in Figure 49, the differences between not modified and tampered vehicles are more pronounced in terms of C-weighted sound pressure level (LCFmax) for all measurement sites. Also for Barcelona, there is not only a difference in median level, but also the overlap of the distributions is significantly lower. This may partly be due to the driving conditions with low engine RPM of many tampered vehicles, leading to more dominant low frequencies suppressed by the A-weighting filter. However, this change in frequency spectrum is probably also part of the sound character often targeted by tampering.

This project has received funding from the European Union's Horizon Europe research and innovation programme under grant agreement No 101056777

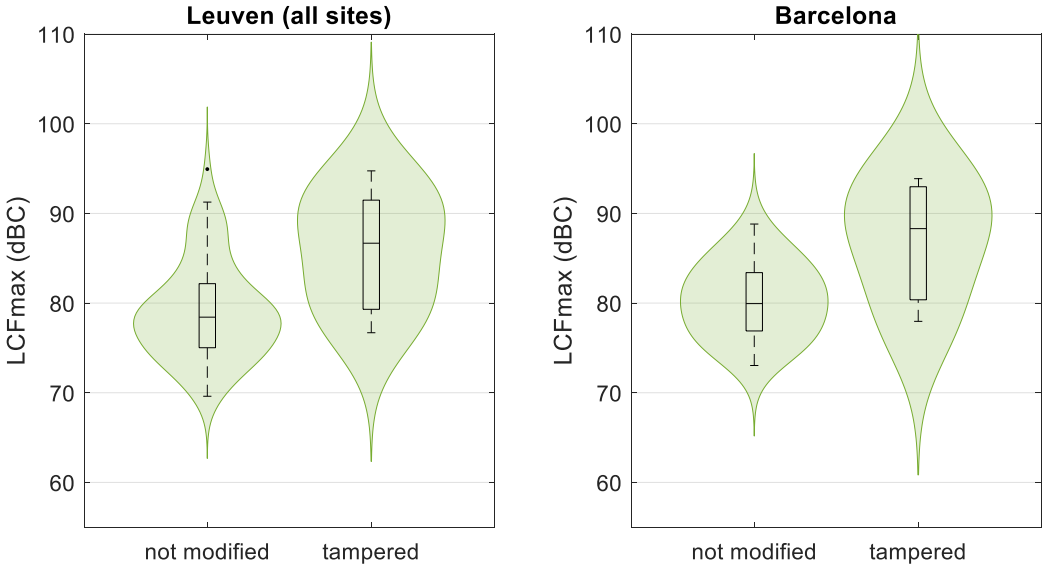

Figure 49. Maximum C-weighted sound pressure level (LCFmax) for all noise recordings corresponding to an inspected LV.

Figure 50 illustrates the relation between the measured sound pressure levels during stationary testing and the sound pressure level measured from the roadside in the Barcelona campaign. It can be observed that overall vehicles with high noise levels in the stationary test also exhibit higher sound pressure levels measured from the roadside. Especially if a C-weighting is applied to the latter, a linear relation between both measurement results is observed. It can also be observed that most tampered vehicles are located in the top right corner of the graph, with high levels measured both in the stationary test and from the roadside. However, there is a large number of non-modified LVs with comparable A-weighted sound pressure levels measured from the roadside and there are a few tampered vehicles with surprisingly low levels in both measurements. From this figure it can be concluded that, although tampered vehicles are often louder, this is not always the case and the difference with not-modified LVs depends on the way the sound pressure level is measured and quantified.

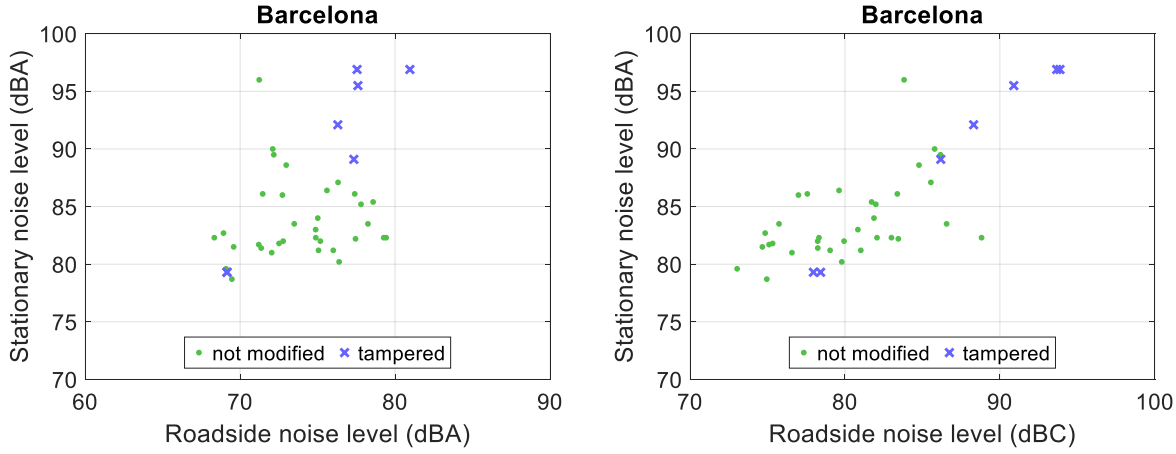

Figure 50. Relation between stationary noise level (dB(A)) and roadside noise level, expressed as maximum A-weighted (LAFmax) and C-weighted (LCFmax) sound pressure level.

This project has received funding from the European Union's Horizon Europe research and innovation programme under grant agreement No 101056777

3.3.3.3 Influence of tampering on psychoacoustic metrics

Besides noise levels, tampering often modifies the sound character of an LV. In the following, the influence of tampering on common psychoacoustic metrics is therefore analyzed. Figures 53, 54 and 55 visualize the effect of tampering on the roughness, fluctuation strength and tonality. It can be observed that the median values for roughness for the fleet of not modified vehicles is in line with the values reported in section 3.3.1 for the complete fleet in section 3.1.12. Tampering seems to increases roughness from a median between 0.25 and 0.3 asper to a median around 0.5 for both measurement sites. There are also a number of vehicles with significantly higher roughness. These results, together with the observations for Dampierre-en-Yvelines in Figure 30, suggest that roughness could be a valuable indicator for detecting tampering.

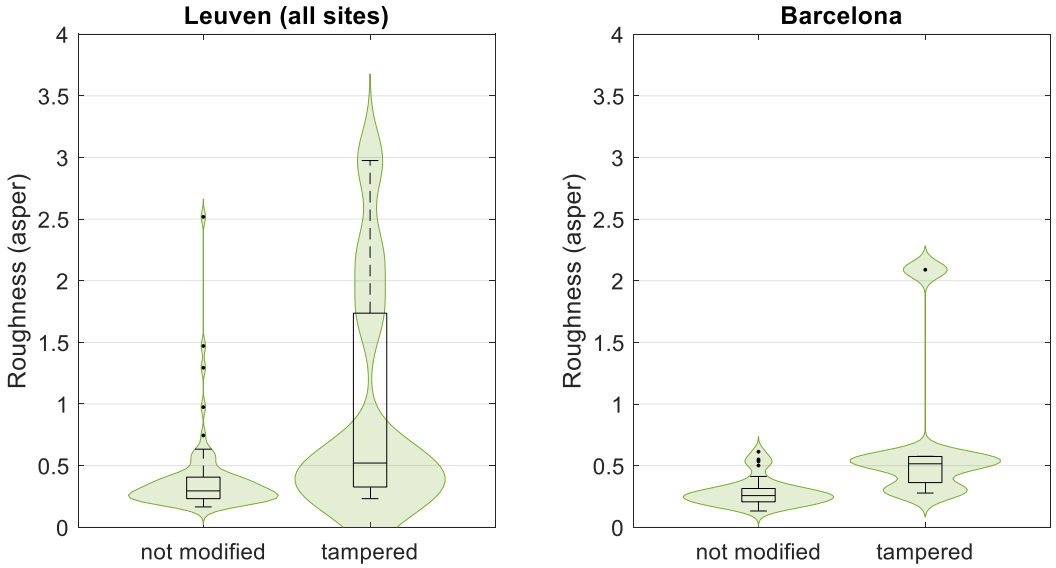

Figure 51. Roughness for all noise recordings corresponding to an inspected LV.

For the fluctuation strength (Figure 52), no clear differences can be observed and the distributions largely overlap. The tonality (Figure 53) remains low for the complete fleet, but a subtle increase from a median of 0.12-0.13 t.u. for not modified LVs to 0.17-0.18 t.u. for tampered LVs can be observed for both measurement sites.

This project has received funding from the European Union's Horizon Europe research and innovation programme under grant agreement No 101056777

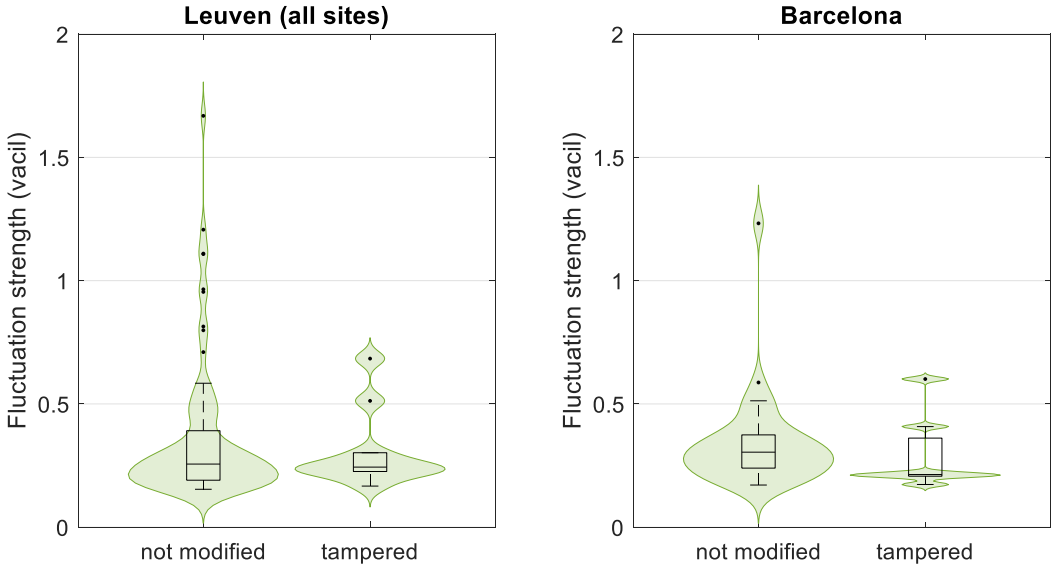

Figure 52. Fluctuation strength for all noise recordings corresponding to an inspected LV.

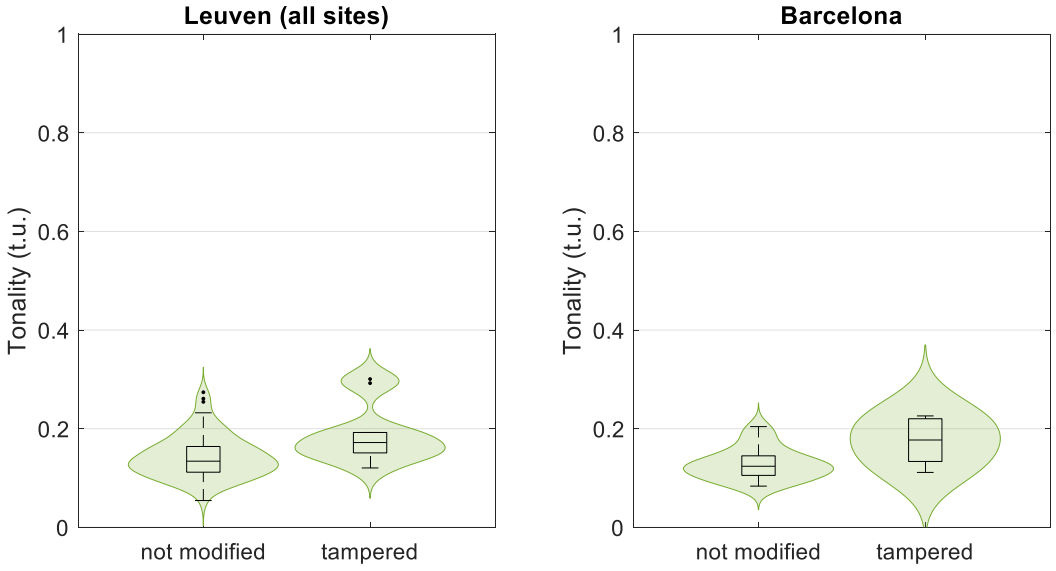

Figure 53. Tonality for all noise recordings corresponding to an inspected LV.

3.3.4 Sound signal features for detecting tampering

Since tampering often changes the character of an LV's sound, it is assumed that tampered vehicles could be detected based on characteristics of their sound signature. A large and diverse set of features originating from various fields has therefore been computed for all inspected LV noise recordings. In particular, features used for vibration analysis for condition monitoring could be interesting tampering indicators since they typically aim to detect the presence of impulsiveness in a signal or quantify the importance of peaks or families of peaks in a spectrum. Besides psychoacoustic metrics (roughness,

This project has received funding from the European Union's Horizon Europe research and innovation programme under grant agreement No 101056777

fluctuation strength, tonality, etc.), among others the following signal characteristics have been investigated:

- **Kurtosis** is a statistical measure that characterizes the "peakiness" of the signal's amplitude distribution. High kurtosis values indicate a distribution with more extreme values.
- **Crest factor (CF)** is the ratio of a signal's peak value to its RMS (Root Mean Square) value. Elevated crest factors can indicate the presence of sharp peaks in the signal.
- **Peak-to-peak (P2P)** is the difference between the maximum positive and maximum negative amplitudes of a signal.
- **Peak-to-peak average power ratio (PAPR)** represents the ratio of the peak power of the signal to its average power, expressed in decibels.
- **75% percentile** is a metric related to the overall amplitude and power of the signal, similar to P2P and PAPR.
- **Shannon entropy** and **Logarithmic Energy Entropy** are used in vibration analysis to quantify the complexity or randomness of a signal. A higher Shannon entropy in a vibration signal suggests more unpredictable or chaotic behaviour [28].
- **4th Figure of Merit (FM4)** is obtained by calculating the fourth normalized statistical moment (normalized kurtosis) of the difference signal, which is obtained by removing frequencies above 1000 Hz from the raw signal. This feature was originally proposed for condition monitoring of gears, for which the difference signal would be primarily Gaussian noise if the gear is in good condition, resulting in a FM4 value of 3 (nondimensional) [29].
- Methods **M6A** and **M8A** are variations of the sixth (M6) and eighth (M8) normalized statistical moments proposed to detect surface damage in gears using vibration signals. M6A and M8A are applied to the same difference signal as defined in the definition of FM4 [29].
- The **Harmonic Product Spectrum** represents the strength of each harmonic component in a signal, revealing tonal characteristics of the signal. The maximum of this spectrum (MHPS) is a metric of tonality in the raw signal [30].
- The **Envelope Harmonic Product Spectrum** similarly represents the strength of each harmonic component on the envelope spectrum, which corresponds to the low frequency cyclic modulations. The maximum of this spectrum (MEHPS) is a measure for the modulation present in the signal.
- **Noise Quality Factor (NQF)** is a measure of signal quality, specifically how well a system stores energy relative to the energy it loses per cycle. A high Q-factor indicates a system that resonates strongly with minimal energy loss, while a low Q-factor suggests significant energy loss and broader resonance [31].
- The **Gini index** has initially been proposed as a measure of sparsity to measure wealth inequality but has also been used for bearing diagnostics [32, 33].
- **L2/L1 norm** is extracted from the signal's envelope and is a sparsity metric equivalent to the spectral kurtosis. It is the extension of the L1/L0 norm and has been used as a sparsity metric in the frequency domain for health monitoring [32, 33].
- Various properties (maximum, number of peaks, etc.) of the **cepstrum**, defined as the inverse Fourier transform of the logarithm of the amplitude spectrum. The cepstrum is a tool to study periodic patterns in a spectrum, such as a series of (engine) orders [34].

This project has received funding from the European Union's Horizon Europe research and innovation programme under grant agreement No 101056777

All of these features have been computed using sliding windows of 0.5s with 50% overlap to account for the time-varying character of the sound. The maximum value occurring in the 3 s recording for each metric is used for further analysis. By studying these features individually, often a large overlap between the distributions for tampered and non-modified LVs can be observed. Nevertheless, some general trends could be detected:

- Features related to the maximum sound pressure level (LAFmax, LZFmax, P2P, 75% percentile) tend to be higher for tampered vehicles than for non-modified vehicles;
- Features quantifying the presence of one or more peaks in the sound spectrum (roughness, fluctuation strength, tonality, MHPS, MEHPS, maximum of the cepstrum) are on average higher for tampered LVs. The same holds for features which quantify the peakiness or complexity of a sound signal (kurtosis, Shannon entropy). Some examples are given in Figure 51, Figure 52, Figure 53, and Figure 54.
- For features originating from gear health monitoring (FM4, M6A, M8A), the lower quartile remains unchanged but the median and IQR increase significantly (see for example Figure 55)
- There is no clear difference between the distributions of the CF and PAPR for tampered and non-modified LVs (see Figure 56);

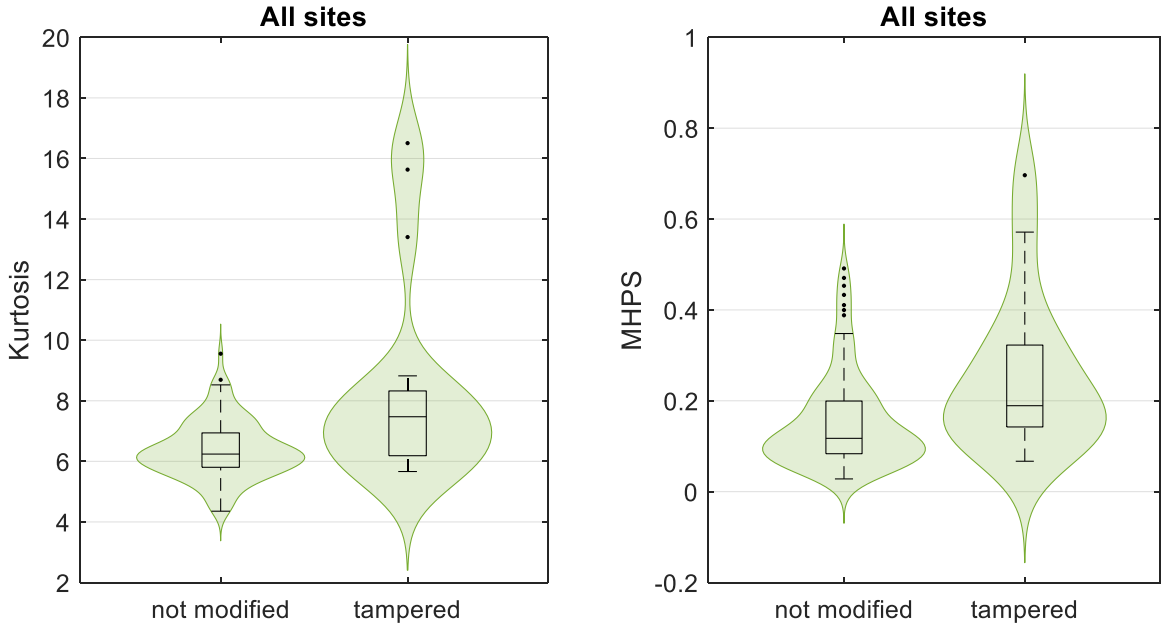

Figure 54. Distribution of the kurtosis (left) and MHPS (right) for all noise recordings corresponding to an inspected LV in the Leuven and Barcelona campaigns.

This project has received funding from the European Union's Horizon Europe research and innovation programme under grant agreement No 101056777

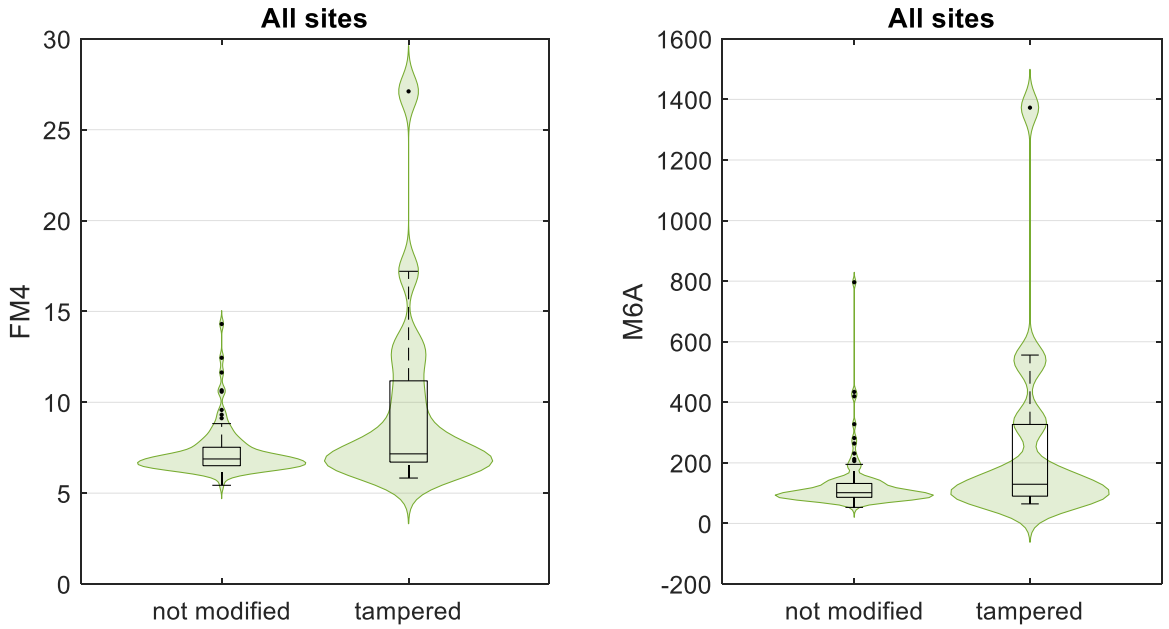

Figure 55. Distribution of the FM4 (left) and M6A (right) for all noise recordings corresponding to an inspected LV in the Leuven and Barcelona campaigns.

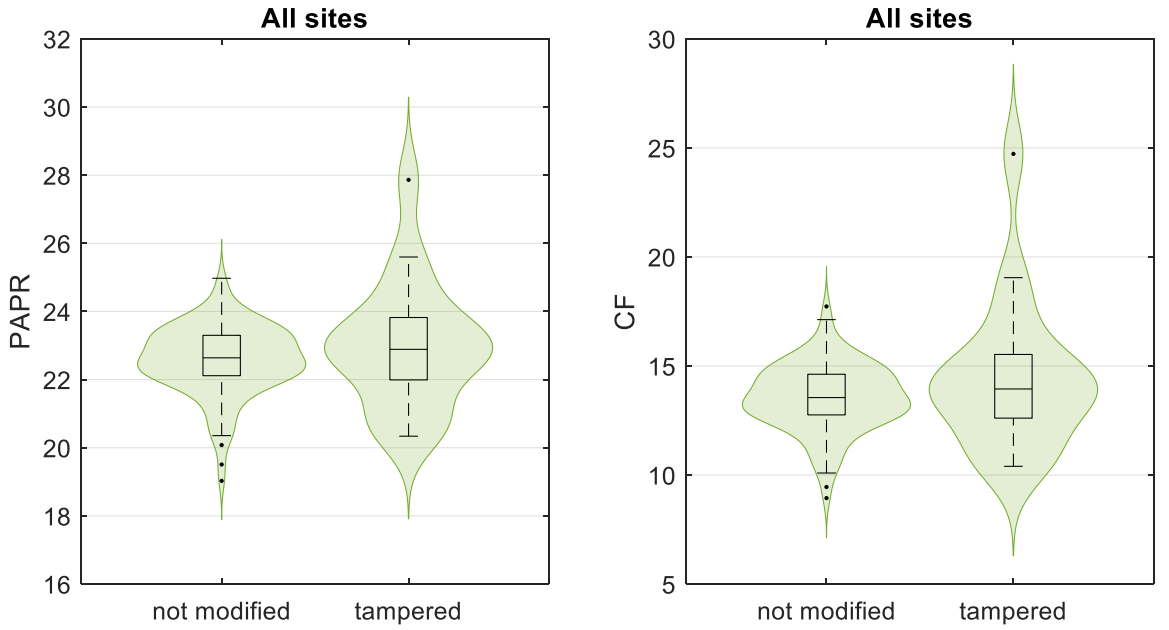

Figure 56. Distribution of the PAPR (left) and CF (right) for all noise recordings corresponding to an inspected LV in the Leuven and Barcelona campaigns.

3.3.5 Classification models

Considering the diversity in sound signatures due to differences in LV types and driving conditions encountered in real life traffic, a much larger dataset of sound recordings of inspected LVs is needed to properly train a classification model that can identify tampering. Nevertheless, it has been attempted to gain some insights in the most interesting features for detecting tampering by training classification models on the limited available data. To limit the diversity in sound character due to LV types in the

This project has received funding from the European Union's Horizon Europe research and innovation programme under grant agreement No 101056777

fleet, it was decided to focus this effort on smaller LVs with an engine displacement up to 250 cc, i.e. mostly mopeds and scooters. As can be seen in Figure 46, this subfleet is for both measurement sites with LV inspections by far the largest one in the noise recordings database (62% for Leuven and 70% for Barcelona), with a comparable share of tampering for both sites (14% for Leuven and 17% for Barcelona).

Different support vector machines and random forest classifiers were trained on the dataset, using different sets of features. Because of the small size of the dataset, with in total only 11 usable recordings of tampered LVs in this category, it was decided to merge the datasets of inspected vehicles in Leuven and Barcelona. Already on the training dataset, the performance of the resulting models is poor. The most relevant outcome of these models is the ranking of the features used by the classifier. Although the ranking strongly depends on the approach and the other features included in the model, P2P, roughness and either Shannon entropy or kurtosis often rank among the most important ones. On the other hand, the NQF is usually among the lowest ranked features and probably doesn't carry much relevant information.

As a final test case, a random forest classifier was trained on the combined data from inspected LVs in Leuven and Barcelona. To avoid overfitting, only the following 3 features were used: P2P (as a measure for the amplitude), roughness (quantifying peaks in the spectrum) and either kurtosis or Shannon entropy (as a measure for peaks in the time signal). The resulting model is clearly overfitted and shows perfect accuracy on the training dataset. Although it is expected to perform poorly on unseen data, the performance of the model was tested on some data which was not used for tampering. Since no ground truth from roadside inspections is available for these LVs, a subjective evaluation was made by listening to the recordings identified as tampered.

In the Leuven dataset, there are 7 recordings corresponding to LVs which have not been inspected, but of which the engine displacement is known to be at most 50 cc by the structure of their license plate. One of these recordings is classified as tampered by both classification models. Based on our evaluation by listening to the recording, it seems plausible that this is indeed a tampered LV. Its sound character gives a more heavy and powerful impression than the majority of LVs in its category. Interesting to note is that this vehicle was consistently classified as tampered by many other attempted classification models, using different feature sets.

The classification model was also applied to all LVs with a known engine displacement up to 250 cc in the Paris dataset. Here only 1 of the 129 recordings were classified as tampered if the Shannon entropy is used as 3rd feature. If the Shannon entropy is replaced by kurtosis, 2 additional recordings are classified as tampered. By listening to the recordings of the LVs suspected of tampering, we assume that the recording highlighted by both classification models could be a tampered scooter but is more likely a cross moto. This is an LV type which was not present in the training dataset and has a very different sound character than the LVs considered for training (mostly mopeds and scooters). Of the other two recordings highlighted as potentially tampered by the classification model using kurtosis, one is clearly due to the driving conditions (rpm burst). The last recording is not highlighted due to driving conditions and tampering can't be excluded, but it's difficult to draw firm conclusions based on only listening to the recording. Further research, requiring a larger dataset of noise recordings for inspected LVs, is needed to improve the classification models and properly evaluate their performance.

This project has received funding from the European Union's Horizon Europe research and innovation programme under grant agreement No 101056777

4 Conclusions

- The on-road/real-world emissions of all regulated pollutants (CO, HC and NO_X) from L-category vehicles have been reduced substantially from around Euro 2 (the early 2000's) to Euro 5 compliant ones, with reductions in the range of ≈ 60 – 90%, depending on pollutant.
- In particular, very strong decreasing on-road emission trends, i.e., 2-3 orders of magnitude, were observed for PN, PN_{23} and PM from Euro 1 to Euro 5.
- Due to the low hit rate in the single-digit percentage range for LVs using point sampling, traffic emission monitoring and detection of tampered LVs in traffic was found to not to be reliably possible by this technique, using the approach validated for passenger-cars and heavy-duty vehicles.
- In order to increase the hit rate for LV emission characterization utilizing point sampling, important factors are, good temporal separation between vehicle passages, high engine load while passing, ensure passage as close to the measurement set-up as safety permits. Furthermore, adaptation of the setup may be considered, such as multiple sampling inlets or closed, tunnel-like measurement passages.
- Schlieren imaging was used successfully to visualize the exhaust of LVs in traffic. Analysis of the images allows us to study the exhaust spread and thus optimize the PS sampling position in the future.
- Despite differences in fleet composition, driving conditions and background noise levels, the median levels at all sites are within 2.5 dB(A) from each other with the higher levels measured at the urban sites. The difference between the 25% and 75% percentiles (the inter quartile range, IQR) was 4 – 6 dB(A) at all measurement sites.
- No clear trends for the A-weighted sound pressure level as a function of Euro class could be observed, and the same holds across all engine sizes. This is most likely due to the driving conditions at the measurement sites, which were not the most noise critical ones for most vehicles. If C-weighted sound pressure levels are used, heavier LVs appear clearly louder than lighter ones.
- Psychoacoustic metrics such as roughness, fluctuation strength and tonality showed consistent values for all measurement sites, with the exception of measurements in the location Dampierre-en-Yvelines where - among others - the average roughness was more than 40% higher.
- In both the two campaigns that hosted roadside inspections (Leuven and Barcelona), the share of modified/tampered LVs was slightly above 10%, including both emission and noise tampering, according to the inspections carried out at the roadside. Since not all tampering options were included in the inspections, e.g., engine speed restrictor tampering or removal, this share represents a minimum confirmed tampering ratio.

This project has received funding from the European Union's Horizon Europe research and innovation programme under grant agreement No 101056777

- Emission modifications/tampering increases the on-road fuel specific emissions of CO, HC and PM (particle mass - UV opacity based measurements) substantially: a factor about 5, 7 and 10, respectively, whereas NO_X emissions tend not to be impacted.
- Noise tampering has an important impact on the noise levels measured in the stationary test, but this difference is much more subtle when looking at sound pressure levels measured from the roadside. The choice of weighting filter (A- or C-weighting) has a big influence on the observed difference in sound pressure level between tampered and not modified vehicles.
- Tampering also changes the sound character of the LV, which can be quantified using various psychoacoustic and other metrics. Especially roughness, an indicator for the rough character of a sound due to high frequency modulation phenomena, tends to clearly increase due to tampering.
- Due to the limited number of usable recordings corresponding to inspected LVs, it was not possible to train a reliable classification model. However, preliminary results show that – with more data – it could be possible to provide an indication of some types of tampering based on their sound signature, taking into account the driving conditions which affect engine speed and loading.
- Finally, based on the results presented in this report, it is believed that the potential end users of this research and the applied methods would be found in areas such as vehicle inspection, legal enforcement and environmental authorities, from the local to the national level.

This project has received funding from the European Union's Horizon Europe research and innovation programme under grant agreement No 101056777

Acknowledgements

- The involved city authorities in Leuven, Rueil Malmaison, Yvelines-en-Dampierre and Barcelona issuing permits for the measurements, and the city police in Leuven and Barcelona for their involvement and strong commitment in the roadside inspections.
- Opus RSE – all the staff taking care of the measurements and Javier Buhigas for preparations and planning, especially in the Barcelona campaign.
- LENS colleagues Roland Oswald at TU Graz and Vojtěch Vobr at Czech University of Life Sciences Prague for their involvement in the Leuven roadside inspections and the measurements in Rueil Malmaison, Paris region.
- LENS colleague Philippe Dégeilh at IFPEN for helping with getting the Paris campaign organized.
- Applus+ for carrying out the vehicular inspections in Barcelona including idle emission and stationary noise tests.

This project has received funding from the European Union's Horizon Europe research and innovation programme under grant agreement No 101056777

References

[1] Regulation (EU) 44/2014, Official Journal of the European Union, 28.1.2014, L 25/1, https://eur-lex.europa.eu/legal-content/EN/TXT/HTML/?uri=CELEX%3A32014R0044.

[2] Batsalia, N., Triantafyllopoulos, G., Tziovas, T., Michael Dittrich, M., Ntziachristos, L. (2023) L-vehicle tampering and undesirable effects. https://www.lens-horizoneurope.eu/wp-content/uploads/2023/10/LENS_D5.1_LVs-tampering-and-undesirable-effectsM14.pdf.

[3] CARES – City Air Remote Emission Sensing, Horizon 2020 research and innovation grant no. 814966. https://cordis.europa.eu/project/id/814966.

[4] NEMO – Noise and Emissions Monitoring and radical mitigation, Horizon 2020 research and innovation grant no. 860441. https://cordis.europa.eu/project/id/860441.

[5] Denayer, H., Gu, H., Gryllias, K., Kupper, M. (2024) Techniques for tampered/high-emitting LV detection https://www.lens-horizoneurope.eu/wp-content/uploads/2025/05/LENS_D5_2_M24.pdf .

[6] Davison, J., Bernard, Y., Borken-Kleefeld, J., Farren, N. J., Hausberger, S., Sjödin, Å., Tate, J.E., Vaughan, A. R., Carslaw, D. C. (2020) Distance-based emission factors from vehicle emission remote sensing measurements. *Science of The Total Environment*, **739**, 139688 https://doi.org/10.1016/j.scitotenv.2020.139688

[7] Bishop, G. A., Starkey, J. R., Ihlenfeldt, A., Williams, W. J., Stedman, D. H. (1989) IR Long-Path Photometry: A Remote Sensing Tool for Automobile Emissions. Analytical Chemistry, **61(10)**, 671A-677A. DOI: https://doi.org/10.1021/ac00185a002.

[8] Dallmann, T., Bernard, Y., Tietge, U., Muncrief, R. (2019) Remote sensing of motor vehicle emissions in Paris https://theicct.org/publication/remote-sensing-of-motor-vehicle-emissions-in-paris/

[9] Bishop, G.A., Starkey, J.R., Ihlenfeldt, A., Williams, W.J., & Stedman, D.H. (1989). IR Long-Path Photometry, A Remote Sensing Tool For Automobile Emissions. Analytical Chemistry, 61(10), 671A-677A. https://doi.org/10.1021/ac00185a002 https://doi.org/10.1021/ac00185a002.

[10] Hu, J., Frey, H. C. (2017) Evaluation of the Effect of Biodiesel on Exhaust Emissions of Locomotive Head End Power Engines. Annual Conference and Exhibition of the Air & Waste Management Association, Pittsburgh, PA, June 2017. https://www.researchgate.net/publication/332696411

[11] Imtiaz, H. H., Schaffer, P., Hesse, P., Kupper, M., Bergmann, A. (2025) Automatic Number Plate Detection and Recognition System for Small-Sized Number Plates of Category L-Vehicles for Remote Emission Sensing Applications. Sensors 2025, 25(11), 3499; https://doi.org/10.3390/s25113499

[12] Imtiaz, H. H., Schaffer, P., Liu, Y., Hesse, P., Bergmann, A., Kupper, M. (2024) Qualitative and Quantitative Analyses of Automotive Exhaust Plumes for Remote Emission Sensing Application Using Gas Schlieren Imaging Sensor System. Atmosphere 2024, 15(9), 1023; https://doi.org/10.3390/atmos15091023

[13] Hallquist Å. M., Jerksjö M., Fallgren H., Westerlund J. and Sjödin Å. (2013) Particle and gaseous emissions from individual diesel and CNG buses, Atmos. Chem. Phys., 13, 5337, https://doi.org/10.5194/ACP-13-5337-2013

This project has received funding from the European Union's Horizon Europe research and innovation programme under grant agreement No 101056777

[14] Liu Q, Hallquist Å. M., Fallgren H., Jerksjö M., Jutterström S., Salberg H., Hallquist M., Le Breton M., Pei X., Pathak R. K., Liu T., Lee B. and Chan C. K. (2019) Roadside assessment of a modern city bus fleet: Gaseous and particle emissions, Atmos. Environ. X, 100044, https://doi.org/10.1016/j.aeaoa.2019.100044
[15] Watne Å. K., Psichoudaki M., Ljungström E., Le Breton M., Hallquist M., Jerksjö M., Fallgren H., Jutterström S. and Hallquist Å., M. (2018) Fresh and Oxidized Emissions from In-Use Transit Buses Running on Diesel, Biodiesel, and CNG, Environ. Sci. & Tech., 52 (14), 7720, https://doi.org/10.1021/ACS.EST.8B01394
[16] Zhou, L., Hallquist Å. M., Hallquist M., Salvador C. M., Gaita S. M., Sjödin Å., Jerksjö M., Salberg H., Wängberg I., Mellqvist, J., Liu Q., Lee B. P. and Chan C. K. (2020) A transition of atmospheric emissions of particles and gases from on-road heavy-duty trucks, Atmos. Chem. Phys., 20, 1701, https://doi.org/10.5194/acp-20-1701-2020
[17] Zhou LY., Salvador C. M., Priestley M., Hallquist M., Liu Q. Y., Chan C. K. and Hallquist Å. M. (2021) Emissions and Secondary Formation of Air Pollutants from Modern Heavy-Duty Trucks in Real-World Traffic–Chemical Characteristics Using On-Line Mass Spectrometry, Environ. Sci. & Tech., 55 (21), 14515, https://doi.org/10.1021/acs.est.1c00412
[18] Le Breton M., Psichoudaki M., Hallquist M., Watne Å. K., Lutz A. and Hallquist Å. M. (2019) Application of a FIGAERO ToF CIMS for on-line characterization of real-world fresh and aged particle emissions from buses, Aerosol Sci. Tech., 53 (3), 244, https://doi.org/10.1080/02786826.2019.1566592
[19] Zhou, L., Liu, Q., Salvador, C. M., Le Breton, M., Hallquist, M., Yu, J. Z., Chan, C. K., and Hallquist, Å. M.: Online characterization of primary and secondary emissions of particulate matter and acidic molecules from a modern fleet of city buses, Atmos. Chem. Phys., 24, 11045–11061, https://doi.org/10.5194/acp-24-11045-2024
[20] Clarke Joan (1998), Evaluation of censored data methods to allow statistical comparisons among very small samples with below detection limit observations, Environ. Sci. Technology, 32 (1), 177-183, https://doi.org/10.1021/es970521v
[21] Knoll, M., Penz, M., Schmidt, C., Pöhler, D., Rossi, T., Casadei, S., Bernard, Y., Hallquist, Å. Sjödin, Å., Bergmann, A. (2024) Evaluation of the point sampling method and inter-comparison of remote emission sensing systems for screening real-world car emissions. Science of The Total Environment, 932, 171710, https://doi.org/10.1016/j.scitotenv.2024.171710
[22] Knoll, M., Penz, M., Juchem, H., Schmidt, C., Pöhler, D., Bergmann (2024) A. Large-scale automated emission measurement of individual vehicles with point sampling Atmos. Meas. Tech., 17, 2481–2505, https://doi.org/10.5194/amt-17-2481-2024
[23] Dittrich, M.; van Mensch, P.; Riemersma, I.; Paschinger, P.; Steven, H.; Karamanlis, N.; Degeilhe, P. (2023) Real world driving conditions and requirements for the LENS test programme - Deliverable 6.1, Public Report, EU Horizon Europe project "LENS".
[24] Felix Greco G., Merino-Martínez R., Osses A. (2023). SQAT: A sound quality analysis toolbox for MATLAB. https://github.com/ggrecow/sqat
[25] Daniel, P., Weber, R. (1997). Psychoacoustical roughness: implementation of an optimized model. Acustica, 83, 113-123.
[26] Osses, A., Garcia A., Kohlrausch, A. (2016) Modelling the sensation of fluctuation strength. Proceedings of Meetings on Acoustics, 28, 050005. https://doi.org/10.1121/2.0000410.

This project has received funding from the European Union's Horizon Europe research and innovation programme under grant agreement No 101056777

[27] Aures, W. (1985) Berechnungsverfahren fuer den sensorischen Wohlklang beliebiger Schallsignale. Acta Acustica united with Acustica, 59, 130-141.
[28] de Novaes Pires Leite G., Araújo A.M., Carvalho Rosas P.A., Stosic T., Stosic B. (2019) Entropy measures for early detection of bearing faults, Physica A: Statistical Mechanics and its Applications, 514, 458-472. https://doi.org/10.1016/j.physa.2018.09.052
[29] Sait A.S., Sharaf-Eldeen Y.I. (2011) A Review of Gearbox Condition Monitoring Based on Vibration Analysis Techniques Diagnostics and Prognostics. Proulx, T. (Eds) Rotating Machinery, Structural Health Monitoring, Shock and Vibration, 5, Conference Proceedings of the Society for Experimental Mechanics Series. Springer, New York, NY. https://doi.org/10.1007/978-1-4419-9428-8_25
[30] Cai Yi, Weihao Zhang, Hu Cao, Lei Yan, Qiuyang Zhou, Ying Shi, Guiting Tang, Le Ran, Jianhui Lin (2024) Cyclostationary harmonic product spectrum with its application for rolling bearing fault resonance frequency band adaptive location. Expert Systems with Applications, 254, 124453. https://doi.org/10.1016/j.eswa.2024.124453
[31] Sekko E., Capdessus C., Attal E. (2023) Noise robust gearbox defect diagnosis. Surveillance, Vibrations, Shock and Noise. https://hal.science/hal-04165865v1
[32] Qi, J., Mauricio, A., and Gryllias, K. (2022) Comparison of Blind Diagnostic Indicators for Condition Monitoring of Wind Turbine Gearbox Bearings. ASME. J. Eng. Gas Turbines Power, 144(4), 041019. https://doi.org/10.1115/GT2020-15278
[33] Dong Wang (2018) Some further thoughts about spectral kurtosis, spectral L2/L1 norm, spectral smoothness index and spectral Gini index for characterizing repetitive transients. Mechanical Systems and Signal Processing, 108, 360-368. https://doi.org/10.1016/j.ymssp.2018.02.034
[34] Randall, R.B. (2017). A history of cepstrum analysis and its application to mechanical problems. Mechanical Systems and Signal Processing, 97, 3-19. https://doi/org/10.1016/j.ymssp.2016.12.026

This project has received funding from the European Union's Horizon Europe research and innovation programme under grant agreement No 101056777

Funded by the European Union. Views and opinions expressed are however those of the author(s) only and do not necessarily reflect those of the European Commission or CINEA. Neither the European Commission nor CINEA can be held responsible for them.

Appendix

Tampering in-field survey measurement sites

A1. Leuven, Belgium

Site 1:

37 Donkerstraat; link to Google Maps: https://maps.app.goo.gl/kVYCZpLtY2nwc2919

Site 2:

55 Tiensestraat; link to Google Maps: https://maps.app.goo.gl/aiyDh9icyTo9YqYo9

This project has received funding from the European Union's Horizon Europe research and innovation programme under grant agreement No 101056777

A2. Paris region, France

Site 1 – Rueil Malmaison:

9 Av. du 18 Juin 1940; link to Google Maps: https://maps.app.goo.gl/2zTy6VQd6X2JZaEg9

Site 2 - Dampierre-en-Yvelines:

12 D91/Route de Versailles; link to Google Maps: https://maps.app.goo.gl/AakMAW2Ptih4oAi87

This project has received funding from the European Union's Horizon Europe research and innovation programme under grant agreement No 101056777

A3 Barcelona, Spain

Site 1:

382 Via Augusta; ; link to Google Maps: https://maps.app.goo.gl/d5tkZucvUPTzpw1U9

This project has received funding from the European Union's Horizon Europe research and innovation programme under grant agreement No 101056777

A4. Roadside inspection results

Leuven

LV no.	Make	Model	2- or 4-stroke	Eng displ cm3	Model year	Euro class	Mileage	% CO idle	ppm HC idle	dB stationary noise	Observations	Modified/Tampered
1	Toscana		2	50		5	3076	3.37	319			No
2	SYM	Fiddle III	4	49		4	24117	4.00	673			No
3	Honda	Zoomer	4	50	2007	3	54529	3.85	869			No
4	SYM	JET 14	4	49	2023	5		0.01	39			No
5	SYM	Orbit II	4	50		4		0.01	13			No
6	SYM	Cirox	4	49	2019	4		3.24	1149		Engine cold	No
7	Kymco	Agility	4	49	2020	4	14552	2.70	490			No
8	Honda	CB 650 F	4	650	2016	3	22274	2.47	266			No
9	SYM	JET 14	4	50	2022	5	6751	1.25	495			No
10	SYM	Orbit II	4	50	2017	2	19679	0.09	205		Hole in exhaust, rusty exhaust pipe	No
11	Yamaha	MT 07 Tracer	4	689	2017	4	14424	3.40	662			No
12	Honda	CB 500 FA	4	500	2023	5	2517	1.23	713			No
13	Suzuki	V Strom 650	4	650	2015	3	11433	1.98	660			No
14	SYM	Fiddle II	4	50	2021	5	17394	0.45	199			No
15	SYM	Mio	4	50	2019	4	10000	4.60	645		Fairings broken	No
16	Honda	BCX	4	125	2012	3	25219	3.46	724			No
17	Honda	BCX	4	125	2022	5	16700	4.65	763			No
18	Honda	Viston	4	49	2015	2	16446	2.75	547			No
19	Kymco	Dink Street	4	125	2016	3	24094	0.71	604			No
20	Vespa	LX50	4	50	2009	3	26650	4.81	792		Old exhaust pipe, rusty	No
21	Vespa	LX50	4	50	2008	3	1756	0.19	14806			No
22	Yamaha	Tracer 9 GTX	4	890	2023	5	21004	0.02	100			No
23	SYM	Orbit II	4	49	2012	3	31403	3.03	1338			No
24	Piaggio	GTS M45	4	278	2016	3	7155	0.03	54			No
25	Piaggio	Prima Vera	4	50	2021	5	5959	0.01	97			No
26	Vespa	Prima Vera	4	50	2021	5	17740	0.06	127			No
27	SYM	Jet 4 RX	4	49	2024	5	568	0.01	134			No
28	Yamaha	DT 125 RE	2	125	2006	3	16570	3.23	11513		Covers missing, exhaust aftermarket, racing muffle	Yes
29	Yamaha	XSR 900	4	900	2023	5	3785	0.06	53			No
30	SYM	Orbit	4	50	2022	5	11206	0.22	24			No
31	Honda	Deaville	4	680	2007	3	49854	0.08	131			No
32	Vespa	LML	2	125	2009	3	58682	2.08	3386		Old and rusty exhaust pipe	No
33	Honda	CBF 600	4	600	2008	3	69761	0.02	88			No
34	BMW	1200 R GS	4	1200	2017	4	66716	0.03	151			No
35	Kawasaki	Z 900 RS	4	900	2019	4	16317	0.02	183			No
36	Turpho	CS 50	2	50	2015	2	10573	5.33	1123			No
37	BMW	GS 1200 R	4	1200	2016	4	33199	0.02	124		Akrapovic muffler	No
38	NECO	Azuru	4	49	2019	4	1830	5.80	769			No
39	Kawasaki	Z1000	4	1000	2018	4	9223	0.04	168		Akrapovic muffler	No
40	Kawasaki	Z650	4	650	2023	5	3269	0.00	182			No

This project has received funding from the European Union's Horizon Europe research and innovation programme under grant agreement No 101056777

LV no.	Make	Model	2- or 4-stroke	Eng displ cm3	Model year	Euro class	Mileage	% CO idle	ppm HC idle	dB stationary noise	Observations	Modified/Tampered
41	SYM	X Pro	4	49	2024	5	3269	0.03	15			No
42	Kymco	Agility	4	50	2023	5	8996	4.31	483			No
43	Piaggio	Sprint	4	50	2021	5	7211	0.01	324			No
44	Peugeot	Kisbee Injection	2	50	2021	5	6870	0.03	41			No
45	BMW	R100 RS	4	1000	1980	0	11994	1.54	180		Old scrambler modified	Yes
46	Kawasaki	1400 GTR	4	1400	2014	3	36252	0.02	22			No
47	Skyteam	Dark 125	4	125	2024	4	7255	0.68	16			No
48	Piaggio	GTS 300	4	300	2012	3	23955	0.28	21			No
49	BMW	F 700 GS	4	700	2014	4	65400	0.01	15			No
50	Quadro	Qooder 4-wheele	4	398	2019	4	9544	0.00	11			No
51	Ducati	Streetfighter	4	950	2023	5	1321	0.01	17			No
52	Malagutti	Bold	4	125	2020	4	15900	1.31	248		Aftermarket muffler	Yes
53	Honda	ZRF 1000	4	1084	2019	4	11991	0.00	8			No
54	Peugeot	Tweet	4	49	2021	4	4847	0.00	38			No
55	Yamaha	R125	4	125	2014	3	37760	2.13	518		GPR muffler bend	Yes
56	BMW	F 900	4	900	2024	5	613	0.00	2		New mc with Akrapovic muffler	No
57	CF Moto	MT 800	4	800	2023	5	7147	0.02	81			No
58	Triumph	Rocket 3	4	2500	2020	5	6261	0.49	61		Aftermarket ZARD muffler	Yes
59	Suzuki	Bandit 1250	4	1250	2012	3	40256	0.01	21		Aftermarket muffler	Yes
60	BMW	R 1250	4	1250	2020	4	31194	0.01	20			No
61	Kymco	Agility	4	50	2019	4	9748	0.00	25			No
62	Yamaha	MT07	4	700	2023	5	5091	0.01	10			No
63	SYM	Fiddle II	4	50	2022	5	4705	0.04	119			No
64	Kawasaki	Kinjo 650	4	650	2017	4	29980	0.01	20			No
65	Piaggio	Liberty	4	50	2020	4	6020	0.04	110			No
66	Honda	NSC 50 R	4	50	2014	4	9805	0.47	172			No
67	Vespa	125 Ivie	4	125	2016	3	12857	0.36	47			No
68	MBK	Nitro	2	50	2019	4	8695	0.80	594		Aftermarket exhaust	Yes
69	Kymco	ZX 50	2	49	2023	5	8868	1.19	6011			No
70	SYM	X Pro 50	4	50	2020	4	21987	0.36	427			No
71	Kymco	Agility 50	4	50	2017	2	3912	3.98	455			No
72	Suzuki	Bandit 650 GSF	4	650	2007	2	33331	0.02	76			No
73	La Souris	Sourini R	4	50	2023	5	1853	0.71	292		Rusty exhaust pipe	No
74	Yamaha	SA46	4	50	2016	2	32640	0.04	34			No
75	Piaggio	Liberty 4 Tempi	4	50	2014	3	15607	0.12	142			No
76	SYM	Fiddle II	4	50	2021	5	6317	0.03	477			No
77	BMW	R 1200	4	1200	2008	3	58000	0.02	147			No
78	SYM	Orbit III	4	50	2020	4	25611	2.47	352			No
79	SYM	Jet 14	4	49	2024	5	731	1.90	224			No
80	Kawasaki	Z 900	4	900	2023	5	12090	0.03	15		Akrapovic muffler	No
81	Yamaha	MT - 09	4	900	2024	5	364	0.02	11			No
82	SYM	Fiddle II	4	50	2020	4	5125	0.06	146			No
83	Vespa	Sprint	4	50	2017	2		1.93	483			No
84	SYM	X Pro 50	4	50	2022	5	4104	0.02	1			No

This project has received funding from the European Union's Horizon Europe research and innovation programme under grant agreement No 101056777

LV no.	Make	Model	2- or 4-stroke	Eng displ cm3	Model year	Euro class	Mileage	% CO idle	ppm HC idle	dB stationary noise	Observations	Modified/Tampered
85	Yamaha	MT - 07	4	700	2014	3	18384	0.79	95		Aftermarket	No
86	Honda	PCX	4	125	2018	4	59107	0.03	18			No
87	Vespa	GTS 250	4	250	2007	3	65512	0.02	21			No
88	Ride	Jump	2	50	2014	2	21324	2.40	6995		Cover broken, race exhaust pipe, other engine	Yes
89	Zoe		4	50			521	4.25	412			No
90	Kymco	Agility 16	4	50	2022	5	12747	0.56	155			No
91	SYM	LM 25	4	250	2010	3	31776	0.87	78			No
92	Kawasaki	Z 900	4	900	2023	5	2563	0.01	20		Akrapovic muffler	No
93	Scooth	Di Lucio 50	4	50	2021	4	7711	5.60	1639			No
94	SYM	Jet 14	4	50	2023	5	2400	0.02	35			No
95	Ducati	Monster	4	937	2021	5	21900				Aftermarket muffler, clutch modified Ducati	Yes
96	SYM	Fiddle II i	4	50	2022	5	4759	0.01	28			No
97	Peugeot	Kimbee	4	50	2020	4	2572	0.02	65			No
98	SYM	Fiddle II	4	50	2021	5	10500	0.01	75		Rusty exhaust pipe	No
99	Kymco	Agility 16	4	50	2018	4	3903	0.93	180			No
100	SYM	Orbit II	4	50	2019	4	17988	0.06	200			No
101	SYM	Jet 14	4	50	2024	4	1830	0.07	160			No
102	SYM	X Pro 50	4	50	2020	4	28021	0.81	182		Rusty exhaust pipe	No
103	SYM	Orbit III	4	50	2022	5	24139	0.00	12			No
104	SYM	X Pro	4	50	2019	4	24599	0.22	529			No
105	SYM	Orbit II	4	50	2020	4	10515	0.01	50			No
106	SYM	Orbit III	4	50	2019	4	21927	0.71	220			No
107	Vespa	S 50	2	50	2010	2	26765	4.39	12670		Exhaust pipe modified, not original	Yes
108	SYM	Orbit III	4	50	2018	4	8299	0.10	360			No
109	Peugeot	Kisbee	4	50	2023	5	9477	0.00	109			No
110	Piaggio	Liberty S	4	50	2019	4	23652	0.14	220		CVT crank bearing bent, cover broken	Yes
111	SYM	X Pro	4	50	2022	5	4153	0.00	36			No
112	SYM	X Pro	4	50	2020	4	42663	0.03	71			No
113	SYM	Jet 14	4	50	2019	4	8695	2.46	375		High idle	No
114	SYM	Orbit II	4	50	2012	3	23830	2.63	292			No
115	GTS	Toscana	4	50	2023	5	3155	0.22	292			No
116	SYM	Fiddle II	4	50	2021	5	6335	0.01	73			No
117	La Souris	Sourini	4	50	2024	5	718	0.23	322			No
118	Honda	CBR 500R	4	500	2013	3	30500	0.01	26			No
119	Peugeot	Kisbee	4	50	2023	5	7125	0.70	183			No
120	SYM	Orbit III	4	50	2020	4	22941	0.92	412		High idle	No
121	SYM	Fiddle 50S	4	50		4	18289	0.00	88			No
122	Kymco	Agility	4	50	2023	5	3973	3.62	286			No
123	Piaggio	Derbi DRD Racing	2	50	2011	3	11000	2.60	11890		Exhaust not original, muffler aftermarket	Yes
124	Kymco	VSR	4	125	2020	4	7088	0.00	231			No
125	SYM	Orbit II	4	50	2016	2	2668	6.32	2104			No
126	Suzuki	TS X	2	50	1988	0		4.10	10861		Exhaust + muffler	Yes

This project has received funding from the European Union's Horizon Europe research and innovation programme under grant agreement No 101056777

LV no.	Make	Model	2- or 4-stroke	Eng displ cm3	Model year	Euro class	Mileage	% CO idle	ppm HC idle	dB stationary noise	Observations	Modified/Tampered
127	KTM	Duke 125	4	125	2018	4	4810	0.00	433			No
128	SYM	Orbit	4	50	2022	5	2751	0.03	159			No
129	SYM	Jet 14	4	50	2024	5	1234	0.05	192			No
130	Triumph	Bonvile	4	980	2003	2	39997	4.70	317		Exhaust not original, carburettor	Yes
131	Peugeot	Kisbee	4	50	2023	5	20210	0.01	55			No
132	SYM	Orbit II	4	50	2020	4	25680	4.35	923			No
133	Kymco	Agility	4	50	2021	4	65930	2.76	265			No
134	SYM	Orbit II	4	50	2016	2	2674	5.27	729			No
135	SYM	Orbit II 50	4	50	2017	2	4444	0.86	239		Exhaust SAI (secondary air injection) missing	Yes
136	SYM	Orbit II	4	50	2017	2	20721	4.91	775			No
137	BMW	F 800 R	4	800	2011	3	28595	0.01	19	88.4		No
138	SYM	Orbit II	4	50	2020	4	14970	0.02	76	84.0		No
139	BMW	R1250 RT	4	1250	2019	4	30894	0.03	31	89.0	Akrapovic muffler	No
140	SYM	Orbit II	4	50	2009	2	22475	1.40	255	80.8		No
141	SYM	Super 8R	4	50	2023	5	5320	1.20	110	81.8		No
142	Peugeot	Kisbee	4	50	2023	5	5564	0.02	45	83.4		No
143	TGB	X Motion	4	125	2011	3	7870	0.03	76	82.3		No
144	Peugeot	ZIP	4	50	2019	4	16287	2.90	210	85.9	Exhaust pipe modified (race)	Yes
145	Piaggio	ZIP	4	50	2023	5	1745	0.02	79	80.6		No
146	Vespa	Prima Vera	4	50	2017	4	9443	1.48	128	83.9		No
147	Yamaha	MT-07	4	700	2024	5	4542	0.07	67	86.9		No
148	Peugeot	V-Clic	4	50	2014	2	10650	7.50	2100	85.0		No
149	Kymco	Agility	4	50	2019	4	10140	2.00	420	96.6	Aftermarket muffler	Yes
150	SYM	Jet 14	4	125	2024	5	60	0.01	59	81.4		No
151	SYM	Jet 4	4	50	2024	5	621			81.0		No
152	SYM	Joy Max 300i	4	300	2017	3	12275	0.02	60	85.5		No
153	Derbi	Sendo Xtreme	2	50	2003	2	19984	4.10	14000	91.9	Aftermarket muffler	Yes
154	Piaggio	Liberty	4	50	2006	2	15500	4.20	590	87.8		No
155	Vespa	LX 125	4	125	2006	3	12955	0.06	22	84.4	Old exhaust pipe	No
156	SYM	X Pro 50	4	50	2020	4	40800	5.40	620	92.0	Rusty exhaust pipe, high idle	No
157	Honda	PCX	4	125	2022	5	5110	0.07	76	85.7		No
158	Piaggio	ZIP	4	50	2023	5	3927	0.01	86	86.0		No
159	Archive	First	4	50	2022	5	858	0.20	60	81.6		No
160	BMW	1200 GS	4	1200	2006	3	78764	0.01	100	86.1		No
161	SYM	X Pro	4	50	2021	4	9484	0.01	100			No
162	Honda	VT 750S	4	750	2011	3	20980	1.00	47	87.1		No
163	BMW	R 1100	4	1150	1998	0	41123	0.42	30	93.6		No
164	Yamaha	X Max	4	125	2015	3	35932	0.95	240	98.2	Akrapovic muffler	No
165	Kymco	Agility	4	50	2020	4	20149	0.03	14	83.8		No
166	SYM	Symphony	4	50	2013	2	47534			83.4		No

This project has received funding from the European Union's Horizon Europe research and innovation programme under grant agreement No 101056777

Barcelona

LV no.	Make	Model	2/4-stroke	Eng displ cm3	Model year	Euro class	Mileage	% CO idle	ppm HC idle	dB stationary noise	Observations	Modified/Tampered
1	Honda	SH125	4	125	2005	2	26202	0.32	50	86.4		No
2	Ducati	Streetfighter V	4	950	2024	5	3	0.03	0	96		No
3	Yamaha	X-max 125	4	125	2021	5	13122	0.16	64	81.8		No
4	Honda	SH125	4	125	2018	4	208677	0.00	0	82		No
5	Kymco	Agility City	4	125	2015	3	25042	0.21	29	85		No
6	Honda	SH350	4	350	2023	5	18436	0.00	0	81		No
7	Kymco	X-Tow	4	300	2023	5	24479	0.70	80	78.5		No
8	BMW	GS800	4	800	2010	3	171275	0.00	0	87.2		No
9	Honda	SH300	4	300	2013	3	75495	1.12	63	87.2		No
10	Kymco	SuperDink300	4	300	2014	3	85927	0.90	100	84		No
11	Honda	SH125	4	125	2018	4	37319	0.69	330	92.1	Muffler changed. No dB Killer. Ref noise 81dB (2test)	Yes
12	Suzuki	GS500	4	500	2007	3	29129	0.90	35	86.1		No
13	BMW	750	4	750	2021	5	11304	0.00	0	88.6		No
14	Yamaha	X-max 125	4	125	2008	3	43819	0.13	70	83.5		No
15	Honda	SH150	4	150	2004	2	78165	0.04	147	85.2		No
16	Yamaha	Tracer900	4	900	2024	5	5711	0.00	0	94.8		No
17	Honda	SH125	4	125	2012	3	45022	1.08	76	84.2		No
18	Yamaha	MT03	4	300	2023	5	11657	-	-	97.5	Exhaust changed. Cannot insert lead	Yes
19	SYM	HL125	4	125	2013	3	68738	0.00	0	82.3		No
20	Yamaha	Tracer900	4	900	2023	5	13204	0.00	0	91.9	Original Yamaha Akrapovic	No
21	Honda	Vision	4	110	2023	5	5019	0.00	0	81		No
22	Honda	PS125	4	125	2010	3	24747	0.42	50	84		No
23	Suzuki	Burgman 125	4	125	2003	2	17624	0.00	0	82.2		No
24	Yamaha	MT07	4	700	2020	5	30009	0.50	130	108.2	Muffler changed, ref noise 90dB	Yes
25	Honda	Vision	4	110	2014	3	50057	0.00	10	85		No
26	Honda	Forza 125	4	125	2020	5	32121	0.20	50	84.7		No
27	Kymco	SuperDink350	4	350	2023	5	3759	0.00	0	84.1		No
28	Kymco	Vitality	2	49	2017	4	20300	4.50	14250	85		No
29	Yamaha	X-max 125	4	125	2018	4	31650	0.00	21	84.2		No
30	Yamaha	MT09	4	900	2017	4	25271	1.05	220	108.3	Muffler changed. No dB Killer. Ref noise 93dB	Yes
31	Kymco	Superdink125	4	125	2021	5	33797	0.02	9	85.6	Ref noise 80dB	Yes
32	Kymco	Agility City 125	4	125	2020	5	12064	1.87	53	81.7		No
33	Yamaha	Aerox	2	49	2018	4		0.60	160	81.7		No
34	Honda	PCX125	4	125	2012	3	23809	0.00	0	83.7		No
35	BMW	F900R	4	900	2024	5	912	0.00	0	90.7		No
36	Honda	Vision	4	110	2014	3	32490	0.15	16	80		No
37	Kymco	Agility	4	125	2014	3	38660	0.38	34	82		No
38	Honda	CB650R	4	650	2019	4	12611	0.00	21	95.8		No
39	Yamaha	T-Max	4	530	2018	4	32873	0.16	29	96.9	Original Akrapovic . No Dbkiller. Ref noise 87db	Yes
40	Yamaha	X-max 125	4	125	2024	5	6329	0.02	61	80.4		No

This project has received funding from the European Union's Horizon Europe research and innovation programme under grant agreement No 101056777

LV no.	Make	Model	2/4-stroke	Eng displ cm3	Model year	Euro class	Mileage	% CO idle	ppm HC idle	dB stationary noise	Observations	Modified/Tampered
41	Honda	SH125	4	125	2021	5	12092	0.00	0	83.1		No
42	Yamaha	Tricity	4	125	2021	5	45678	0.05	39	81.4		No
43	Honda	Shmode	4	125	2021	5	4500	1.12	149	81.8		No
44	Yamaha	X-MAX 400	4	400	2020	5	18373	1.73	61	82.8		No
45	Yamaha	x-max 125	4	125	2013	3	48355	0.09	26	82.6		No
46	Kymco	Agility	4	125	2020	5	25688	0.00	3	79.9		No
47	Kymco	People	4	125	2018	4	12755	0.13	45	80.4		No
48	BMW	GS1200	4	1250	2016	3	51383	0.03	6	94.7		No
49	BMW	F800R	4	800	2018	4	50585	0.35	21	90.9		No
50	Honda	Shmode	4	125	2017	4	32629	0.00	0	84.3		No
51	Yamaha	Tracer 700	4	700	2019	4	31724	0.51	52	89	Exhaust changed..	Yes
52	Honda	CB500X	4	500	2024	5	3336	0.00	0	90		No
53	Honda	Vision	4	110	2013	3	18467	0.02	60	78.7		No
54	Honda	SH300	4	300	2017	4	19115	0.00	0	82.3		No
55	Piaggio	Zip	4	49	2008	3	32450	0.03	480	78.5		No
56	Honda	SH300	4	300	2010	3	33082	1.19	159	88.3		No
57	Yamaha	X-Max250	4	250	2012	3	70937	0.08	12	84.4		No
58	Honda	SH125	4	125	2008	3	67623	1.00	115	86.1		No
59	Honda	SH125	4	125	2022	5	10862	0.00	0	84.8		No
60	Honda	Dylan	4	125	2003	2	No hay le	0.23	113	86		No
61	Kymco	Agility	4	125	2016	3		3.80	2377	83.5		No
62	Aprilia	RX125	4	125	2023	5	16010	1.15	281	89.1	Original Arrow . No dB Killer.	Yes
63	Honda	SH125	4	125	2018	4	28114	0.00	10	84.7		No
64	Piaggio	Liberty	4	125	2024	5	7885	0.14	11	81.5		No
65	Yamaha	MT09	4	900	2019	4	13655	0.63	140	103.4	Exhaust changed without homologation. Ref noise 93dB	Yes
66	Piaggio	Liberty	4	125	2020	5	11756	0.00	0	80.2		No
67	Yamaha	T-Max	4	530	2012	3	31000	0.03	13	87.1	Original Akrapovic	No
68	SYM	Symphony	4	49	2018	4	34991	0.00	6	78.7		No
69	BMW	GS650	4	650	2004	2	68750	0.04	23	83		No
70	Honda	SH125	4	125	2020	5	27810	0.00	0	82.3		No
71	Honda	CBR125R	4	125	2024	5	2966	0.02	0	79.3	Exhaust changed without homologation	Yes
72	Honda	CB650R	4	650	2022	5	13628	0.00	0	96		No
73	Suzuki	GSR	4	600	2006	3	63854	0.08	70	90.3		No
74	KTM	Duke125	4	125	2021	5	10344	0.00	0	81.2		No
75	SYM	Symphony	4	125	2024	5	944	0.00	0	82.7		No
76	Yamaha	X-Max	4	250	2017	4	67391	0.61	5	85.8	MIL ON	Yes
77	Honda	Forza 125	4	125	2023	5	18019	0.00	0	85.4		No
78	Honda	CB500F	4	500	2018	4	24189	0.00	0	86.4		No
79	Yamaha	Xenter	4	125	2013	3	25000	0.04	14	79.6		No
80	Triumph	Speed	4	400	2024	5	2539	0.00	0	87.8		No

This project has received funding from the European Union's Horizon Europe research and innovation programme under grant agreement No 101056777

LV no.	Make	Model	2/4-stroke	Eng displ cm3	Model year	Euro class	Mileage	% CO idle	ppm HC idle	dB stationary noise	Observations	Modified/Tampered
81	Yamaha	N-Max	4	125	2024	5	850	0.00	3	82		No
82	Yamaha	X-Max125	4	125	2011	3	22894	0.10	44	82.2		No
83	BMW	R850	4	850	2005	2	48457	2.80	152	85.2		No
84	Honda	CB500	4	500	2020	5	17161	0.00	0	89.5		No
85	Kawasaki	Z900	4	900	2019	4	29006	0.00	43	89.3		No
86	BMW	R850R	4	850	2006	3	151435	0.09	42	88.3		No
87	BMW	650 Sport	4	650	2019	4	24310	0.04	23	95.5	Original Akrapovic . Ref noise 91db	Yes
88	Honda	Vision	4	110	2020	5	9624	0.00	0	83.2		No
89	Suzuki	Burgman200	4	200	2013	3	54719	0.06	0	90		No
90	BMW	GS1200	4	1200	2007	3	162323	0.01	14	88.4		No
91	Honda	PCX125	4	125	2023	5	10915	0.02	22	85.3		No
92	Honda	SH125	4	125	2017	4	68888	0.00	0	82.7		No
93	Yamaha	X-Max	4	300	2021	5	27022	0.00	0	83.3		No
94	BMW	GS1250	4	1250	2020	5	21164	0.00	0	92.9		No

This project has received funding from the European Union's Horizon Europe research and innovation programme under grant agreement No 101056777